NCHRP
REPORT 478

NATIONAL COOPERATIVE HIGHWAY RESEARCH PROGRAM

Relationship of Superpave Gyratory Compaction Properties to HMA Rutting Behavior

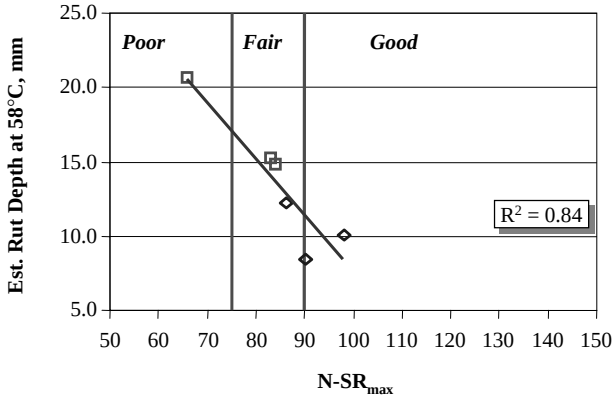

TRANSPORTATION RESEARCH BOARD
OF THE NATIONAL ACADEMIES

TRANSPORTATION RESEARCH BOARD EXECUTIVE COMMITTEE 2002 (Membership as of July 2002)

OFFICERS

Chair: *E. Dean Carlson, Secretary of Transportation, Kansas DOT*
Vice Chair: *Genevieve Giuliano, Professor, School of Policy, Planning, and Development, University of Southern California, Los Angeles*
Executive Director: *Robert E. Skinner, Jr., Transportation Research Board*

MEMBERS

WILLIAM D. ANKNER, *Director, Rhode Island DOT*
THOMAS F. BARRY, JR., *Secretary of Transportation, Florida DOT*
MICHAEL W. BEHRENS, *Executive Director, Texas DOT*
JACK E. BUFFINGTON, *Associate Director and Research Professor, Mack-Blackwell National Rural Transportation Study Center, University of Arkansas*
SARAH C. CAMPBELL, *President, TransManagement, Inc., Washington, DC*
JOANNE F. CASEY, *President, Intermodal Association of North America*
JAMES C. CODELL III, *Secretary, Kentucky Transportation Cabinet*
JOHN L. CRAIG, *Director, Nebraska Department of Roads*
ROBERT A. FROSCH, *Senior Research Fellow, John F. Kennedy School of Government, Harvard University*
SUSAN HANSON, *Landry University Professor of Geography, Graduate School of Geography, Clark University*
LESTER A. HOEL, *L. A. Lacy Distinguished Professor, Department of Civil Engineering, University of Virginia*
RONALD F. KIRBY, *Director of Transportation Planning, Metropolitan Washington Council of Governments*
H. THOMAS KORNEGAY, *Executive Director, Port of Houston Authority*
BRADLEY L. MALLORY, *Secretary of Transportation, Pennsylvania DOT*
MICHAEL D. MEYER, *Professor, School of Civil and Environmental Engineering, Georgia Institute of Technology*
JEFF P. MORALES, *Director of Transportation, California DOT*
DAVID PLAVIN, *President, Airports Council International, Washington, DC*
JOHN REBENSDORF, *Vice President, Network and Service Planning, Union Pacific Railroad Co., Omaha, NE*
CATHERINE L. ROSS, *Executive Director, Georgia Regional Transportation Agency*
JOHN M. SAMUELS, *Senior Vice President-Operations Planning & Support, Norfolk Southern Corporation, Norfolk, VA*
PAUL P. SKOUTELAS, *CEO, Port Authority of Allegheny County, Pittsburgh, PA*
MICHAEL S. TOWNES, *Executive Director, Transportation District Commission of Hampton Roads, Hampton, VA*
MARTIN WACHS, *Director, Institute of Transportation Studies, University of California at Berkeley*
MICHAEL W. WICKHAM, *Chairman and CEO, Roadway Express, Inc., Akron, OH*
M. GORDON WOLMAN, *Professor of Geography and Environmental Engineering, The Johns Hopkins University*

MIKE ACOTT, *President, National Asphalt Pavement Association (*ex officio*)*
REBECCA M. BREWSTER, *President and CEO, American Transportation Research Institute, Atlanta, GA (*ex officio*)*
JOSEPH M. CLAPP, *Federal Motor Carrier Safety Administrator, U.S.DOT (*ex officio*)*
THOMAS H. COLLINS (Adm., U.S. Coast Guard), *Commandant, U.S. Coast Guard (*ex officio*)*
JENNIFER L. DORN, *Federal Transit Administrator, U.S.DOT (*ex officio*)*
ELLEN G. ENGLEMAN, *Research and Special Programs Administrator, U.S.DOT (*ex officio*)*
ROBERT B. FLOWERS (Lt. Gen., U.S. Army), *Chief of Engineers and Commander, U.S. Army Corps of Engineers (*ex officio*)*
HAROLD K. FORSEN, *Foreign Secretary, National Academy of Engineering (*ex officio*)*
JANE F. GARVEY, *Federal Aviation Administrator, U.S.DOT (*ex officio*)*
EDWARD R. HAMBERGER, *President and CEO, Association of American Railroads (*ex officio*)*
JOHN C. HORSLEY, *Executive Director, American Association of State Highway and Transportation Officials (*ex officio*)*
MICHAEL P. JACKSON, *Deputy Secretary of Transportation, U.S.DOT (*ex officio*)*
ROBERT S. KIRK, *Director, Office of Advanced Automotive Technologies, U.S. Department of Energy (*ex officio*)*
WILLIAM W. MILLAR, *President, American Public Transportation Association (*ex officio*)*
MARGO T. OGE, *Director, Office of Transportation and Air Quality, U.S. Environmental Protection Agency (*ex officio*)*
MARY E. PETERS, *Federal Highway Administrator, U.S.DOT (*ex officio*)*
JEFFREY W. RUNGE, *National Highway Traffic Safety Administrator, U.S.DOT (*ex officio*)*
JON A. RUTTER, *Federal Railroad Administrator, U.S.DOT (*ex officio*)*
WILLIAM G. SCHUBERT, *Maritime Administrator, U.S.DOT (*ex officio*)*
ASHISH K. SEN, *Director, Bureau of Transportation Statistics, U.S.DOT (*ex officio*)*
ROBERT A. VENEZIA, *Earth Sciences Applications Specialist, National Aeronautics and Space Administration (*ex officio*)*

NATIONAL COOPERATIVE HIGHWAY RESEARCH PROGRAM

Transportation Research Board Executive Committee Subcommittee for NCHRP

E. DEAN CARLSON, *Kansas DOT* (Chair)
GENEVIEVE GIULIANO, *University of Southern California, Los Angeles*
LESTER A. HOEL, *University of Virginia*
JOHN C. HORSLEY, *American Association of State Highway and Transportation Officials*
MARY E. PETERS, *Federal Highway Administration*
JOHN M. SAMUELS, *Norfolk Southern Corporation, Norfolk, VA*
ROBERT E. SKINNER, JR., *Transportation Research Board*

NATIONAL COOPERATIVE HIGHWAY RESEARCH PROGRAM

NCHRP REPORT 478

Relationship of Superpave Gyratory Compaction Properties to HMA Rutting Behavior

R. MICHAEL ANDERSON
PAMELA A. TURNER
ROBERT L. PETERSON
Asphalt Institute
Lexington, KY

AND

RAJIB B. MALLICK
Worcester Polytechnic Institute
Worcester, MA

SUBJECT AREAS
Materials and Construction

Research Sponsored by the American Association of State Highway and Transportation Officials
in Cooperation with the Federal Highway Administration

TRANSPORTATION RESEARCH BOARD

WASHINGTON, D.C.
2002
www.TRB.org

NATIONAL COOPERATIVE HIGHWAY RESEARCH PROGRAM

Systematic, well-designed research provides the most effective approach to the solution of many problems facing highway administrators and engineers. Often, highway problems are of local interest and can best be studied by highway departments individually or in cooperation with their state universities and others. However, the accelerating growth of highway transportation develops increasingly complex problems of wide interest to highway authorities. These problems are best studied through a coordinated program of cooperative research.

In recognition of these needs, the highway administrators of the American Association of State Highway and Transportation Officials initiated in 1962 an objective national highway research program employing modern scientific techniques. This program is supported on a continuing basis by funds from participating member states of the Association and it receives the full cooperation and support of the Federal Highway Administration, United States Department of Transportation.

The Transportation Research Board of the National Academies was requested by the Association to administer the research program because of the Board's recognized objectivity and understanding of modern research practices. The Board is uniquely suited for this purpose as it maintains an extensive committee structure from which authorities on any highway transportation subject may be drawn; it possesses avenues of communications and cooperation with federal, state and local governmental agencies, universities, and industry; its relationship to the National Research Council is an insurance of objectivity; it maintains a full-time research correlation staff of specialists in highway transportation matters to bring the findings of research directly to those who are in a position to use them.

The program is developed on the basis of research needs identified by chief administrators of the highway and transportation departments and by committees of AASHTO. Each year, specific areas of research needs to be included in the program are proposed to the National Research Council and the Board by the American Association of State Highway and Transportation Officials. Research projects to fulfill these needs are defined by the Board, and qualified research agencies are selected from those that have submitted proposals. Administration and surveillance of research contracts are the responsibilities of the National Research Council and the Transportation Research Board.

The needs for highway research are many, and the National Cooperative Highway Research Program can make significant contributions to the solution of highway transportation problems of mutual concern to many responsible groups. The program, however, is intended to complement rather than to substitute for or duplicate other highway research programs.

Note: The Transportation Research Board of the National Academies, the National Research Council, the Federal Highway Administration, the American Association of State Highway and Transportation Officials, and the individual states participating in the National Cooperative Highway Research Program do not endorse products or manufacturers. Trade or manufacturers' names appear herein solely because they are considered essential to the object of this report.

NCHRP REPORT 478

Project D9-16 FY'99

ISSN 0077-5614

ISBN 0-309-06767-7

Library of Congress Control Number 2002112945

Price $15.00

NOTICE

The project that is the subject of this report was a part of the National Cooperative Highway Research Program conducted by the Transportation Research Board with the approval of the Governing Board of the National Research Council. Such approval reflects the Governing Board's judgment that the program concerned is of national importance and appropriate with respect to both the purposes and resources of the National Research Council.

The members of the technical committee selected to monitor this project and to review this report were chosen for recognized scholarly competence and with due consideration for the balance of disciplines appropriate to the project. The opinions and conclusions expressed or implied are those of the research agency that performed the research, and, while they have been accepted as appropriate by the technical committee, they are not necessarily those of the Transportation Research Board, the National Research Council, the American Association of State Highway and Transportation Officials, or the Federal Highway Administration, U.S. Department of Transportation.

Each report is reviewed and accepted for publication by the technical committee according to procedures established and monitored by the Transportation Research Board Executive Committee and the Governing Board of the National Research Council.

Published reports of the

NATIONAL COOPERATIVE HIGHWAY RESEARCH PROGRAM

are available from:

Transportation Research Board
Business Office
500 Fifth Street, NW
Washington, DC 20001

and can be ordered through the Internet at:

http://www.national-academies.org/trb/bookstore

Printed in the United States of America

THE NATIONAL ACADEMIES

Advisers to the Nation on Science, Engineering, and Medicine

The **National Academy of Sciences** is a private, nonprofit, self-perpetuating society of distinguished scholars engaged in scientific and engineering research, dedicated to the furtherance of science and technology and to their use for the general welfare. On the authority of the charter granted to it by the Congress in 1863, the Academy has a mandate that requires it to advise the federal government on scientific and technical matters. Dr. Bruce M. Alberts is president of the National Academy of Sciences.

The **National Academy of Engineering** was established in 1964, under the charter of the National Academy of Sciences, as a parallel organization of outstanding engineers. It is autonomous in its administration and in the selection of its members, sharing with the National Academy of Sciences the responsibility for advising the federal government. The National Academy of Engineering also sponsors engineering programs aimed at meeting national needs, encourages education and research, and recognizes the superior achievements of engineers. Dr. William A. Wulf is president of the National Academy of Engineering.

The **Institute of Medicine** was established in 1970 by the National Academy of Sciences to secure the services of eminent members of appropriate professions in the examination of policy matters pertaining to the health of the public. The Institute acts under the responsibility given to the National Academy of Sciences by its congressional charter to be an adviser to the federal government and, on its own initiative, to identify issues of medical care, research, and education. Dr. Harvey V. Fineberg is president of the Institute of Medicine.

The **National Research Council** was organized by the National Academy of Sciences in 1916 to associate the broad community of science and technology with the Academy's purposes of furthering knowledge and advising the federal government. Functioning in accordance with general policies determined by the Academy, the Council has become the principal operating agency of both the National Academy of Sciences and the National Academy of Engineering in providing services to the government, the public, and the scientific and engineering communities. The Council is administered jointly by both the Academies and the Institute of Medicine. Dr. Bruce M. Alberts and Dr. William A. Wulf are chair and vice chair, respectively, of the National Research Council.

The **Transportation Research Board** is a division of the National Research Council, which serves the National Academy of Sciences and the National Academy of Engineering. The Board's mission is to promote innovation and progress in transportation by stimulating and conducting research, facilitating the dissemination of information, and encouraging the implementation of research results. The Board's varied activities annually engage more than 4,000 engineers, scientists, and other transportation researchers and practitioners from the public and private sectors and academia, all of whom contribute their expertise in the public interest. The program is supported by state transportation departments, federal agencies including the component administrations of the U.S. Department of Transportation, and other organizations and individuals interested in the development of transportation. **www.TRB.org**

www.national-academies.org

COOPERATIVE RESEARCH PROGRAMS STAFF FOR NCHRP REPORT 478

ROBERT J. REILLY, *Director, Cooperative Research Programs*
CRAWFORD F. JENCKS, *Manager, NCHRP*
EDWARD T. HARRIGAN, *Senior Program Officer*
EILEEN P. DELANEY, *Managing Editor*
HILARY FREER, *Associate Editor II*

NCHRP PROJECT D9-16 PANEL
Field of Materials and Construction—Area of Bituminous Materials

RITA B. LEAHY, *Fugro-BRE, Inc., Austin, TX* (Chair)
JOHN BUKOWSKI, *FHWA*
GERALD HUBER, *Heritage Research Group, Indianapolis, IN*
THOMAS E. KEITH, *Henley, MO*
THOMAS W. KENNEDY, *University of Texas—Austin*
CARL L. MONISMITH, *University of California—Berkeley*
JAMES A. MUSSELMAN, *Florida DOT*
DAVID E. NEWCOMB, *National Asphalt Pavement Association*
RONALD A. SINES, *P. J. Keating Co., Fitchburg, MA*
JAMES P. WALTER, *Washington State DOT*
THOMAS HARMAN, *FHWA Liaison Representative*
FREDERICK HEJL, *TRB Liaison Representative*

FOREWORD

By Edward T. Harrigan
Staff Officer
Transportation Research Board

This report presents the findings of a research project to examine whether there is a relationship between any property of hot mix asphalt (HMA) measurable with the Superpave gyratory compactor and the rutting behavior of HMA pavements in service. Its main finding is that the parameter $N\text{-}SR_{max}$, the number of gyrations at maximum stress ratio, may be used within certain limits to identify mix designs likely to show gross instability under the shear stresses produced by traffic in HMA pavements. The report will be of particular interest to materials engineers in state highway agencies, as well as to materials suppliers and paving contractor personnel responsible for HMA design and quality control.

The Superpave volumetric mix design procedure (AASHTO MP2 and PP28) developed in the Asphalt Research Program (1987–1993) of the Strategic Highway Research Program (SHRP) does not include a simple, mechanical "proof" test analogous to the Marshall stability and flow tests or the Hveem stabilometer method. Instead, the original Superpave method relied on strict conformance to the material specifications and volumetric mix criteria to ensure satisfactory performance of mix designs intended for low-traffic-volume situations (defined as no more than 10^6 equivalent single axle loads [ESALs] applied over the service life of the pavement). For higher trafficked projects, the original SHRP Superpave mix analysis procedures[1] required a check for tertiary creep behavior with the repeated shear at constant stress ratio test (AASHTO TP7) and a rigorous evaluation of the mix design's potential for permanent deformation, fatigue cracking, and low-temperature cracking using several other complex test methods in AASHTO TP7 and TP9.

User experience with the Superpave mix design and analysis method, combined with the long-standing problems associated with the original SHRP Superpave performance models supporting what was then termed "level 2 and 3" analyses, demonstrated the need for simpler, quicker procedures to screen out mixes susceptible to permanent deformation early in the design process. Since the mid-1990s, FHWA and NCHRP have initiated several research projects with the goal of identifying such tests or procedures for inclusion in the Superpave volumetric mix design method.

The principal tool of volumetric mix design is the Superpave gyratory compactor (SGC). A satisfactory mix design is one that meets rigorous volumetric requirements at initial and design levels of gyration (N_{ini} and N_{design}, respectively); these levels are, in turn, determined by the total traffic, expressed in ESALs, expected on the pavement over its projected service life (usually 20 years). Intuitively, then, properties of the SGC densification curve are believed to correlate in some manner with pavement performance and, in particular, permanent deformation, but the property-performance relationship has not been quantified.

Under NCHRP Project 9-16, "Relationship Between Superpave Gyratory Compaction Properties and Permanent Deformation of Pavements in Service," the Asphalt Institute was assigned the tasks of (1) determining the relationship between hot mix asphalt (HMA) properties measurable during Superpave gyratory compaction and per-

[1] *The Superpave Mix Design Manual for New Constructions and Overlays*, Report SHRP-A-407, Strategic Highway Research Program, National Research Council, Washington, DC (1994).

manent deformation of pavements in service and (2) recommending any practical modifications to existing SGCs, test methods, or both, to measure the identified properties. The research team (1) conducted a literature review to determine which, if any, gyratory compaction parameters have been related to HMA performance; (2) analyzed compaction data from laboratory and field studies to identify candidate parameters most likely to correlate with actual HMA field performance; and (3) carried out a statistically designed program of laboratory testing to validate these parameter-performance relationships with the goal of identifying one suitable for use with the Superpave volumetric mix design procedure. Emphasis was placed on parameters derivable from unmodified, commercially available SGCs meeting the requirements set out in AASHTO T312. However, as noted above, the research team was given the latitude to examine *practical* modifications to such SGCs (for example, the addition of an externally mounted sensor) or to the compaction procedure (for example, a change in the angle of gyration) if they were judged likely to produce a useful mix design tool.

Of the candidate SGC parameters identified through the literature review and survey of research results, the one that offered the greatest early promise was *k x AV*, the product of the compaction slope and the percent air voids. However, the laboratory testing program failed to validate the general utility of this parameter for mixes from several field projects, including NCHRP Project 9-7, the 1992 LTPP SPS-9 pilot projects, the WesTrack experiment, and several LTPP GPS projects used in the original development of the SGC N_{design} levels in the SHRP Asphalt Research Program.

The research team then tested a second good candidate, $N\text{-}SR_{max}$, the number of gyrations at maximum stress ratio. The team found that $N\text{-}SR_{max}$ was capable of correctly grouping laboratory mixes with good, fair, and poor expected rutting resistance and that this finding was reasonably validated by the data from the field projects described above. The parameter is directly obtainable from any commercial SGC capable of measuring shear stress during compaction; for compactors not meeting this criterion, the use of an auxiliary external device, such as the Gyratory Load Cell Plate Assembly developed by the University of Wisconsin, may produce acceptable results.

The research results suggest that the $N\text{-}SR_{max}$ provides a rapid means of identifying gross HMA mix instability or rutting potential during volumetric mix design. Thus, it can serve as a useful screening or indicator parameter; it is not, however, a fundamental material property for predicting the development of permanent deformation. Moreover, although $N\text{-}SR_{max}$ is reasonably sensitive to aggregate structure and binder volume, it cannot detect the effect of changes in asphalt binder stiffness (i.e., the performance grade of the asphalt binder) on mix stability. The research team has also prepared a draft test method in AASHTO standard format for screening HMA mix designs for gross mix instability by measurement of $N\text{-}SR_{max}$ during compaction with the SGC.

The final report includes a summary of the literature review, a detailed description of the experimental program, a discussion of the research results, and six supporting appendixes:

- Appendix A: NCHRP 9-7 Field Projects;
- Appendix B: Additional Details from LPI Experiment;
- Appendix C: Experiment Evaluating the Effect of Binder Stiffness on SGC Properties;
- Appendix D: Draft AASHTO Procedure for Estimating the Rutting Performance of Asphalt Mixtures Using Shear Stress Measurements During Compaction in the Superpave Gyratory Compactor;
- Appendix E: Literature Review Summaries; and
- Appendix F: Task 2 Data Sheets.

This published report includes the main text and Appendix D; the other appendixes are available on request from NCHRP. The entire contractor's final report is also planned for publication in the CRP CD-ROM Bituminous Materials Research Series. The research results and the draft test method have been referred to the TRB Mixtures and Aggregate Expert Task Force Group for its review and possible recommendation to the AASHTO Highway Subcommittee on Materials for action.

CONTENTS

AUTHOR ACKNOWLEDGMENTS

The research reported herein was performed under NCHRP Project 9-16 by the Asphalt Institute (Lexington, Kentucky), the University of Kentucky (Lexington, Kentucky), Worcester Polytechnic Institute (Worcester, Massachusetts), and Frankfort Testing Laboratory (Frankfort, Kentucky). The Asphalt Institute was the contractor for this study. The work performed at the University of Kentucky, Worcester Polytechnic Institute, and Frankfort Testing Laboratory was under subcontracts with the Asphalt Institute.

R. Michael Anderson, Director of Research, was the principal investigator for the Asphalt Institute. Also contributing to the research from the Asphalt Institute were Robert L. Peterson, Asphalt Materials Engineer; Pamela A. Turner, Asphalt Materials Engineer; Dwight E. Walker, Associate Director of Research and Technical Services; Dr. John Haddock, District Engineer (currently Professor of Civil Engineering, Purdue University); Gary Irvine, Asphalt Materials Technologist; Mark Beavin, Asphalt Materials Technician; and Shay Emmons, Asphalt Materials Technician.

Dr. Kamyar C. Mahboub, Associate Professor of Civil Engineering, directed the work at the University of Kentucky.

Dr. Rajib B. Mallick, Assistant Professor of Civil Engineering, directed the work at Worcester Polytechnic Institute.

R. Scott Quire, Lab Manager and Testing Engineer, directed the efforts at Frankfort Testing Laboratory.

Also contributing to this research were Mr. Mike Butcher, Supervising Asphalt Scientist for the South Australia Department for Transport, and Dr. Dennis Smith, Statistical Consultant.

RELATIONSHIP OF SUPERPAVE GYRATORY COMPACTION PROPERTIES TO HMA RUTTING BEHAVIOR

SUMMARY

At the time the NCHRP Project 9-16 research was initiated, the Superpave mix design procedure did not include any testing to evaluate a design asphalt mixture for adequate resistance to permanent deformation. This gap in the Superpave mix design process was originally intended to be filled by the advanced performance tests and analyses developed during the Strategic Highway Research Program (SHRP). Unfortunately, the cost of purchasing a Superpave shear tester to validate asphalt mixture performance and the experience required to execute the tests and perform the associated analyses were prohibitive. Without performance-related tests, users became increasingly uncomfortable relying strictly on mixture volumetric properties and component material requirements. Consequently, many state agencies began using supplemental tests, such as loaded wheel tests, to complement the Superpave material selection and mix design process.

The common problem with most performance tests has been the cost of the test devices. A commercially available, loaded wheel test device may cost as much as $80,000. Scaled-down versions of the Superpave shear tester may range in cost from $75,000 to $100,000. Although research is not complete, it appears likely that the cost of test equipment needed to perform axial testing (e.g., dynamic complex modulus and repeated load axial tests) may approach $50,000. These tests also require well-trained, experienced personnel to execute the testing and analyze the results properly.

The NCHRP 9-16 project was developed to determine if a relationship can be identified relating permanent deformation resistance to some compaction parameters generated during compaction of an asphalt mixture specimen in the Superpave gyratory compactor (SGC). The benefits of such a relationship are clear. In addition to savings in cost and complexity, an SGC compaction parameter related to permanent deformation resistance would provide a relatively quick response compared with most performance-related tests, thus permitting use of the parameter in a quality control (QC) environment and thereby minimizing the probability for placement of poorly designed or produced asphalt mixture placed on the road.

The NCHRP Project 9-16 research evaluated several compaction parameters that could be obtained without modification of either the SGC equipment or compaction procedure. An initially promising parameter meeting these qualifications was the product

of compaction slope and the percentage air voids ($k \times AV$). This parameter better accounted for the volume of asphalt binder in a mixture than compaction slope by itself.

Although the $k \times AV$ parameter indicated some relationship with mixture stiffness, it did not appear as promising as another parameter identified during the laboratory experiments. The number of gyrations at which the maximum shear stress occurred during compaction (identified as $N\text{-}SR_{max}$ in the report) appeared capable of correctly grouping mixtures with good, fair, and poor expected rutting resistance. The findings of the laboratory experiment were reasonably validated using mixtures from several actual projects, including the Long-Term Pavement Performance (LTPP) SPS-9 mixtures, General Paving Studies (GPS) mixtures used in the SHRP experiments, and WesTrack mixtures.

The $N\text{-}SR_{max}$ parameter was measured in this research using a modified version of the AFG1 SGC produced by Pine Instruments. However, the parameter should be available from any SGC capable of measuring shear stress during compaction. For those compactors without the capability to measure shear stress, the use of an external device, such as the Gyratory Load Cell Plate Assembly (GLPA) developed at the University of Wisconsin—Madison, may be capable of producing similar information.

The advantage of using the $N\text{-}SR_{max}$ parameter as a rapid method of identifying gross mixture instability or rutting potential is that it is information that can be obtained immediately following compaction. An experienced asphalt mixture technologist should be able to recognize within 10 min after loading the SGC mold whether or not an asphalt mixture sample will have unacceptable rutting potential. As such, the $N\text{-}SR_{max}$ parameter serves as a screening, or indicator, parameter to identify when further performance-related testing is needed.

One of the disadvantages of the $N\text{-}SR_{max}$ parameter identified by the research is that it is not able to identify the effects of asphalt binder stiffness (or performance grade [PG]) on the rutting potential of an asphalt mixture. The parameter apparently only indicates aggregate structure and asphalt binder volume effects. In other words, an increase in rounded aggregates or asphalt binder content probably can be identified by the $N\text{-}SR_{max}$ parameter, but changing from a PG 76-22 binder to a PG 64-22 binder cannot. This limitation may decrease the usefulness of the $N\text{-}SR_{max}$ parameter for some users.

There are several implementation issues with the $N\text{-}SR_{max}$ parameter. The principal one is that there are currently few models of SGCs with the capability of measuring shear stress during compaction. Retrofitting of existing equipment, redesign of new equipment, and adaptation of the GLPA for use in other SGCs are all options for the user to obtain the $N\text{-}SR_{max}$ parameter.

Although the research indicated that the $N\text{-}SR_{max}$ parameter has potential as a rapid indicator of asphalt mixture rutting potential, further validation with a wide variety of mixture types and users is needed to confirm or reject its general use as a tool for mix design and QC operations. The $N\text{-}SR_{max}$ parameter is not intended to serve as a replacement for performance-related testing. The parameter can serve as a relatively simple, inexpensive, and rapid indicator of expected mixture performance. The $N\text{-}SR_{max}$ parameter is a useful tool for asphalt technologists involved in mix design and quality control to minimize the incidence of rutting-susceptible asphalt mixture being placed on the roadway.

CHAPTER **1**

INTRODUCTION AND RESEARCH APPROACH

Superpave mix design is based on (1) properties of the asphalt binder and aggregate and (2) volumetric properties of hot mix asphalt (HMA). The characteristics of the densification curve obtained during gyratory compaction of HMA are believed to be related to the strength of the aggregate skeleton. The strength of the aggregate skeleton can give an indication of the asphalt mixture strength and, consequently, the expected pavement performance. As such, many asphalt technologists believe that SGC data can be used to evaluate asphalt mixture strength properties.

The SGC operates by applying constant conditions of vertical pressure (600 kPa), angle of gyration (1.25 deg), and rotational speed (30 rpm) to an asphalt mixture during the compaction process. The SGC operates differently from other compaction devices in several respects. First, the ability to monitor change in specimen height during compaction is a feature shared only by the Corps of Engineers Gyratory Test Machine (GTM). The Marshall, Hveem (kneading), and Texas gyratory compaction processes do not have this ability. For these three compaction methods, measurement of mixture properties occurs only at the end of the compaction process. The user has no indication in the Marshall and Hveem compaction processes how rapidly the density of the asphalt mixture changes during compaction. In the Texas gyratory compaction process, however, an experienced technologist may have an indication as to how rapidly the mixture is compacting, based on the number of three-gyration "bursts" required to reach the end-point condition. Still, there is no measurement associated with this compaction procedure.

Another major difference between the SGC procedure and the Marshall and Hveem compaction procedures is in the compaction effort applied to the asphalt mixture specimen. In the Marshall procedure, a fixed amount of energy is imparted into the asphalt mixture specimen through impact compaction. A 4.5-kg (10-lb) sliding weight falls through a distance of 0.45 m (18 in.) and impacts the face of the asphalt mixture specimen, generating approximately 20 J (15 ft-lb) of energy per blow. The compaction process will generate a fixed amount of compaction energy (3 kJ or 2,250 ft-lb for a 75-blow Marshall design) imparted to the specimen during the compaction process. The same is true of the Hveem compaction procedure where a specified number of tamps is used with a specified pressure. For these devices, the stiffness of the asphalt mixture has a significant effect on the densification of the mixture. For example, a stiff asphalt mixture (i.e., good aggregate skeleton and/or low asphalt content) may compact to 4% air voids at the end of the compaction process, while a weak asphalt mixture (i.e., poor aggregate skeleton and/or high asphalt content) may compact to 2% air voids with the same compaction effort.

By contrast, the SGC applies a constant amount of shear strain to the specimen, regardless of the mixture stiffness. The energy input to the specimen is not constant, but increases with stiffer asphalt mixtures to permit a constant shear strain to create compaction. As a consequence, the rate of compaction in the SGC is very much related to the aggregate characteristics (i.e., gradation, particle shape, and texture). At high compaction temperatures (135°C), the aggregate contributes greatly to the mixture strength, while the asphalt binder contributes little. As an example, research performed at the Asphalt Institute indicated that the shear stiffness of a specific asphalt mixture was 3,000 kPa at 70°C. By contrast, the shear stiffness of the asphalt binder used in the mix was approximately 3 kPa at the same temperature. This indicates that the stiffness of the asphalt mixture, measured in the linear viscoelastic region, is dominated by the aggregate structure. This also explains why the SGC indicates no apparent sensitivity of mixture density to changes in compaction temperature (because aggregate, which dominates compaction rate, is practically insensitive to temperature changes) as suggested by previous research *(1)*. Research, completed at the University of Wisconsin—Madison as part of NCHRP Project 9-10, validates these findings. A change in asphalt stiffness of two orders of magnitude (2 Pa-s to 200 Pa-s) resulted in no significant change in the asphalt mixture density through the SGC *(2)*.

That aggregate characteristics, rather than asphalt binder characteristics, dominate the rate of compaction in the SGC is evident in *Strategic Highway Research Program (SHRP) Report A-407 (3)* where the Superpave mix design procedure recommends horizontally shifting compaction curves from trial gradations to estimate properties at the design asphalt binder content. In the Superpave mix design process, little difference exists in the compaction slope for different asphalt binder contents with the same aggregate structure. The compaction curves are very close to being parallel lines when plotted on a semi-logarithmic graph. An example is presented in

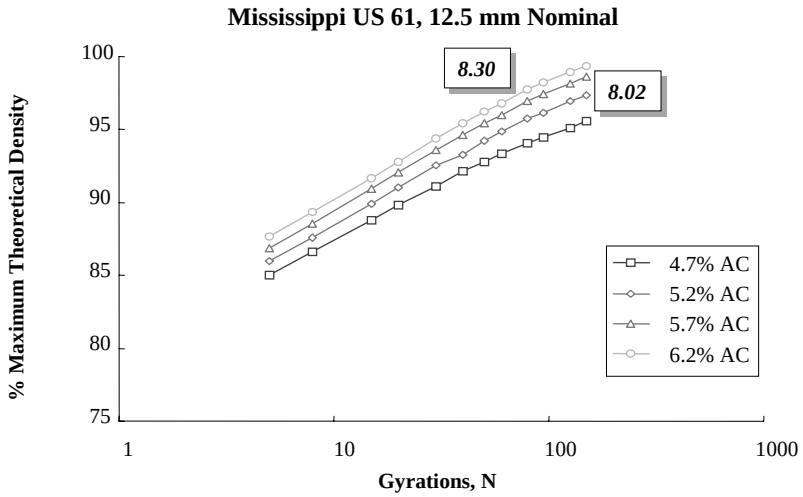

Figure 1. Effect of asphalt binder content on compaction slope.

Figure 1. Figure 2 presents the compaction slopes of different gradations of the same aggregate. In the SHRP A-407 report, compaction slope is calculated as follows:

$$\text{Compaction slope} = 100 * \frac{C_{des} - C_{ini}}{\log(N_{des}) - \log(N_{ini})}$$

where C_{des} and C_{ini} are the levels of compaction achieved (density) at the design number of gyrations (N_{des}) and initial number of gyrations (N_{ini}), respectively.

As noted in Figure 2, finer gradations tend to have lower compaction slopes. More rounded aggregates, or those with less internal friction, also tend to produce lower compaction slopes. This is illustrated in Figure 3 where the aggregate gradations are similar for the two mixtures, but one gradation uses uncrushed river gravel (compaction slope of 6.14) and the other uses crushed limestone (compaction slope of 8.84).

Some previous research has attempted to correlate mixture stiffness properties (or permanent deformation resistance) to compaction slope in the SGC with mixed results. In a study involving Watsonville Granite *(4)*, some differences were noted in the mixture's shear stiffness and development of permanent shear strain as compaction slope changed. These results are presented in Figure 4. Unfortunately, although the trends matched expectations (i.e., higher compaction slope mixtures had higher shear stiffness and lower permanent shear strain), the differences between the mixture properties were not as great as expected for the wide range in compaction slopes.

Testing performed as part of the NCHRP 9-7 project also indicated some relationship between compaction slope and

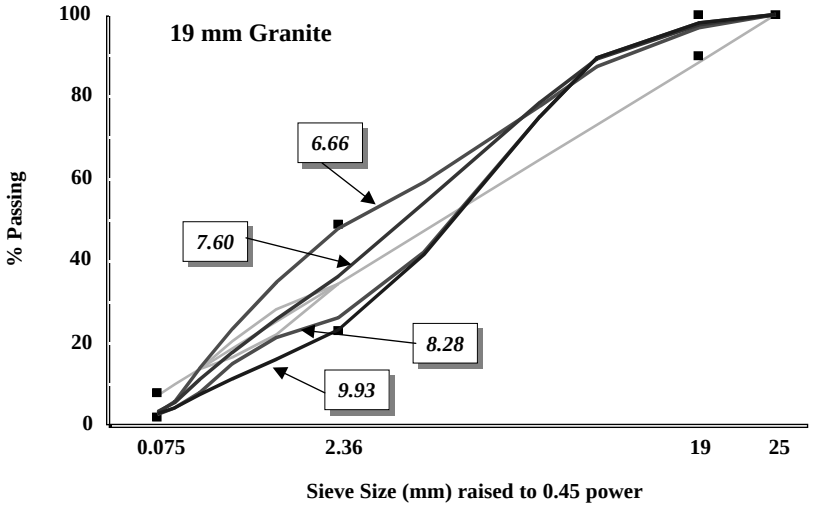

Figure 2. Effect of aggregate gradation on compaction slope.

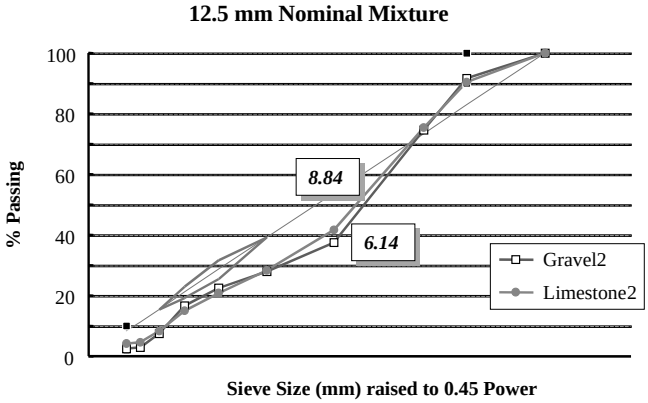

Figure 3. Effect of aggregate type (angularity) on compaction slope.

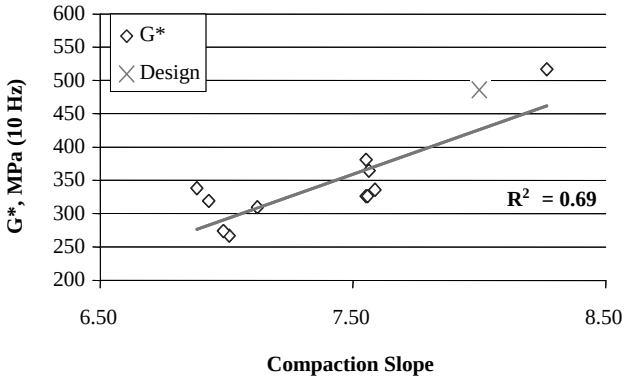

Figure 5. Relationship between shear stiffness and compaction slope—Mississippi US-61, 12.5 mm mixture.

mixture stiffness for a mixture placed on Mississippi US 61 in 1994. The results, presented in Figure 5, are from QC testing performed by the Asphalt Institute in support of the NCHRP 9-7 research *(5)*.

Repeated shear testing was also performed by the Asphalt Institute on several asphalt mixtures from Northeast Texas *(6)*. The data in Figure 6 indicate a general trend to higher permanent shear strain as the percentage of sand is increased or as the compaction slope becomes smaller (i.e., flatter). These data are not conclusive, given that there are some outliers, but the general trend supports conventional expectations from experience.

Ultimately, the main problem in relating compaction slope to mixture performance properties is that the compaction slope, unlike mixture performance, is not sensitive to asphalt binder content. This was verified in the NCHRP 9-7 experiment, "Sensitivity of Superpave Mixture Tests to Changes in Mixture Components" *(7)*. This research indicated that paired blends with the same aggregate structure, but asphalt contents different by 1.0%, may have similar compaction slopes, but different mix properties. A good example is given by a comparison of Blends 4 and 12, which have the same aggregate structure, but different asphalt binder contents. An excerpt from the data is presented in Table 1.

Although the compaction slope, as typically calculated, is apparently not sensitive to asphalt binder properties, other SGC compaction parameters may provide a link with expected mixture performance.

ANTICIPATED RESEARCH RESULTS AND EXPECTED BENEFITS

A common problem with most performance tests proposed for the Superpave mix design method is the cost of the test devices. A commercially available, loaded wheel test device may cost as much as $80,000. Scaled-down versions of the Superpave shear tester (that were studied in NCHRP Project 9-18) may range in cost from $75,000 to $100,000. Of equal importance is that executing the testing and properly analyzing the results requires well-trained, experienced personnel.

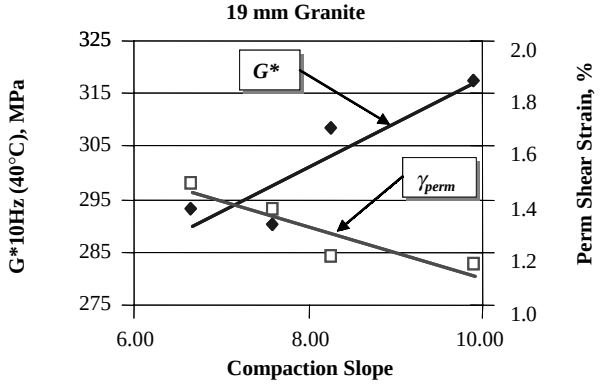

Figure 4. Relationship between high temperature mix properties and compaction slope.

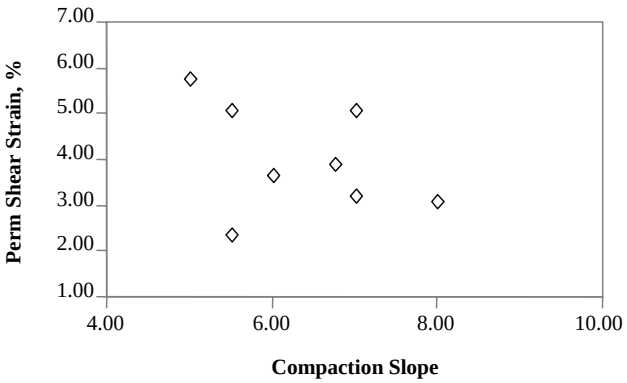

Figure 6. Relationship between shear strain and compaction slope—Texas mixtures.

TABLE 1 Data from NCHRP 9-7 field sensitivity experiment

Blend	Asphalt Content	Slope	Perm. Shear Strain	G^*_{10Hz} (26°C), MPa
4	4.2%	9.76	5.53%	907
12	5.2%	9.81	7.80%	862

If a relationship can be identified relating permanent deformation resistance to some compaction parameters generated during SGC compaction of an asphalt mixture specimen, then the benefits to the user should be clear. Test results would be relatively quick compared with most performance-related tests, thus permitting use of the parameter in a QC environment and thereby minimizing the probability of placing poorly designed or produced asphalt mix.

It was expected that the NCHRP Project 9-16 research would result in a new SGC parameter, measured during compaction, which relates to the asphalt mixture's resistance to rutting. It was envisioned that this parameter could be obtained with little or no modification to existing SGC devices. Consequently, it was expected that users would be able to estimate the rutting resistance of an asphalt mixture without adding significant cost to the laboratory or increasing testing time. In the best-case scenario, it was envisioned that an SGC parameter could be identified that was strongly related to the rutting potential of an asphalt mixture, thus alleviating the need for a simple performance test. The more likely scenario for the research was that some SGC parameter could be identified that was capable of identifying mixture instability that could lead to catastrophic rutting failures.

PROJECT OBJECTIVES

The primary objectives of this project were to do as follows:

- Determine the relationship between mix properties measurable during Superpave gyratory compaction and permanent deformation of pavements in service; and
- Recommend any practical modifications to existing Superpave gyratory compactors, test methods, or both, to measure the identified properties.

RESEARCH APPROACH

The general approach of the NCHRP Project 9-16 research was as follows:

1. Conduct a literature review to determine if any compaction parameters from the SGC (or similar compaction equipment) have been related to asphalt mixture performance.
2. Analyze all of the existing parameters currently available from the SGC compaction curve (principally compaction slope) and relate the individual parameters to performance properties of the asphalt mixture (using laboratory testing and, preferably, field performance data).
3. If tentative relationships are identified, then validate the relationships with a statistically designed laboratory experiment. This is an important part of the research because none of the research referenced earlier focused on compaction slope as a primary response variable. In most cases, compaction parameters were merely collateral information.
4. If no strong relationship is identified between performance and compaction slope, explore SGC compaction parameters from alternative approaches such as measuring the inclination force required to create a constant angle of gyration, calculation of shear stress by moment *(8)*, calculation of gyratory ratio *(9)*, and calculation of compaction energy and traffic densification indexes *(10)*. If these approaches are followed, it is likely that some modification of the SGC will be required to execute the research. Validate the alternative approach or approaches with a statistically designed laboratory experiment.
5. Recommend SGC parameters related to expected mixture performance for permanent deformation.
6. Recommend modifications, if necessary, to the SGC, or, indicate that no relationship exists between SGC compaction parameters and resistance to permanent deformation.

CHAPTER **2**

FINDINGS

LITERATURE REVIEW

The research team completed searches of the Transportation Research Information Services (TRIS), Compendex Plus, and Australian Road Research Board (ARRB) databases. Abstracts from papers and reports related to gyratory compaction and/or permanent deformation through 2000 were collected and summarized.

As expected, the literature search was limited by the fact that the Superpave gyratory compactor came into existence less than 10 years ago. Information on compaction properties from the SGC, particularly compaction slope, was not available in many papers. Reports by McGennis and Anderson at TRB in 1997 were some of the earliest papers reviewed that discussed compaction slope. SGC compaction properties, including compaction slope, are discussed also in the reports of NCHRP Projects 9-7 (Field Procedures and Equipment to Implement SHRP Asphalt Specifications) and 9-9 (Refinement of the Superpave Gyratory Compaction Procedure).

A list of the key concepts and findings of some of the previous papers is provided in Table 2.

The literature review was subdivided into three general categories:

- Papers or reports with conventional SGC compaction slope included,
- Papers or reports with alternative SGC compaction properties, and
- Papers or reports involving shear measurements of asphalt mixtures during compaction.

In the first category (SGC Compaction Slope), papers by McGennis *(6),* Anderson and Bahia *(4),* Anderson et al. *(5, 7),* Langlois and Beaudoin *(11),* and Tarn et al. *(12)* indicate some relationship between compaction slope and aggregate type or gradation. The papers also indicate little effect of asphalt binder stiffness or volume on SGC compaction slope. This finding is also confirmed by some of the NCHRP Project 9-9 research *(13).*

In the second category (Alternative SGC Compaction Properties), papers by Mallick *(9),* Bahia et al. *(10),* and Vavrik and Carpenter *(14)* provide some alternative methods for using the SGC compaction data. The procedures by Mallick *(9)* and Vavrik and Carpenter *(14)* rely on data from a small portion of the compaction curve. The procedure by Bahia et al. *(10)* relies on total area under the compaction curve.

In the third category (Shear Measurement of Mixtures During Compaction), papers by Butcher *(15),* West and Ruth *(16),* and Guler et al. *(17)* provide procedures for measuring the shear resistance of asphalt mixtures during compaction. The paper by West and Ruth uses the Corps of Engineers Gyratory Testing Machine (GTM) gyratory shear at 200 gyrations for stone mastic asphalt (SMA) mixtures. The paper by Butcher discusses use of maximum shear stress with the Servopac gyratory compactor. It notes that mixtures using softer asphalt binders appear to have lower maximum shear stresses than mixtures with harder asphalt binders. The paper by Guler et al. discusses development of a shear testing plate accessory that can identify reduction in shear resistance. Analysis indicates that mixtures with higher asphalt contents experience a collapse in shear resistance after a specified number of gyrations.

From the literature review, the research team assembled information useful in the execution of the research. The gyratory ratio (Mallick) and compaction energy (Bahia et al.) concepts were easily added to the analysis of existing SGC data. The effect of asphalt binder stiffness (Langlois and Beaudoin), asphalt binder volume (Anderson et al. *[7]* and Anderson et al. *[13]),* and sand percentage (McGennis *[6]*) aided in the development of the experimental plan for the laboratory experiment. Similarly, the shear testing plate (Guler et al.) and other shear measurements (Butcher, and West and Ruth) were considered for addition to the laboratory experiment.

ANALYSIS OF SGC COMPACTION PARAMETERS FROM EXISTING DATA

Before beginning a statistically designed laboratory experiment, it was necessary to analyze data from existing projects where the SGC was used for mix design or QC testing. The objective of this analysis was to identify whether any relationships exist between mix properties measured during compaction and permanent deformation in service for mixes meeting all Superpave volumetric requirements.

To accomplish the objective, projects were identified that have SGC compaction data and either actual performance

TABLE 2 Key concepts from literature review

Author	Year	Key Concept
West (*16*)	1995	Gyratory shear correlated with Hveem stabilometer for SMA
Moutier (*29*)	1996	Shear stress concepts discussed at international workshop
Hall (*30*)	1996	SGC compaction properties not influenced by mass below 3.5 kg
McGennis (*6*)	1997	Compaction slope lowered with increase in rounded, field sands
Anderson (*4*)	1997	Same aggregate; different gradations lead to different slope; similar mechanical properties
Vavrik (*14*)	1998	"Locking point" concept of SGC compaction
Habib (*31*)	1998	Kansas comparison of Marshall and Superpave compaction
Anderson (*7*)	1998	Binder content has little effect on compaction slope
Langlois (*11*)	1998	Binder has less influence on SGC properties than on LCPC rut tests
Butcher (*15*)	1998	Shear resistance measurements during compaction using Servopac
Bahia (*10*)	1998	Compaction energy concepts introduced; terminal densification index
Mallick (*9*)	1999	Gyratory ratio concepts introduced; GTM data included
Anderson (*5*)	1999	Increased compaction slope, increased mix stiffness (for one mix)
Guler (*17*)	2000	Development of shear testing plate for SGC
Tarn (*12*)	1998	Traditional mixes (poor performing) have lower slope than Superpave

data or expected performance data from laboratory tests. These projects consisted of the following:

- 1992 SPS-9(P) projects;
- NCHRP 9-7 (Field Procedures and Equipment to Implement SHRP) field projects;
- Accelerated Load Facilities and Test Tracks;
- SHRP Laboratory Experiments; and
- FHWA Pooled Fund Study 176.

Data from these projects were analyzed using the parameters identified in Table 3. All of the Table 3 parameters were obtained from the conventional SGC compaction data.

1992 SPS-9(P) Projects

Analysis of compaction data was conducted for the 1992 SPS-9(P) projects in Wisconsin (IH-94 and IH-43), Indiana (IH-65), and Maryland (IH-70). These four projects were the first projects designed using the Superpave mix design procedure. Because of the Asphalt Institute's involvement in the SHRP A-001 contract, the Asphalt Institute conducted mix design and field production testing on each of the project mixtures. In addition, some accelerated performance testing was conducted on the field-produced asphalt mixture samples *(18)*. Finally, a site survey was conducted in 1998 by Asphalt Institute staff to assess pavement condition.

Individual densification data and analysis for each surface mixture were examined and are summarized in Table 4. Figures 7 through 10 illustrate the data in Table 4 as a function of a rutting rate parameter (mm/ESAL$^{1/2}$).

The data in Table 4 and Figures 7 through 10 indicate some relationship between the selected parameter and the rutting rate of the 1992 SPS-9(P) surface mixtures. In Figures 7 through 9, the Maryland IH-70 surface mixture does not follow the expected trend. In Figure 10, the Indiana IH-65 surface mixture does not follow the expected trend.

TABLE 3 Response parameters from conventional SGC compaction data

Parameter	Abbr.	Description
Compaction Slope (Linear)	k	
C_1 Intercept (Linear)	C_1	
Compaction Slope (Power Exponent)	b	Power Law: $y=ax^b$
C_1 Intercept (Power)	a	Power Law: $y=ax^b$
Number of Gyrations to 92% Density	N_{92}	
Number of Gyrations to 95% Density	N_{95}	
Number of Gyrations to 96% Density	N_{96}	
Number of Gyrations to 98% Density	N_{98}	
Ratio of N_{95} to N_{92}	N_{95}/N_{92}	
Ratio of N_{98} to N_{95}	N_{98}/N_{95}	
Ratio of N_{98} to N_{96}	N_{98}/N_{96}	
Compaction Energy Index from C_1 to 92%	CEI_{92}	
Compaction Energy Index from N_{ini} to 92%	$CEI_{Nini-92}$	
Densification Energy Index from 92% to 96%	DEI_{92-96}	
Terminal Densification Index from 96% to 98%	TDI_{96-98}	
Terminal Densification Index from 92% to 98%	TDI_{92-98}	

TABLE 4 Summary of densification data from 1992 SPS-9 surface mixtures

Project	Wisconsin IH-94	Wisconsin IH-43 (PG 3-4)	Indiana IH-65	Maryland IH-70
Design Traffic (20-yr ESAL)	24,640,000	11,921,000	55,000,000	11,340,000
Accum. Traffic (ESAL)	7,392,000	3,576,300	16,500,000	3,402,000
Rut Depth, mm	2	2	5	6
Rutting Rate (mm/ESAL$^{1/2}$)	0.00074	0.00106	0.00123	0.00325
Compaction Slope				
Conventional Semi-Log (N_{des})	9.525	7.833	7.317	7.883
Conventional Semi-Log (Regr.)	9.452	7.541	6.958	7.689
Exponent (b) from Power Law	0.0454	0.0352	0.0334	0.0361
Power Law Slope at N_{des}	0.0428	0.0339	0.0313	0.0346
Gyrations for Target Density				
N_{92}	58	27	60	29
N_{95}	117	67	157	63
N_{96}	148	90	214	81
N_{98}	232	162	398	135
Gyratory Ratio				
N_{96}/N_{92}	2.55	3.35	3.58	2.83
N_{98}/N_{95}	1.98	2.42	2.54	2.14
N_{98}/N_{96}	1.57	1.80	1.85	1.66
$Log(N_{96})/Log(N_{92})$	1.23	1.37	1.31	1.31
$Log(N_{98})/Log(N_{95})$	1.14	1.21	1.18	1.18
$Log(N_{98})/Log(N_{96})$	1.09	1.13	1.12	1.11
Energy Indices				
CEI_{92}	667	190	529	239
$CEI_{Nini-92}$	206	151	371	122
DEI_{92-96}	91	79	201	58
TDI_{96-98}	616	148	491	191
TDI_{92-98}	636	517	1,304	393

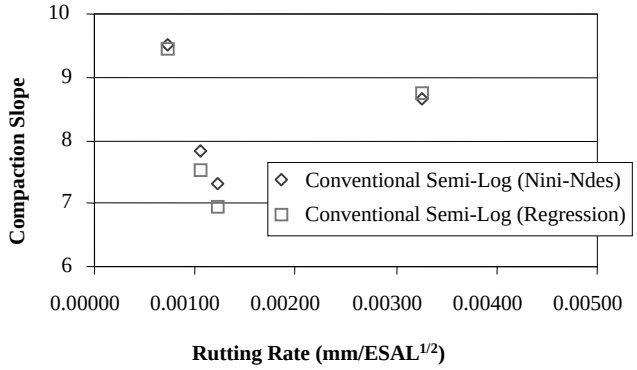

Figure 7. Conventional compaction slope for 1992 SPS-9(P) mixtures.

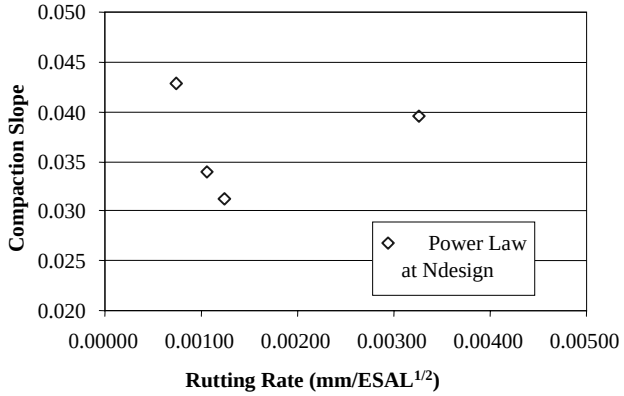

Figure 8. Compaction slope (power law) for 1992 SPS-9(P) mixtures.

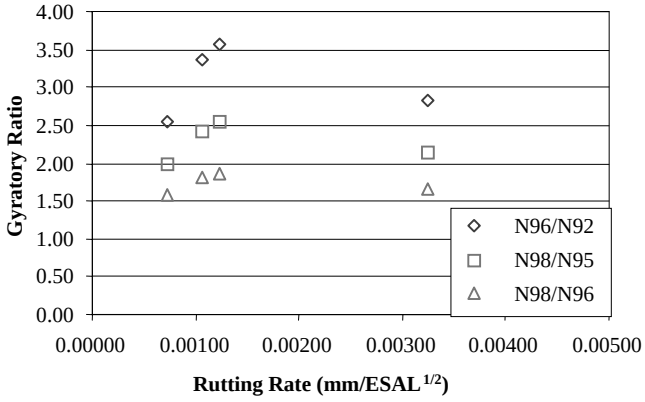

Figure 9. Gyratory ratios for 1992 SPS-9(P) mixtures.

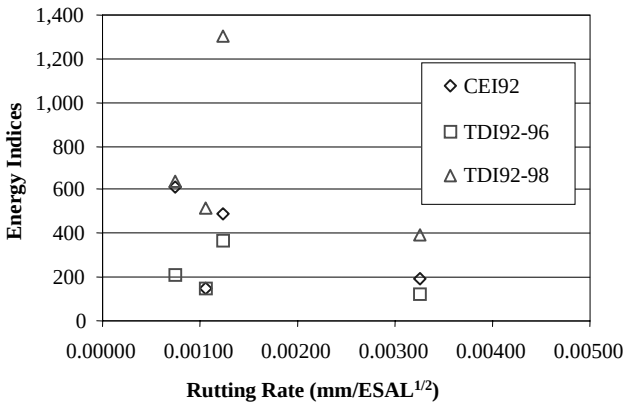

Figure 10. Calculated energy indices for 1992 SPS-9(P) mixtures.

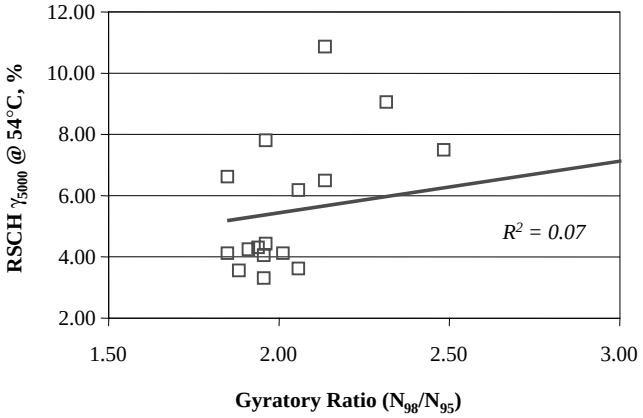

Figure 12. Relationship between calculated gyratory ratio and permanent shear strain for NCHRP Project 9-7.

NCHRP 9-7 Field Sensitivity Experiment

Data were analyzed from the NCHRP Project 9-7 field sensitivity experiment *(19).* This experiment was a half-factorial (2^5 design) with variables, including asphalt binder content, fine gradation (minus 0.3-mm), coarse gradation (plus 4.75-mm), intermediate gradation, and natural sand content. Low and high levels of each variable were assigned to create 16 different mixtures, in addition to the control (baseline) mixtures. The high level of asphalt binder content was 1.0% higher than the low level. The high natural sand blends had 20% natural (river) sand and 12% crushed limestone fine aggregate. The low natural sand blends had 0% natural sand and 32% crushed limestone fine aggregate.

All 17 mixtures were tested using the shear frequency sweep at constant height test (FSCH) to establish mixture stiffness and the repeated shear test at constant height (RSCH) to establish mixture rutting potential *(20).* Figures 11 through 13 represent the relationship between the permanent shear strain at 5,000 loading cycles (γ_{5000}) from the RSCH and the various SGC parameters.

Figures 11 through 13 do not indicate any strong relationships between permanent shear strain from the RSCH and the SGC parameters. The best R^2 value is only 0.32, although all of the trendlines appear to follow the correct direction hypothesized for each parameter (i.e., increased shear resistance with increased energy index or decreased shear resistance with decreased gyratory ratio). Of the three figures, the relationship between shear resistance and energy indexes (Figure 13) appears to provide the best relationship (although weak).

Figure 11 illustrates one of the problems with the use of the conventional SGC compaction slope. Asphalt binder content apparently does not significantly affect compaction slope *(21),* but does affect permanent shear strain. To account for the effects of asphalt binder content, it was hypothesized that a parameter involving either the percentage of air voids (AV) or the percentage of voids filled with asphalt (VFA) was necessary. To explore this concept, the compaction slope was multiplied by the percentage of air voids (expressed as 4.2 rather than 0.042) for the field sensitivity mixtures. The result is illustrated in Figure 14.

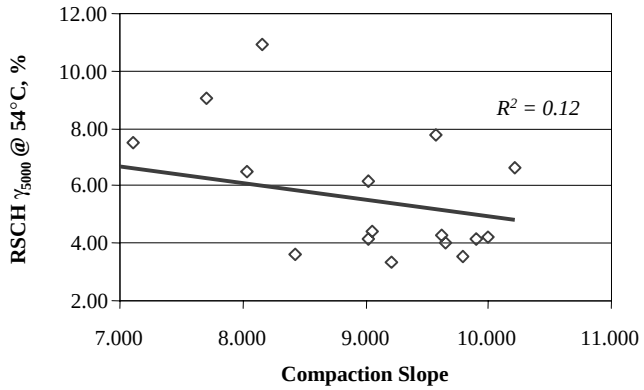

Figure 11. Relationship between compaction slope and permanent shear strain for NCHRP Project 9-7.

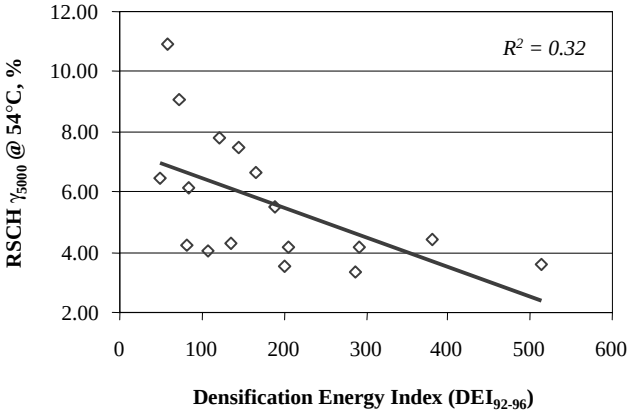

Figure 13. Relationship between $DEI_{92\text{-}96}$ and permanent shear strain for NCHRP Project 9-7.

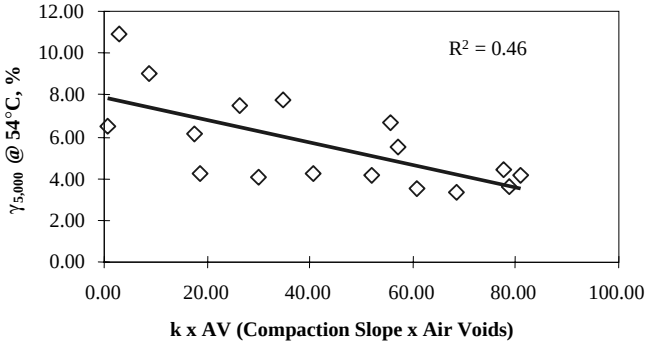

Figure 14. Relationship between the product of compaction slope and voids and permanent shear strain for NCHRP Project 9-7.

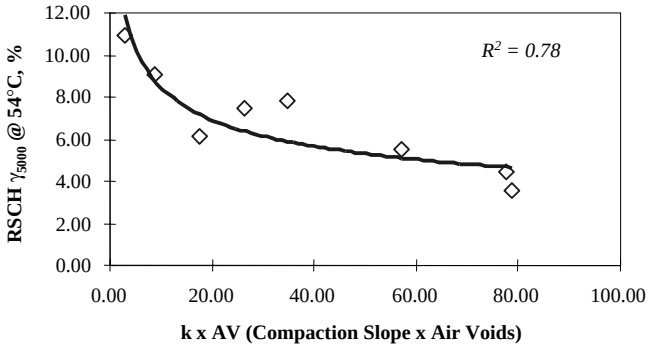

Figure 16. Relationship between the product of compaction slope and voids and permanent shear strain for the high sand blends for NCHRP Project 9-7.

The product of compaction slope and percentage of air voids significantly improved the relationship (from $R^2 = 0.12$ to $R^2 = 0.46$), but it was still not a good correlation. Upon examination of the data and the correlation equation, six blends were identified that provided the worst fit. Further analysis indicated that, for five of the six blends, natural sand content appeared to cause the measured permanent shear strain to be different from that calculated with the equation. In each of the five cases, higher natural sand resulted in worse permanent shear strain than predicted by the equation using the interaction of compaction slope and percentage of air voids. Conversely, lower natural sand resulted in better permanent shear strain than accounted for in the equation using the interaction of compaction slope and percentage of air voids. Only Blend 3 did not follow this trend. Separating the data between blends with high natural sand contents and low natural sand contents yielded the data illustrated in Figures 15 and 16.

The separation of the natural sand contents significantly improve the relationships between permanent shear strain in the RSCH test and the product of compaction slope and percentage of air voids. The low sand blends have an R^2 value of 0.85 with Blend 3 removed as an outlier. The high sand blends have an R^2 value of 0.78. Figure 17 represents a combination of Figures 15 and 16.

Figure 17 indicates that the high sand blends appear to be more sensitive to changes in the product of compaction slope and air voids ($k \times AV$) than the low sand blends. At high values of $k \times AV$, the shear resistance of the blends are comparable. As the value of $k \times AV$ decreases, the shear resistance of the high sand blends becomes significantly worse than the low sand blends. This indicates that the combination of high sand content and high asphalt binder content (or a high percentage of voids filled with asphalt binder) may significantly degrade an asphalt mixture's shear resistance.

Figures 18 and 19 duplicate Figures 12 and 13 with the blends separated. Figure 20 illustrates the relationship between permanent shear strain and terminal densification energy index ($TDI_{92\text{-}98}$).

Figure 18 does not indicate any better relationship with the sand content of the blends separated into low and high blends. However, Figures 19 and 20 indicate a significant improvement in correlation between permanent shear strain and the densification energy indexes.

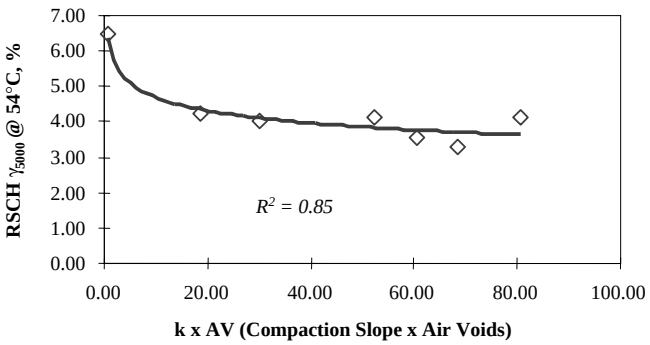

Figure 15. Relationship between the product of compaction slope and voids and permanent shear strain for the low sand blends for NCHRP Project 9-7.

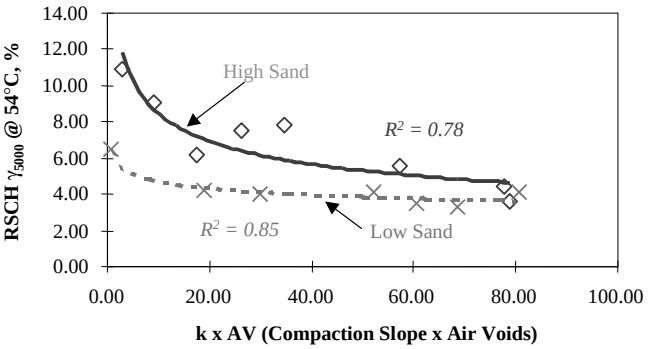

Figure 17. Relationship between the product of compaction slope and voids and permanent shear strain for NCHRP Project 9-7.

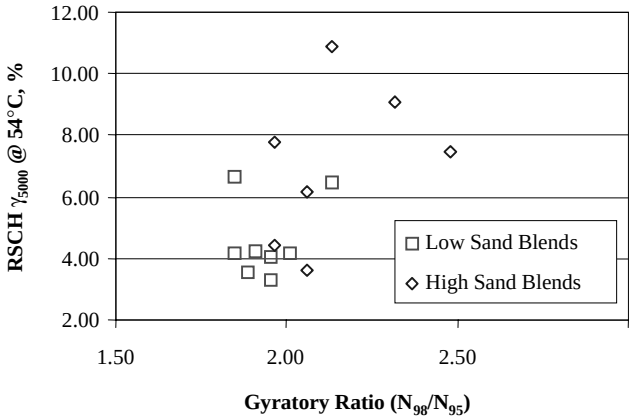

Figure 18. Relationship between calculated gyratory ratio and permanent shear strain (with sand percentage separated) for NCHRP Project 9-7.

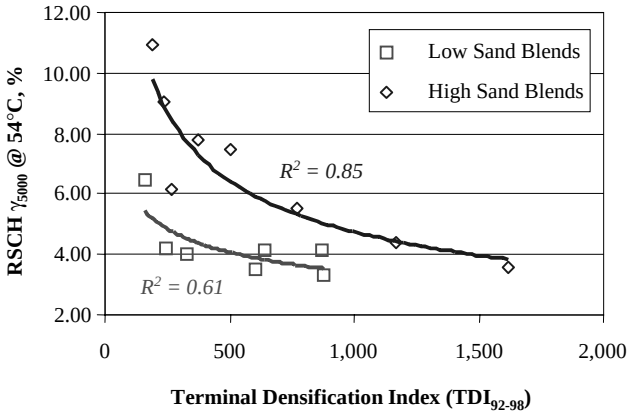

Figure 20. Relationship between $TDI_{92\text{-}98}$ and permanent shear strain (with sand percentage separated) for NCHRP Project 9-7.

Based on analysis of the NCHRP Project 9-7 field sensitivity experiment data, combining compaction slope and percentage of air voids appears to provide a better correlation with rutting susceptibility than compaction slope alone. This combined term allows for the effect of asphalt binder to be considered.

The data from the field sensitivity experiment also favor the use of a densification energy index ($DEI_{92\text{-}96}$). Both the $DEI_{92\text{-}96}$ and $TDI_{92\text{-}98}$ correlated well with permanent shear strain.

1992 SPS-9 Mixtures—Continuing Analysis

The review of the 1992 SPS-9 data indicated that the one outlier that did not indicate a good relationship between compaction slope and actual rutting was the Maryland IH-70 data point. These data indicated a relatively high compaction slope with the highest rutting rate. Field QC data indicated that the Maryland IH-70 mixture had an average percentage of air voids of less than 1.0% at N_{design}. Combining the percentage of air voids with the compaction slope into the $k \times AV$ parameter resulted in the data in Figure 21.

The product of compaction slope and percentage of air voids results in a significant improvement in correlation for the 1992 SPS-9 mixtures. Even though there are only four data points, there is an apparent trend to higher rutting rates as the product of compaction slope and air voids decreases.

NCHRP 9-7 Projects

Seven field projects from the NCHRP 9-7 research project were evaluated to assess the relationship between conventional SGC compaction parameters ($k \times AV$ and $TDI_{92\text{-}98}$) and either actual rutting performance or estimated rutting performance from mechanical property tests conducted in the laboratory. These projects consisted of the following:

- Kentucky IH-64/75;
- Mississippi US-61;

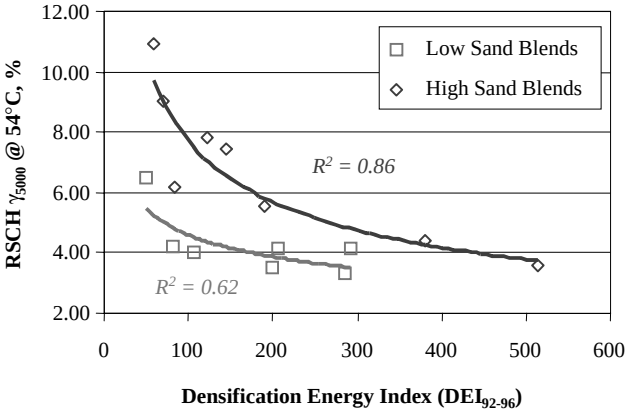

Figure 19. Relationship between $DEI_{92\text{-}96}$ and permanent shear strain (with sand percentage separated) for NCHRP Project 9-7.

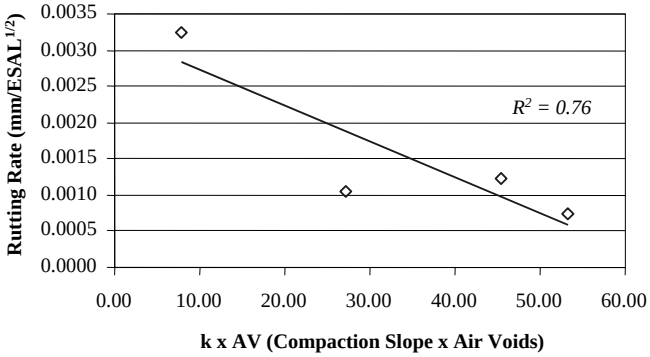

Figure 21. Relationship between rutting rate of 1992 SPS-9 mixtures and the product of compaction slope and voids ($k \times AV$).

- Florida US-301;
- Kansas IH-70;
- Maryland IH-68;
- Maryland US-40; and
- Kentucky SR-676.

Analysis of the Kentucky IH-64/75 project indicated that, contrary to expectations, the product of compaction slope and percentage of air voids ($k \times AV$) and $TDI_{92\text{-}98}$ were much lower than the Indiana IH-65 project (SPS-9 project), even though the actual field performance (i.e., rutting rates of 0.00119 and 0.00123, respectively) and laboratory high-temperature shear stiffness (i.e., 376 and 371 MPa, respectively) were similar.

Analysis of the Mississippi US-61 project indicated that the mix design samples exhibit a decrease in shear stiffness as the $k \times AV$ and $TDI_{92\text{-}98}$ values decrease. Compacted specimens from plant-produced mixture do not indicate a significant relationship between shear stiffness and SGC compaction parameters. The rutting performance of the mixture has been reported as good. The average mixture shear stiffness is comparable (342 MPa) with the Indiana IH-65 and Kentucky IH-64/75 mixtures (i.e., 371 and 376 MPa, respectively), which have indicated low rutting rates.

Analysis of the Florida US-301 project indicated that the mix design samples exhibit a decrease in shear stiffness as the $k \times AV$ and $TDI_{92\text{-}98}$ values decrease. Similarly, compacted specimens from plant-produced mixture also exhibit a decrease in shear stiffness as the $k \times AV$ and $TDI_{92\text{-}98}$ values decrease. However, the same $k \times AV$ or $TDI_{92\text{-}98}$ value results in different shear stiffness for the two subsets of data (i.e., mix design and plant-produced). The average mixture shear stiffness is high (532 MPa) compared with other surface mixtures (341–376 MPa), which have indicated low rutting rates.

Analyses of the Kansas IH-70, Maryland IH-68, Maryland US-40, and Kentucky SR-676 mixtures all indicate average $k \times AV$ and $TDI_{92\text{-}98}$ values comparable with the preceding NCHRP 9-7 projects.

Accelerated Load Facilities and Test Tracks

WesTrack

Several of the WesTrack mixtures were also analyzed for relationships between SGC compaction parameters and rutting performance. Samples of WesTrack mixtures have been stored at the Asphalt Institute's laboratory since the construction of WesTrack in 1995. These samples are identified in Table 5.

The NCHRP Project 9-7 contractor (Fugro-BRE) provided compaction data for 12 mixtures. Mixtures 26, 7, and 15 represent mixtures with the same relative asphalt binder content (low) and construction air voids (high). Only the gradation of the mixtures was a variable. Data for these three mixtures are presented in Table 6. Because rutting can be affected by construction air voids, it was desired to analyze the mixtures grouped by construction air voids.

TABLE 5 WesTrack samples at Asphalt Institute laboratory

Section	Mix	Gradation	% AC	% Voids[1]	Rut Depth, mm
25	25	Coarse	High	Low	27
18	9	Fine	High	Low	7
9	14	Fine Plus	High	Low	30
24	24	Coarse	Med.	Med.	26
15	6	Fine	Med.	Med.	10
11	16	Fine Plus	Med.	Med.	11
26	26	Coarse	Low	High	19
16	7	Fine	Low	High	9
10	15	Fine Plus	Low	High	12

[1] Construction air voids, not SGC air voids.

Figures 22 and 23 illustrate some of the SGC parameters in Table 6 as a function of rut depth.

Figure 22 indicates that rut depth increases as compaction slope increases. This is contrary to the findings of the 1992 SPS-9 mixtures and the NCHRP 9-7 field sensitivity experiment mixtures.

Figure 23 indicates that rut depth increases as densification index decreases. This matches the results of the field sensitivity experiment.

Figure 24 was generated to examine the relationship between rut depth and the interaction of compaction slope and air voids. Unlike the field sensitivity mixtures and the 1992 SPS-9 mixtures, the $k \times AV$ parameter did not provide a good correlation with rutting.

Data analysis was completed for 12 mixture samples representing each of the three gradations (i.e., Coarse, Fine, and Fine Plus) at the low and high asphalt binder contents. Table 7 contains a summary of the compaction data for the six mixtures.

TABLE 6 WesTrack mixtures—high construction air voids

Mixture	26 (Coarse)	7 (Fine)	15 (Fine+)
Accum. Traffic (ESAL)	2,800,000	2,800,000	2,800,000
Rut Depth, mm	19	9	12
Rutting Rate (mm/ESAL$^{1/2}$)	0.01135	0.00538	0.00717
Compaction Slope			
Conventional Semi-Log (N_{des})	8.957	6.023	6.382
Conventional Semi-Log (Regr.)	9.058	6.136	6.512
Exponent (b) from Power Law	0.0433	0.0293	0.0308
Power Law Slope at N_{des}	0.0415	0.0276	0.0294
Gyrations for Target Density			
N_{92}	38	44	29
N_{95}	80	130	82
N_{96}	101	186	116
N_{98}	163	376	226
Gyratory Ratio			
N_{96}/N_{92}	2.67	4.27	3.98
N_{98}/N_{95}	2.05	2.89	2.74
N_{98}/N_{96}	1.61	2.02	1.95
Energy Indices			
CEI_{92}	367	307	186
$CEI_{Nini\text{-}92}$	147	350	211
$DEI_{92\text{-}96}$	67	211	122
$TDI_{96\text{-}98}$	317	273	149
$TDI_{92\text{-}98}$	460	1,320	773

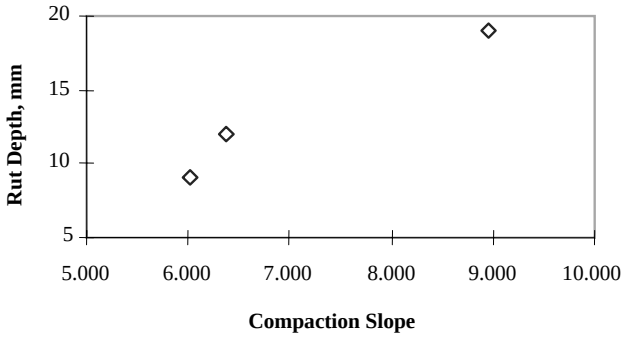

Figure 22. WesTrack mixtures—compaction slope (semi-log), low asphalt content, high air voids.

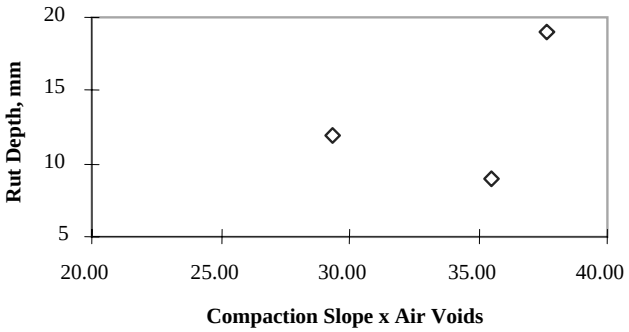

Figure 24. WesTrack mixtures—product of compaction slope and air voids, low asphalt content, high air voids.

Average compaction data in Table 7 indicate that the lowest SGC properties are associated with the Coarse, High mixtures. The SGC data suggest that these mixtures would be expected to perform poorest overall. The highest SGC properties are associated with the Fine, Low mixtures. These data suggest that these mixtures would be expected to perform best overall. These findings are in general agreement with the actual rutting performance of the WesTrack mixtures.

FHWA Accelerated Loading Facility

The FHWA's Accelerated Loading Facility (ALF) experiment was initiated in 1993 to validate the Superpave high temperature parameter ($G^*/\sin\delta$) for asphalt binders related to rutting.

A 19-mm surface course mixture was designed using diabase and natural sand (8%) as aggregates. Five different asphalt binders were used: AC-5 (PG 58-34), AC-10 (PG 58-28), AC-20 (PG 64-22), Novaphalt (PG 76-22), and Styrelf (PG 82-22). The design asphalt content (4.85%) was determined using the Marshall mix design procedure (75 blows). Specimens of plant-produced mixture were compacted with the SGC using an N_{design} of 109 gyrations. More project information can be found in the complete report *(22).* The ALF SGC compaction data and the performance data are summarized in Table 8.

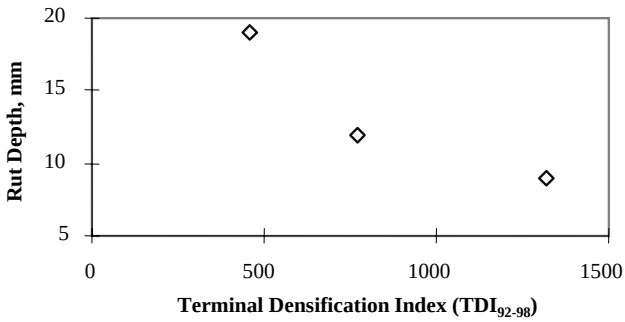

Figure 23. WesTrack mixtures—terminal densification index ($TDI_{92\text{-}98}$), low asphalt content, high air voids.

The data in Table 8 indicate that the shear tests (i.e., simple shear, shear frequency sweep, and repeated shear) and loaded wheel tests match actual ALF performance well. Higher actual rut depths in the ALF correspond with higher rut depths in the loaded wheel tests, greater permanent shear strain in the repeated shear test, and lower shear stiffness in the FSCH test. None of the SGC parameters identify the difference in rutting performance among the test sections. This matches the findings of Langlois and Beaudoin *(11),* discussed in the literature review, that binder stiffness has little influence on SGC compaction properties.

SHRP Lab Experiments

SHRP Field Sensitivity Experiment

The purpose of the field sensitivity experiment was to determine if the SGC could identify changes in key mixture components during production, including asphalt binder content; dust (percent passing 0.075-mm sieve) content; intermediate aggregate content (percent passing the 2.36-mm sieve); nominal aggregate size; and natural (uncrushed) sand content. Details of the experiment can be found in the SHRP A-408 report *(21).*

TABLE 7 WesTrack mixtures—summary of compaction data

Gradation	Asphalt Content	k x AV	$TDI_{92\text{-}98}$
Coarse	Low	36.58	453
Coarse	High	3.20	189
Fine	Low	34.79	1,145
Fine	High	11.37	294
Fine Plus	Low	29.85	773
Fine Plus	High	6.72	234

TABLE 8 Summary of FHWA ALF experimental data

	AC-5	AC-10	AC-20	Styrelf	Novaphalt
Asphalt Content, %	4.85	4.85	4.85	4.85	4.85
Air Voids at N_{design}, %	2.4	3.0	3.1	2.1	2.8
VMA at N_{design}, %	13.4	13.6	13.7	13.0	13.7
VFA at N_{design}, %	81.8	78.2	77.4	83.9	79.4
Rutting Performance Data (58C)					
ALF Wheel Passes at 15 mm RD	480	1,050	1,030	32,610	>200K
ALF Wheel Passes at 20 mm RD	1,410	1,880	2,640	>200K	>200K
GTM Tests (60C)					
Static Shear Strength (S_g), kPa	370	430	370	370	370
Gyratory Stability Index (GSI)	1.10	1.15	1.15	0.95	1.10
Gyr. Elasto-Plastic Index (GEPI)	1.00	1.05	0.90	0.80	0.95
Loaded Wheel Tests					
French - %Rutting at 60C (30K)	15.5	13.8	6.4	3.7	2.6
Georgia – RD at 40C (8K)	7.4 mm	5.4 mm	3.7 mm	1.9 mm	1.4 mm
Hamburg – RD at 50C (10K)	>30 mm	22.8 mm	6.8 mm	2.6 mm	1.4 mm
Shear Test Data[1]					
Max Shear Strain – SSCH (40C)	25,500	20,400	19,200	4,020	2,020
Shear Stiffness – FSCH (40C)	62	134	222	281	409
Perm. Shear Strain – RSCH (40C)	11,100	8,520	7,410	1,740	915
Compaction Slope	8.937	8.922	8.779	8.703	8.373
K x AV	21.72	26.41	27.20	18.19	23.66
Gyratory Ratio N_{98}/N_{95}	2.14	2.13	2.15	2.21	2.25
$TDI_{92\text{-}98}$	352	397	417	331	405

[1] Shear test data has units of μ strain for the SSCH and RSCH tests and MPa for the FSCH test.

For each variable, a high and a low value were assigned. All other values remained at the medium, or control level. For example, if asphalt binder content was the selected response variable, three mixes would be analyzed representing asphalt contents at the design (optimum), 0.6% below design, and 0.6% above design. All other variables (i.e., dust content, intermediate gradation, nominal aggregate size, and natural sand content) remained at the control levels. The effect each variable has on SGC compaction properties is summarized in Table 9.

Although there is no mechanical mixture testing associated with the data in Table 9, previous testing on laboratory-prepared specimens (e.g., Mississippi US-61, Florida US-301, and Kansas IH-70) indicates that decreasing values of the SGC compaction properties ($k \times AV$ or $TDI_{92\text{-}98}$) are associated with reduced mixture stiffness. The data in Table 9 indicate that increasing the asphalt binder, dust, or natural sand content results in decreasing SGC compaction properties. This is expected to produce a decrease in mixture stiffness or shear resistance.

TABLE 9 SHRP field sensitivity experiment

Blend	Description	Asphalt Content	Air Voids	Compaction Slope	k x AV	$TDI_{92\text{-}98}$
Asphalt Content						
2	Opt –0.6%	4.7%	9.4%	6.567	61.73	4,409
1	Opt	5.3%	7.1%	6.767	48.05	1,809
3	Opt +0.6%	5.9%	5.1%	7.433	37.91	846
Dust Content						
1	Control	5.3%	7.1%	6.767	48.05	1,809
4	Medium $P_{0.075}$	5.3%	3.4%	7.633	25.95	504
5	High $P_{0.075}$	5.3%	1.3%	8.100	10.53	311
$P_{2.36}$ Content						
6	Low $P_{2.36}$	5.3%	7.7%	7.167	55.19	1,916
1	Control	5.3%	7.1%	6.767	48.05	1,809
7	High $P_{2.36}$	5.3%	6.3%	6.733	42.42	1,574
Nominal Agg. Size						
8	High Nominal	5.3%	7.6%	6.667	50.67	2,177
1	Control	5.3%	7.1%	6.767	48.05	1,809
9	Low Nominal	5.3%	7.5%	7.033	52.75	1,930
Natural Sand Content						
11	Low Sand	5.3%	9.9%	6.767	66.99	4,559
1	Control	5.3%	7.1%	6.767	48.05	1,809
10	High Sand	5.3%	4.9%	6.767	33.16	974

TABLE 10 FHWA Pooled Fund Study 176

	19L39B	19L44A	19L44B	19L50A
Coarse Aggregate	Limestone	Limestone	Limestone	Limestone
Fine Aggregate	River Sand	Limestone	Limestone	Granite
FAA	39	44	44	50
Gradation	Below RZ	Above RZ	Below RZ	Above RZ
Asphalt Content, %	5.5	4.6	4.6	5.9
APT Rut Depth, mm	15.7	4.3	8.0	9.3
Compaction Slope	8.653	7.839	9.671	9.977
k x AV	34.61	31.36	38.68	39.91
$TDI_{92\text{-}98}$	770	574	453	398

FHWA Pooled Fund Study 176

The FHWA Pooled Fund Study 176 was executed by Purdue University. The research involved the production of mixtures from two coarse aggregates and four fine aggregates having different fine aggregate angularity (FAA) values.

A PG 64-22 asphalt binder was used for all mixtures. Rutting results were determined from the Purdue Accelerated Pavement Tester (APT) at the high density (low construction air voids) for each mixture. A summary of the test results using crushed limestone coarse aggregate is presented in Table 10.

Figures 25 and 26 illustrate the relationship between APT rut depth and SGC compaction properties ($k \times AV$ and $TDI_{92\text{-}98}$, respectively).

As indicated in Figures 25 and 26, neither SGC compaction property exhibits a strong relationship with actual rut depth. As the $k \times AV$ term increases, the rut depth generally increases. The exception to this is the 19L39B mixture, which has the second lowest $k \times AV$ value, but highest rut depth. Figure 26 indicates that the $TDI_{92\text{-}98}$ values generally decrease as rut depth increases. This pattern does match expectations. However, the 19L39B mixture again is an anomaly with the highest $TDI_{92\text{-}98}$ value and the highest rut depth.

LABORATORY EXPERIMENTS RELATING SGC PROPERTIES TO RUTTING

Laboratory experiments were developed to address two main questions:

- Can a parameter be identified during SGC compaction that is related to the rutting resistance of an asphalt mixture?
- If a parameter is identified, can the relationship to rutting potential be validated through the performance of mixtures in service?

Based on the analysis of SGC parameters from existing data, two potential parameters available from conventional SGC compaction data were the product of compaction slope and percentage of air voids ($k \times AV$) and the terminal densification index from 92% to 98% ($TDI_{92\text{-}98}$). These two parameters were selected for further evaluation in the laboratory experiments.

In addition, other non-conventional compaction parameters were examined to determine if any provided a good correlation with rutting potential. These included the following:

- Shear stress measurements, using the Servopac Gyratory Compactor and the modified Pine AFG1 SGC;
- Lateral pressure indicator (LPI), using a modified SGC mold; and
- Shear force measurements, using the Gyratory load cell plate assembly (GLPA).

Using Compaction Slope and Percentage of Air Voids ($k \times AV$) to Estimate Rutting

Using a combination of the compaction slope and percentage of air voids ($k \times AV$) appeared to account for the

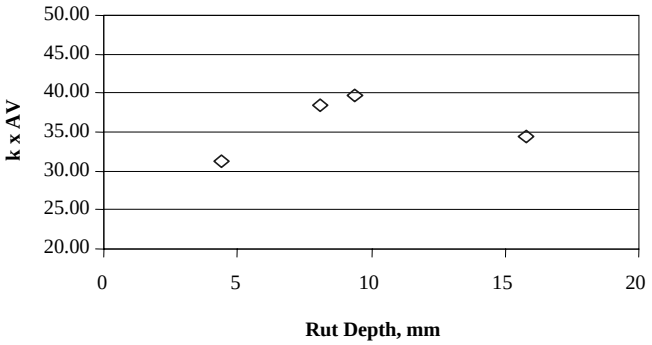

Figure 25. FHWA Pooled Fund Study 176—relationship between rut depth and $k \times AV$.

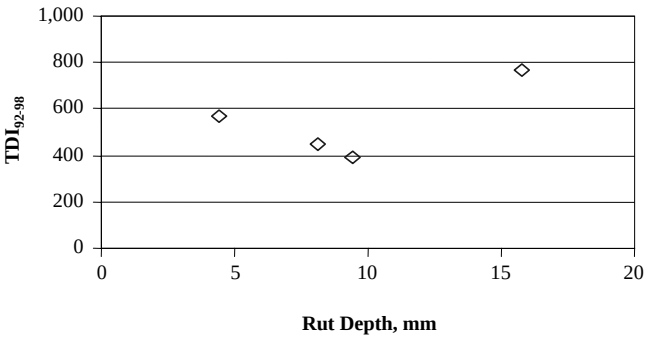

Figure 26. FHWA Pooled Fund Study 176—relationship between rut depth and $TDI_{92\text{-}98}$.

TABLE 11 Evaluation of the sensitivity of conventional SGC parameters for determining shear resistance

		Target k x AV	
		Gravel Fine 9.5-mm 40% Sand PG 64-22	Limestone Coarse 9.5-mm 0% Sand PG 76-22
Asphalt Binder Content	**Target Air Voids**		
Optimum	4.0%	24.34	34.61
Optimum – 0.5%	5.2%	31.64	45.00
Optimum + 0.5%	2.8%	17.04	24.23
Optimum + 1.0%	1.5%	9.13	12.98

problem of the compaction slope being insensitive to asphalt binder volume. One question that remained, however, was if mixtures with the same $k \times AV$ values would be expected to have the same rutting potential. The experiment conducted to answer this question involved two mixtures at different asphalt binder contents (to create different percentages of air voids) as indicated in Table 11.

For each of the eight cells, triplicate specimens were compacted to 100 gyrations (N_{design}) to verify the target $k \times AV$ values. Another set of triplicate specimens was then compacted to 3.0 ± 0.5% air voids for each cell. These specimens were tested using the RSCH test at 58°C to determine the rutting resistance of the asphalt mixtures. The data were analyzed by plotting estimated rut depth from the RSCH test as a function of $k \times AV$ values, as illustrated in Figure 27.

The null hypothesis of the experiment was that two mixtures with similar $k \times AV$ values, but different design compaction slopes (k) will perform the same in shear resistance (as measured by the RSCH test). Acceptance of the null hypothesis indicates that the $k \times AV$ value may serve as a universal measure of shear resistance during the mix design process. Rejection of the null hypothesis (i.e., the two sets of data do not fall on the same curve as indicated in Figure 27) indicates that the $k \times AV$ value may be used only as an indication of rutting susceptibility within a given mixture (i.e., for production quality control rather than mix design).

Average test data are presented in Table 12 and Figures 28 and 29.

As seen in Table 12 and Figure 28, the 9.5-mm Limestone Coarse (0% Sand) mixtures have higher values of $k \times AV$ than the 9.5-mm Gravel Fine (40% Sand) mixtures. The $k \times AV$ of the two mixtures begin to coincide at a value of approximately 30. This point represents the Opt-0.5% asphalt binder content for the Gravel mix and the Opt+0.5% asphalt binder content for the Limestone mix.

While the $k \times AV$ values show a continual decrease as the asphalt binder content increases, the compaction slope of the mixtures remains relatively unresponsive to changes in asphalt binder content, as indicated in Figure 29.

Figures 28 and 29 also clearly indicate that asphalt binder stiffness has no effect on either the compaction slope, k, or the product with percentage of air voids, $k \times AV$. The PG 76-22 asphalt binder curves are virtually identical to the PG 64-22 asphalt binder curves for each mixture.

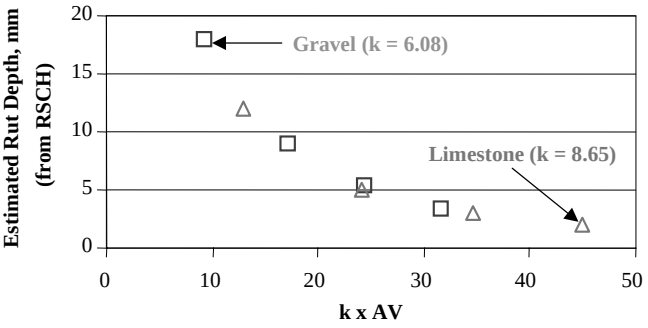

Figure 27. Anticipated output from conventional SGC parameters ($k \times AV$) experiment.

TABLE 12 Sensitivity of conventional SGC parameters for determining shear resistance

		Asphalt Binder Content			
		Opt – 0.5%	Opt.	Opt + 0.5%	Opt + 1.0%
Mixture	**Binder**	**k x AV**			
9.5-mm Gravel Fine, 40% Sand	PG 64-22	29.94	22.13	16.31	11.19
	PG 76-22	28.95	20.47	18.17	10.69
9.5-mm Limestone Coarse, 0% Sand	PG 64-22	55.47	43.08	34.25	20.53
	PG 76-22	50.16	49.38	32.86	27.20
Mixture	**Binder**	**k**			
9.5-mm Gravel Fine, 40% Sand	PG 64-22	6.04	6.20	6.06	5.91
	PG 76-22	5.91	5.99	6.31	5.95
9.5-mm Limestone Coarse, 0% Sand	PG 64-22	9.16	9.25	9.50	9.69
	PG 76-22	9.34	9.17	9.33	9.60

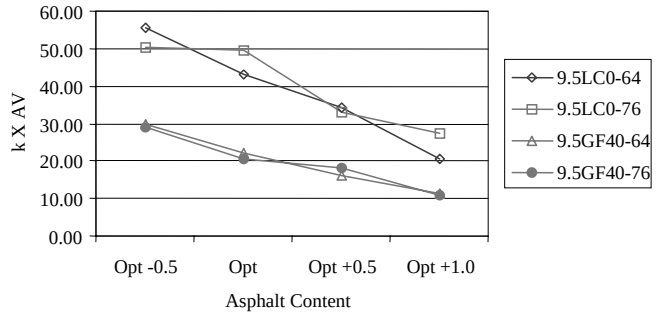

Figure 28. Sensitivity of $k \times AV$ values to asphalt binder content.

In addition to the volumetric specimens, another set of triplicate specimens was compacted to 3.0 ± 0.5% air voids for each cell. These specimens were tested using the RSCH test at 58°C to determine the rutting resistance of the asphalt mixtures.

Data from the RSCH tests on the 9.5-mm Gravel Fine mixture are presented in Figures 30 and 31.

The data in Figures 30 and 31 indicate that the PG 64 mixture shows a strong relationship toward increasing rut depth with increasing compaction slope (k) and decreasing $k \times AV$ values. The PG 76 mix shows a slight trend toward increasing rut depth with increasing compaction slope (k) and decreasing $k \times AV$ values, but appears to be much less sensitive to changes in asphalt binder content than the PG 64 mixtures. The 9.5-mm Limestone Coarse mixtures (not shown) follow the same pattern as the 9.5-mm Gravel Fine mixtures in Figures 30 and 31.

Figure 32 includes all of the data for each asphalt binder, assuming mixture type is ignored. Figure 33 presents the same data with the mixture type indicated.

The PG 64 asphalt mixtures validate the null hypothesis that $k \times AV$ values are related to the estimated rut depth of the asphalt mixtures, regardless of mixture type. The higher $k \times AV$ value of the 9.5-mm Gravel Fine mixture reasonably overlaps with the lower $k \times AV$ values of the 9.5-mm Limestone Coarse mixtures.

The PG 76 asphalt mixtures show very little change in estimated rut depth with $k \times AV$ values. It is thought that this lack

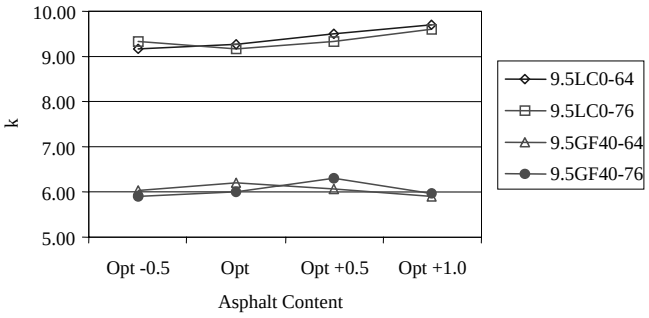

Figure 29. Sensitivity of compaction slope to asphalt binder content.

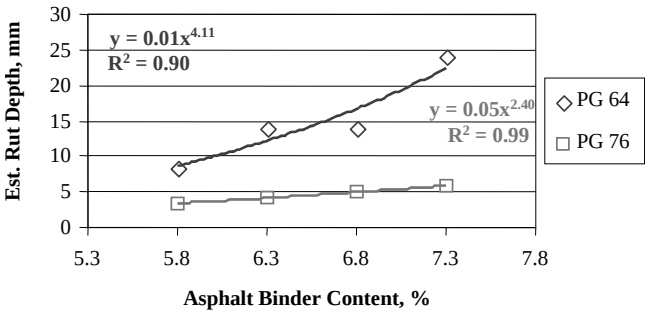

Figure 30. Relationship between rut depth and asphalt binder content (9.5GF Mix).

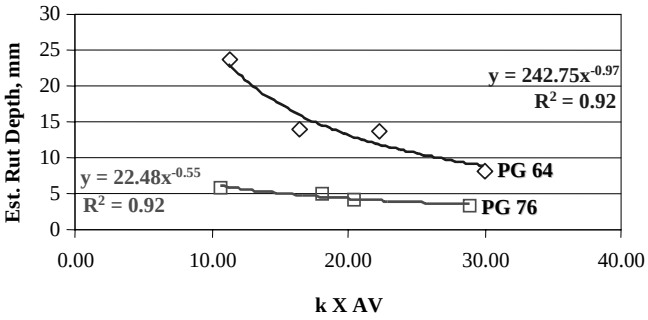

Figure 31. Relationship between rut depth and $k \times AV$ values (9.5GF Mix).

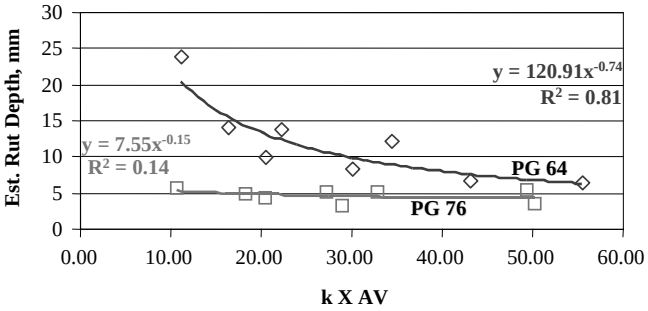

Figure 32. Relationship between estimated rut depth and $k \times AV$ values.

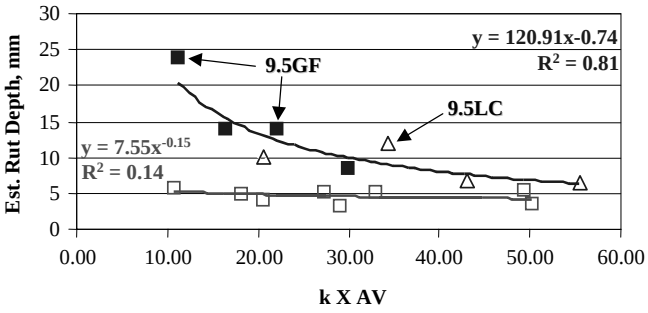

Figure 33. Relationship between estimated rut depth and $k \times AV$ values (mixture type identified).

of response resulted from the selected test temperature. The stiffness of the PG 76 asphalt binder is approximately 4 times greater than the PG 64 asphalt binder at 58°C. If the test temperature were increased for the PG 76 mixtures (e.g., 70°C) a similar response as the PG 64 mixtures would be expected.

In either case, data indicate that it may be possible to select a $k \times AV$ value as a minimum requirement during compaction to provide adequate rutting resistance. This concept was further explored in the main laboratory experiment evaluating the effects of changes in mixture components on asphalt mixture rutting resistance.

Evaluation of Shear Measurements

Servopac Gyratory Compactor Shear Stress Measurements

Research presented by Professor Byron Ruth (University of Florida) at an Asphalt Mixtures Expert Task Group (ETG) Meeting *(23)* indicated that the Servopac gyratory compactor could distinguish between asphalt mixtures when a compaction angle of 2.5 deg was used, but not when the standard angle of 1.25 deg was used.

The Servopac gyratory compactor was designed so that the critical parameters of compaction could be simply and quickly adjusted. Pressure transducers installed in the pressure lines of the three gyratory actuators allow the measurement of shear resistance of a sample during compaction.

A small experiment was developed to validate the research conducted at the University of Florida and explore the concept of shear stress measurement during SGC compaction. The Asphalt Institute prepared four mixtures for compaction on the Servopac gyratory compactor at the University of Florida:

- 9.5-mm NMS Limestone Coarse, 0% Sand, PG 76-22, Optimum
- 9.5-mm NMS Limestone Coarse, 0% Sand, PG 64-22, Optimum
- 9.5-mm NMS Gravel Fine, 40% Sand, PG 64-22, Optimum
- 9.5-mm NMS Gravel Fine, 40% Sand, PG 64-22, Optimum Plus

The mixtures were prepared and aged at the Asphalt Institute laboratory and then shipped to the University of Florida. A member of the research team accompanied the samples to Florida to assist with and observe the compaction of the specimens. Four samples were compacted to $N_{maximum}$ (160 gyrations) on the Servopac gyratory compactor at two compaction angles (2.5 deg and 1.25 deg) for each of the four mixtures.

Limestone Blends. Figures 34 and 35 illustrate the compaction data for the Limestone Coarse, 0% natural sand mixes.

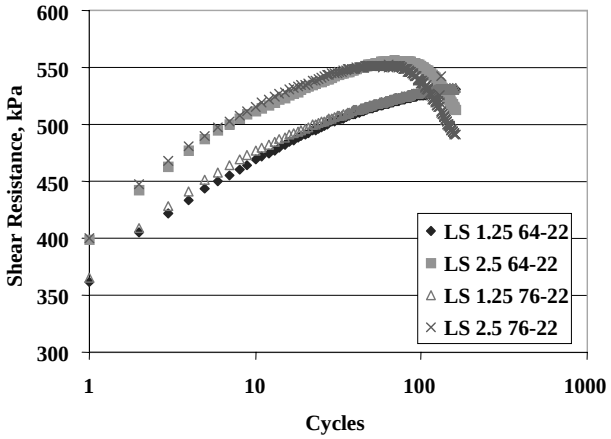

Figure 34. Measured shear resistance—limestone mixtures.

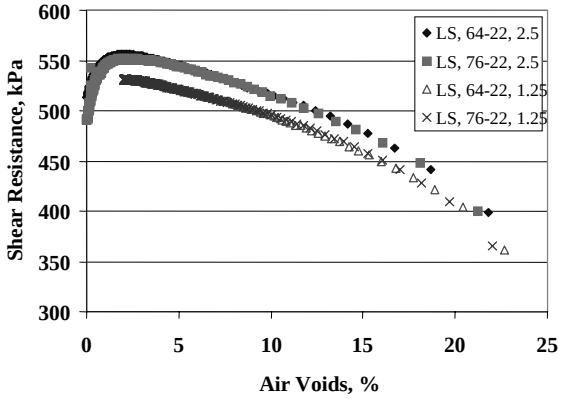

Figure 35. Measured shear resistance as a function of air voids—limestone mixtures.

Table 13 shows the average properties for each Limestone mixture and compaction angle. Tables 14 and 15 show the maximum shear resistance and number of cycles to maximum shear resistance for each of the individual specimens.

The data shown in Figures 34 and 35 indicate that the measured shear resistance of the specimens compacted at the lower compaction angle increased steadily throughout compaction and was about the same for both the PG 76-22 and the PG 64-22 binders. The measured shear resistance for the specimens compacted at the higher compaction angle

TABLE 13 Average compaction properties—limestone coarse mixtures

Asphalt Binder	Angle Deg.	Max Shear kPa	Air Voids %	Height mm
64-22	1.25	531	2.38	114.8
	2.50	556	0.03	111.2
76-22	1.25	532	2.00	114.5
	2.50	552	0.03	111.2

TABLE 14 Maximum shear resistance (kPa)—limestone coarse mixtures

		Asphalt Binder			
		64-22		76-22	
	Angle	1.25	2.50	1.25	2.50
Specimen	1	527	560	533	554
	2	533	552	528	551
	3	529	557	531	--
	4	534	558	537	555
	Average	531	556	532	552

TABLE 15 Cycles to maximum shear resistance—limestone coarse mixtures

		Asphalt Binder			
		64-22		76-22	
	Angle	1.25	2.50	1.25	2.50
Specimen	1	160	66	160	62
	2	160	76	160	51
	3	160	75	160	--
	4	160	111	160	69
	Average	160	82	160	61

increased to a maximum value, then decreased with additional cycles.

A statistical *t*-test analysis of the individual specimen data in Table 14 indicates that the maximum shear values for the 2.5-deg specimens were statistically higher than the maximum shear values (final shear values) for the 1.25-deg specimens. There was no statistical difference, however, between the PG 64-22 and PG 76-22 at either angle. In other words, no distinction could be made between the performance of the two asphalt binders at either compaction angle.

Based on the comparison shown in Figure 35, the maximum shear resistance for all specimens occurred at approximately 2.0% air voids.

Gravel Blends. Figures 36 and 37 illustrate the compaction data for the Gravel Fine, 40% natural sand mixes.

TABLE 16 Average compaction properties—gravel fine mixtures

% Binder	Angle Deg.	Max Shear kPa	Air Voids %	Height mm
7.3	1.25	506	0.80	117.9
	2.50	528	0.26	117.4
6.3	1.25	517	2.28	117.5
	2.50	543	0.66	115.6

Table 16 shows the average properties for each Gravel mixture. Tables 17 and 18 show the maximum shear resistance and number of cycles to maximum shear resistance for each of the individual specimens.

Examining the compaction results illustrated in Figure 36, it is apparent that the gravel mixes with 6.3% asphalt content reached higher maximum shear resistance value than the 7.3%

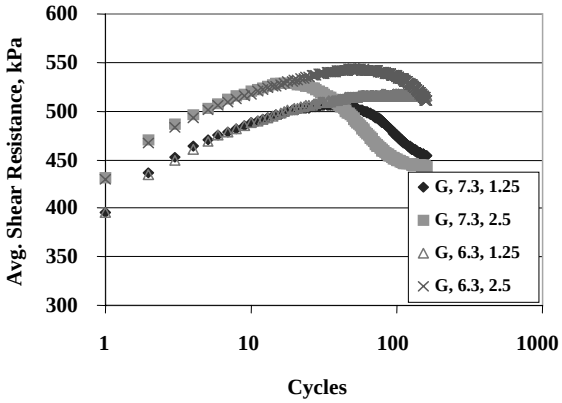

Figure 36. Measured shear resistance—gravel mixtures.

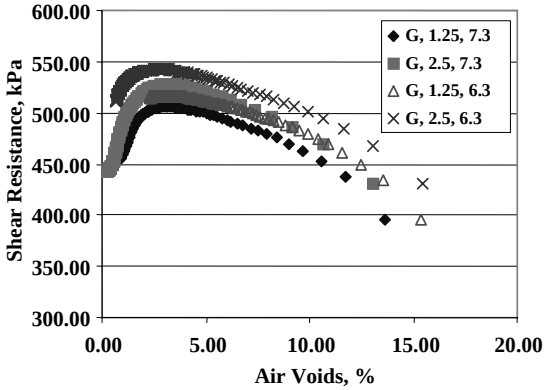

Figure 37. Measured shear resistance as a function of air voids—gravel mixtures.

TABLE 17 Maximum shear resistance (kPa)—gravel fine mixtures

		Asphalt Binder Content, %			
		7.3		6.3	
	Angle	1.25	2.50	1.25	2.50
Specimen	1	502	537	520	547
	2	503	524	514	541
	3	511	525	517	545
	4	511	539	517	538
	Average	506	528	517	543

TABLE 18 Cycles to maximum shear resistance—gravel fine mixtures

		Asphalt Binder Content, %			
		7.3		6.3	
	Angle	1.25	2.50	1.25	2.50
Specimen	1	36	14	81	53
	2	40	26	147	53
	3	49	22	109	54
	4	34	26	149	47
	Average	40	22	122	51

asphalt content specimens. The 6.3% specimens also required more gyrations before reaching the maximum shear resistance than the 7.3% specimens. Higher shear resistance and longer cycles to maximum shear resistance should indicate a better performing mix. However, it should be noted that for each angle the specimens start off following the same curve, then the higher asphalt content specimens reach a maximum shear resistance level and drop off at approximately half the number of cycles as the lower asphalt content specimens.

From the comparison of shear resistance as a function of the percentage of air voids in Figure 37, it can be seen that all of the mixes reach maximum shear resistance at approximately 3% air voids.

A statistical *t*-test analysis of the shear resistance data in Table 17 indicates that all four conditions are statistically different. At a compaction angle of 2.5 deg, one could conclude that the gravel mix with 6.3% asphalt content would perform better than the gravel mix with 7.3% asphalt content. The same conclusion could also be reached based on the 1.25-deg data.

Comparison of Mixture Types. Figures 38 and 39 show a comparison of the Limestone and Gravel mixtures at each compaction angle.

Comparing Figures 38 and 39, it can be seen that the same trends are evident at both compaction angles. At 1.25 deg, there is a statistical difference between the maximum shear resistance values for the gravel mixes and the maximum shear resistance values for the limestone mixes. There is no statistical difference between the maximum shear resistance values for the two limestone mixes. The gravel mix with the high asphalt content indicates statistically lower shear resistance values than the gravel mix at optimum asphalt content. At the 2.5-deg compaction angle, the same trends are observed. The paired comparisons are also indicated in Table 19.

The data in Table 19 indicate that, for a given compaction angle, the 9.5-mm Limestone Coarse mixtures using two different asphalt binders have substantially the same measured maximum shear values. This comparison (asphalt binder stiffness) does not indicate any differences in maximum shear as a function of asphalt binder stiffness.

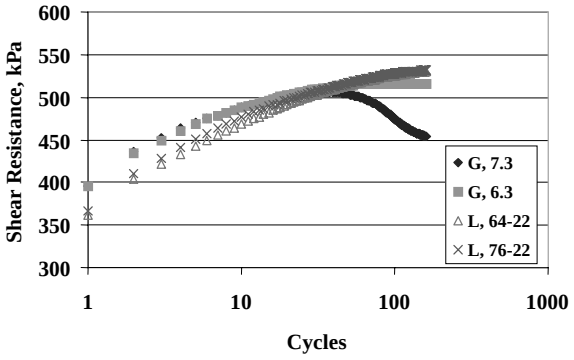

Figure 38. Measured shear resistance—1.25-degree compaction angle.

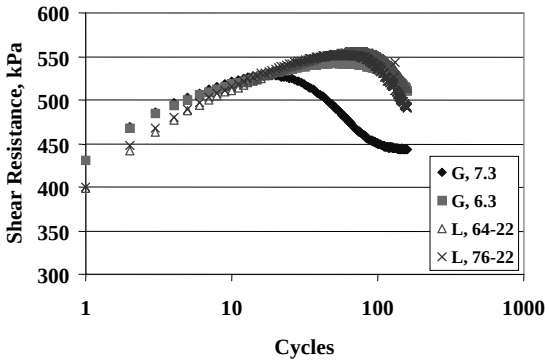

Figure 39. Measured shear resistance—2.5-degree compaction angle.

TABLE 19 Paired comparisons for ServoPac experiment

			Max Shear, kPa		% Air Voids at Max Shear	
Aggregate	**Binder**	**% AC**	**1.25°**	**2.50°**	**1.25°**	**2.50°**
Limestone	PG 64	Opt.	531	556	2.6	2.2
Limestone	PG 76	Opt.	532	552	2.2	2.0
Limestone	PG 64	Opt.	531	556	2.6	2.2
Gravel	PG 64	Opt.	517	543	2.8	3.0
Gravel	PG 64	Opt.	517	543	2.8	3.0
Gravel	PG 64	Opt +	506	528	3.3	3.5

In the second paired comparison, the 9.5-mm Limestone Coarse mixture has higher values of maximum shear at both compaction angles compared with the 9.5-mm Gravel Fine mixture. This comparison (mixture type) matches expectations of rutting potential. The higher maximum shear value corresponds with the mixture expected to have the greatest rutting resistance (9.5-mm Limestone Coarse, 0% Sand).

In the third paired comparison, the 9.5-mm Gravel Fine mixture at Optimum asphalt binder content has higher values of maximum shear at both compaction angles compared with the same mixture at the Optimum Plus asphalt binder content. This comparison (asphalt binder content) matches expectations of rutting potential. The higher maximum shear value corresponds with the mixture expected to have the greatest rutting resistance (9.5-mm Gravel Fine, Optimum).

Although the maximum shear values in Table 19 are higher for the specimens compacted at 2.50 deg, the trend is the same as for the specimens compacted at 1.25 deg. The data in Table 19 also indicate that the percentage of air voids at the maximum shear value is essentially the same for the two compaction angles. This is an indication that although the specimens compacted at 2.50 deg show more of a decrease in shear for some mixtures (Figures 34 and 36), the decrease is related to the specimens reaching a critical percentage of air voids. In other words, the percentage of air voids is lower for specimens compacted at 2.50 deg at the same number of gyrations compared with the specimens compacted at 1.25 deg. In the opinion of the research team, this indicates no specific advantage to using a compaction angle of 2.50 deg as compared with 1.25 deg for shear measurement in the Servopac gyratory compactor. The same shear curves could be expected for the 1.25 deg specimens by compacting to a higher number of gyrations (lower percentage of air voids).

Finally, the data in Table 19 indicate that the percentage of air voids at the measured maximum shear value may be related to the expected shear resistance of the four mixtures. The lowest percentage of air voids, at 1.25 deg, corresponds with the mixture expected to have the best rutting resistance of the four mixtures (9.5-mm Limestone Coarse, 0% Sand, PG 76-22, Opt). The highest percentage of air voids, at 1.25 deg, corresponds with the mixture expected to have the worst rutting resistance of the four mixtures (9.5-mm Gravel Fine, 40% Sand, PG 64-22, Optimum Plus).

Because the number of gyrations controls the percentage of air voids in a specimen, lower air voids would roughly equate to higher gyrations at maximum shear value. Table 20 indicates the number of gyrations at which the maximum shear occurs for each of the mixtures.

Data in Table 20 indicate that the number of gyrations at which the maximum shear occurs is generally higher for mixtures with good expected rutting resistance. Paired comparisons indicate that aggregate structure (mixture type) and asphalt binder volume have an effect on the number of gyrations at the maximum shear. Binder stiffness does not appear to have an effect as noted earlier.

Lateral Pressure Indicator

Dr. Rajib Mallick developed a procedure that uses a modified Pine SGC mold with load cell to measure lateral pressure during compaction. The Lateral Pressure Indicator (LPI), developed at Worcester Polytechnic Institute (WPI), records the pressure on the sides of the gyratory mold during the compaction of an asphalt mixture specimen. The LPI was designed to measure pore pressure in a compacted asphalt mixture sample to determine if pressure readings could be correlated with pavement performance.

WPI used a Pine AFG1A Superpave gyratory compactor for this experiment. The SGC at WPI was ordered with the optional shear measurement capabilities offered by Pine Instruments. In addition to the factory shear measurement capabilities, the WPI research team cut a rectangular piece from the side of the mold and installed a load cell behind it to record pressure during compaction. The signal from the load cell was recorded on a computer and later the data were merged with the compaction data file.

Pine Instruments later produced a special mold for WPI that was outfitted with two loose plates and load cells placed 90 deg apart in the mold walls. In addition, the internal G1 computer was modified to accept signals from the load cells and include the data in the regular compaction data file.

TABLE 20 Number of gyrations at maximum shear (1.25 deg)

Aggregate	**Binder**	**% AC**	***N* at Max Shear**	**Ratio N_{shear}/N_{max}**
Limestone	PG 64	Opt.	151	0.94
Limestone	PG 76	Opt.	148	0.92
Limestone	PG 64	Opt.	151	0.94
Gravel	PG 64	Opt.	114	0.71
Gravel	PG 64	Opt.	114	0.71
Gravel	PG 64	Opt +	34	0.21

The lateral pressure indicatory (LPI) can be measured during compaction as a ratio between the lateral stress (measured) and vertical stress (applied). The concept appears to be very similar to the Hveem stabilometer.

Developmental research conducted by Dr. Mallick indicated that the LPI is sensitive to asphalt binder content, aggregate gradation, and aggregate particle shape. It was also noted that the LPI provided results that are consistent with observed, documented mix performance data.

To aid in validation of the LPI, the research team generated data on the four mixes used in testing on the Servopac gyratory compactor. Triplicate specimens were batched, mixed, and conditioned in accordance with AASHTO PP2 at the Asphalt Institute and shipped to WPI. In addition, triplicate specimens were shipped to WPI from two WesTrack mixes. A Coarse mix (Section 25) with 27-mm rutting and a Fine mix (Section 18) with 7-mm rutting were used for compaction.

Data for the four laboratory mixtures are indicated in Table 21.

The four laboratory mixtures exhibited LPI trends consistent with expectations. The two Limestone mixtures (PG 64-22, Optimum, and PG 76-22, Optimum) had lower LPI values at 100 gyrations (N_{design}) than the two Gravel mixtures (PG 64-22, Optimum and Optimum Plus). The Limestone mixtures and the Gravel mixture at the optimum asphalt binder content exhibited relatively flat LPI values after the initial compaction. According to the research by Dr. Mallick, this is a desirable indication of a stable mixture. Each of these three mixtures did exhibit a slight increase in LPI after approximately 150 gyrations. At this compaction level, the percentage of air voids in the mixture had decreased to approximately 3%.

The Gravel mixture with an asphalt binder content 1% higher than optimum exhibited a higher LPI at 100 gyrations and a steadily increasing LPI throughout the compaction process. According to the research, this is an indication of an increasingly unstable mixture.

The LPI at 100 gyrations appeared to provide a consistent ranking with the expected shear (rutting) resistance of the four laboratory mixtures. The Limestone mixture with the Optimum PG 76-22 asphalt binder had the lowest LPI (32). The next lowest LPI (35) was the Limestone mixture with the Optimum PG 64-22 asphalt binder, followed by the Gravel mixture with the Optimum PG 64-22 asphalt binder (LPI = 40), and the Gravel mixture with the Optimum Plus PG 64-22 asphalt binder (LPI = 45). Unfortunately, variability in the test data caused the paired comparisons to be considered statistically equal (*t*-test with $\alpha = 0.05$). Thus, the Limestone PG 64-22 mixture had statistically the same LPI as the Gravel PG 64-22 mixture; the Limestone PG 64-22 mixture had statistically the same LPI as the Limestone PG 76-22 mixture; and the Gravel PG 64-22 mixture at Optimum asphalt binder content had statistically the same LPI as the Gravel PG 64-22 at Optimum-Plus asphalt binder content.

The WesTrack mixtures did not match expectations. Analysis indicated that the Section 18 mixture (Fine, Optimum Plus) had higher LPI at all gyrations than the Section 25 mixture (Coarse, Optimum Plus) and a steadily increasing LPI curve during compaction. This mixture had indicated relatively little rutting during trafficking (7 mm after 2.8-million ESALs) and in the RSCH test (conducted for the WesTrack project) compared with the Section 25 mixture (27 mm after 2.8-million ESALs). The Section 25 mixture did indicate an unusual hump in the LPI curve at approximately 70 gyrations. It was hypothesized that after this point the aggregate structure began to deteriorate into a less interlocked, more random pattern. The LPI values peaked almost 7 psi higher than the LPI at 70 gyrations.

The relationship between the expected rutting resistance of an asphalt mixture and the LPI for the four laboratory mixtures matched expectations, although the paired comparisons did not indicate any statistically significant differences. Based on these findings, the LPI experiment was continued with the 16 mixtures selected for the main laboratory experiment.

Results and Analyses of Experimental Mixtures

For any mix that has higher than optimum asphalt content, it is expected that the mix will not have a chance to form a stable aggregate structure because the pore pressure quickly builds and prevents the formation of any stable aggregate

TABLE 21 LPI data for laboratory mixtures

		Limestone PG 64-22 Optimum	Limestone PG 76-22 Optimum	Gravel PG 64-22 Optimum	Gravel PG 64-22 Optimum +
LPI @ N=100	Rep 1	43.5	33.7	43.0	47.3
	Rep 2	34.2	28.9	34.7	45.9
	Rep 3	34.6	34.3	40.5	43.7
	Rep 4	29.2	33.3	n/a	43.2
	Average	**35.4**	**32.5**	**39.4**	**45.0**
LPI @ N=160	Rep 1	44.4	33.0	43.5	50.4
	Rep 2	35.9	31.9	34.7	47.3
	Rep 3	32.0	31.6	39.2	50.2
	Rep 4	33.0	32.8	n/a	46.9
	Average	**36.4**	**32.3**	**39.2**	**48.7**

structure. Therefore, for these mixes, the slope of Voids in Total Mixture (VTM) versus lateral pressure plot should not decrease and should probably increase at voids lower than 2%.

Another way to examine these data is to look at the change in pressure when the percentage of air voids changes from 7% to 4%. Barksdale *(24)* observed a residual stress of 2 psi (13.7 kPa) in compacted aggregate bases. Applying this approach, a difference of approximately 14 kPa would indicate a good mix. A larger difference would indicate a poor aggregate structure that could rut.

Change in residual pressure for the 16 experimental mixtures is shown in Table 22. This can also be seen graphically on a plot of pressure as a function of gyrations. Steep slopes indicate a weak mixture, while flat slopes indicate a stable mixture. If the slope of the mix varies, it is an indication that the aggregate structure is constantly changing, and is, therefore, unstable. A couple of mixes show a negative difference from 7% to 4%. This indicates a mixture in which the aggregate structure is unstable and changes under pressure.

A simpler approach is to look at the pressure indicated by the LPI at a specified number of gyrations. This gives a quick method of ranking the mixes. Using this analysis procedure, a lower pressure indicates a stronger mix. Results of LPI readings at 100 and 160 gyrations are indicated in Table 23.

TABLE 22 Residual pressure in mixture during compaction from 7% to 4% air voids

	Residual Pressure (kPa)			
	Sample Number			
Mix	1	2	3	Average
A	7.03	-9.20	2.17	**0.00**
B	37.41	30.34	46.00	**37.92**
C	2.62	-7.55	10.45	**1.84**
D	-23.17	19.47	19.27	**5.19**
E	8.40	0.24	1.55	**3.40**
F	23.43	-1.42	34.95	**18.99**
G	5.45	13.79	-1.48	**5.92**
H	17.98	-4.04	17.02	**10.32**
I	13.57	14.35	0.00	**13.96**
J	-16.90	-6.75	-22.97	**-15.54**
K	11.53	9.81	13.53	**11.63**
L	45.12	42.10	61.91	**48.71**
M	9.35	25.65	45.93	**26.98**
N	-9.40	-2.00	3.32	**-2.69**
O	17.82	2.91	20.53	**13.75**
P	36.30	22.80	55.91	**38.34**

Effect of Changes in Mixture Components on Shear Stiffness and Rutting Resistance

This main experiment consisted of determining the effects of changes in mixture components on SGC compaction parameters and mixture properties related to mixture stiffness and permanent deformation resistance. The objective of the experiment was to address whether the SGC parameters selected for evaluation are affected by specific variables that should affect mixture performance, such as asphalt binder content, percentage of rounded fine aggregate, and asphalt binder stiffness. The experimental design is shown in Table 24.

The design is a 2^6 factorial consisting of 64 cells. All of the main factors were selected to provide contrasts in the expected permanent deformation resistance of the mixtures. For example, it was expected that mixtures produced at the optimum asphalt content should have better permanent deformation resistance than mixtures produced at an asphalt content 0.8% higher than the optimum. Similarly, mixtures produced with a PG 76-22 asphalt binder or no rounded sand were expected to have better rutting resistance than mixtures produced with a PG 64-22 asphalt binder or a high percentage of rounded sand.

Sixteen mix designs were developed to identify Optimum and Optimum Plus asphalt binder contents. Each mix design was conducted using an N_{design} of 100 gyrations ($N_{maximum}$ of 160 gyrations). The optimum asphalt binder content was

TABLE 23 LPI measured at different gyrations

	LPI @ 100 Gyrations				LPI @ 160 Gyrations			
Mix	Rep 1	Rep 2	Rep 3	Average	Rep 1	Rep 2	Rep 3	Average
A	330	85	219	**211**	320	85	215	**206**
B	245	145	207	**199**	285	168	230	**228**
C	179	275	178	**211**	211	284	174	**223**
D	143	154	188	**162**	156	146	186	**163**
E	73	20	188	**94**	80	22	186	**96**
F	116	106	252	**158**	122	116	264	**167**
G	78	120	166	**121**	122	142	194	**153**
H	155	47	227	**143**	139	33	209	**127**
I	136	152		**144**	139	163		**151**
J	149	211	251	**204**	143	213	251	**202**
K	164	132	201	**166**	165	152	213	**176**
L	235	258	275	**256**	234	257	300	**264**
M	171	195	380	**249**	177	204	389	**256**
N	158	184	244	**195**	153	167	244	**198**
O	110	210	237	**186**	115	230	228	**191**
P	235	153	300	**229**	259	182	334	**258**

TABLE 24 Assessment of the effects of changes in mixture components experiment

				PG 64-22		PG 76-22	
Aggregate	**Gradation**	**Size, mm**	**% Sand**	**Opt.**	**Opt. +**	**Opt.**	**Opt. +**
Limestone	Coarse	9.5	0				
			40				
		19	0				
			40				
	Fine	9.5	0				
			40				
		19	0				
			40				
Gravel	Coarse	9.5	0				
			40				
		19	0				
			40				
	Fine	9.5	0				
			40				
		19	0				
			40				

determined as the asphalt binder content required to achieve 4.0% air voids at N_{design}.

The experiment was conducted using one-eighth (⅛) factorials as building blocks. The first ⅛ factorial is indicated by the dark-shaded cells in Table 24. Based on the analysis of the first ⅛ factorial, the second ⅛ factorial, represented by the light-shaded cells, was chosen.

For each cell, three SGC specimens were compacted to $N_{maximum}$ (160 gyrations) using the modified Pine AFG1 SGC so that conventional SGC compaction parameters and measured stress ratio could be evaluated for each of the cells. Three additional specimens were compacted to N_{design} (100 gyrations) for the Optimum Plus cells.

Shear testing was conducted using the Superpave Shear Tester (SST) to evaluate the resistance of the asphalt mixture to permanent deformation. The FSCH test was conducted at 40°C, 46°C, and 52°C to characterize the high-temperature shear stiffness of the asphalt mixture. The principal response parameter was the complex shear modulus (G^*) at a specified loading frequency (usually 10 Hz).

The RSCH test was also conducted at 58°C to characterize the development of permanent shear strain in the asphalt mixture. The response variable from this test is permanent shear strain at 5,000 cycles. Using a transfer function developed during SHRP, permanent shear strain was converted into an estimated rut depth *(25)*.

The null hypothesis of the experiment was that the SGC parameters derived from the Pine AFG1 SGC (stress ratio, $k \times AV$, $TDI_{92\text{-}96}$) are directly related to the mixture shear stiffness and inversely related to the mixture permanent shear strain.

SGC Compaction Parameters

The SGC parameters selected for evaluation included conventional parameters identified in Tasks 1 and 2, as well as several new compaction parameters that use the shear measurement capabilities of the modified AFG1 SGC. These compaction parameters were as follows:

- Maximum stress ratio (shear stress ÷ normal stress), SR_{max};
- Stress ratio at the final gyration compared with the maximum stress ratio, $SR_{final} \div SR_{max}$;
- Stress ratio at 160 gyrations compared with the maximum stress ratio, $SR_{160} \div SR_{max}$;
- Percentage of compaction at the maximum stress ratio, $\%G_{mm}$ @ SR_{max};
- Number of gyrations at the maximum stress ratio, $N\text{-}SR_{max}$; and
- Performance factor at the final gyration, PF_{final}.

The performance factor at the final gyration, PF_{final}, is a separate parameter calculated by the AFG1 software that the manufacturer believed could be related to mixture rutting performance. Data for each of these factors is presented in Tables 25 through 32.

Three separate statistical analyses were conducted to determine the effects of the input variables on the response variables. These three analyses were identified as the "Equal Voids," "100 Gyrations," and "160 Gyrations" cases. The "Equal Voids" case used data from specimens compacted to 100 gyrations for the Optimum Plus cells and data from specimens compacted to 160 gyrations for the Optimum cells. Because the Optimum Plus cells were 0.8% higher in asphalt binder content than the Optimum cells, the reduction to 100 gyrations should have produced specimens with approximately equal percentages of air voids as the Optimum specimens compacted to 160 gyrations.

The mechanical property testing was conducted on the specimens from the "Equal Voids" case. This was done because the mechanical property tests (shear stiffness and permanent shear strain) are sensitive to the percentage of air

TABLE 25 Compaction slope, *k*

				PG 64-22		PG 76-22	
Aggregate	**Gradation**	**Size, mm**	**% Sand**	**Opt.**	**Opt. +**	**Opt.**	**Opt. +**
Limestone	Coarse	9.5	0	8.481			
			40				5.114
		19	0				8.526
			40	3.997			
	Fine	9.5	0			8.426	
			40		5.358		
		19	0		8.417		
			40			4.091	
Gravel	Coarse	9.5	0		9.464		
			40			4.789	
		19	0			8.362	
			40		4.638		
	Fine	9.5	0				9.400
			40	5.752			
		19	0	7.901			
			40				4.973

TABLE 26 Densification Energy Index, $DEI_{92\text{-}96}$

				PG 64-22		PG 76-22	
Aggregate	**Gradation**	**Size, mm**	**% Sand**	**Opt.**	**Opt. +**	**Opt.**	**Opt. +**
Limestone	Coarse	9.5	0	226			
			40				71
		19	0				95
			40	237			
	Fine	9.5	0			201	
			40		97		
		19	0		102		
			40			289	
Gravel	Coarse	9.5	0		90		
			40			281	
		19	0			177	
			40		81		
	Fine	9.5	0				89
			40	188			
		19	0	208			
			40				64

TABLE 27 Maximum stress ratio, SR_{max}

				PG 64-22		PG 76-22	
Aggregate	**Gradation**	**Size, mm**	**% Sand**	**Opt.**	**Opt. +**	**Opt.**	**Opt. +**
Limestone	Coarse	9.5	0	0.7598			
			40				0.8329
		19	0				0.7362
			40	0.9496			
	Fine	9.5	0			0.7542	
			40		0.8520		
		19	0		0.7911		
			40			0.8861	
Gravel	Coarse	9.5	0		0.7616		
			40			0.8608	
		19	0			0.7786	
			40		0.8975		
	Fine	9.5	0				0.7911
			40	0.8523			
		19	0	0.8175			
			40				0.9220

TABLE 28 Ratio of stress ratio at final gyration to maximum, $SR_{final} \div SR_{max}$

				PG 64-22		PG 76-22	
Aggregate	**Gradation**	**Size, mm**	**% Sand**	**Opt.**	**Opt. +**	**Opt.**	**Opt. +**
Limestone	Coarse	9.5	0	0.9962			
			40				0.9505
		19	0				0.9957
			40	0.9925			
	Fine	9.5	0			0.9683	
			40		0.9878		
		19	0		0.9960		
			40			0.9837	
Gravel	Coarse	9.5	0		0.9960		
			40			0.9852	
		19	0			0.9916	
			40		0.9922		
	Fine	9.5	0				0.9819
			40	0.9796			
		19	0	0.9954			
			40				0.9550

TABLE 29 Ratio of stress ratio at 160 gyrations to maximum, $SR_{160} \div SR_{max}$

				PG 64-22		PG 76-22	
Aggregate	**Gradation**	**Size, mm**	**% Sand**	**Opt.**	**Opt. +**	**Opt.**	**Opt. +**
Limestone	Coarse	9.5	0	0.9962			
			40				0.8081
		19	0				0.9949
			40	0.9925			
	Fine	9.5	0			0.9683	
			40		0.9861		
		19	0		0.9911		
			40			0.9837	
Gravel	Coarse	9.5	0		0.8283		
			40			0.9852	
		19	0			0.9916	
			40		0.9871		
	Fine	9.5	0				0.8601
			40	0.9796			
		19	0	0.9954			
			40				0.9281

TABLE 30 Percentage of compaction at the maximum stress ratio, $\%G_{mm} @ SR_{max}$

				PG 64-22		PG 76-22	
Aggregate	**Gradation**	**Size, mm**	**% Sand**	**Opt.**	**Opt. +**	**Opt.**	**Opt. +**
Limestone	Coarse	9.5	0	95.8			
			40				96.3
		19	0				97.5
			40	96.1			
	Fine	9.5	0			95.1	
			40		96.6		
		19	0		97.2		
			40			95.4	
Gravel	Coarse	9.5	0		97.5		
			40			94.9	
		19	0			96.1	
			40		97.4		
	Fine	9.5	0				96.3
			40	96.9			
		19	0	96.3			
			40				96.5

TABLE 31 Number of gyrations at maximum stress ratio, $N\text{-}SR_{max}$

				PG 64-22		PG 76-22	
Aggregate	**Gradation**	**Size, mm**	**% Sand**	**Opt.**	**Opt. +**	**Opt.**	**Opt. +**
Limestone	Coarse	9.5	0	155			
			40				34
		19	0				95
			40	107			
	Fine	9.5	0			110	
			40		61		
		19	0		98		
			40			91	
Gravel	Coarse	9.5	0		95		
			40			82	
		19	0			129	
			40		72		
	Fine	9.5	0				68
			40	153			
		19	0	152			
			40				35

TABLE 32 Performance factor at the final gyration, PF_{final}

				PG 64-22		PG 76-22	
Aggregate	**Gradation**	**Size, mm**	**% Sand**	**Opt.**	**Opt. +**	**Opt.**	**Opt. +**
Limestone	Coarse	9.5	0	1169			
			40				1225
		19	0				1042
			40	1385			
	Fine	9.5	0			1188	
			40		1556		
		19	0		1124		
			40			1538	
Gravel	Coarse	9.5	0		1284		
			40			1466	
		19	0			1121	
			40		1661		
	Fine	9.5	0				1339
			40	1642			
		19	0	1366			
			40				1261

voids in the test specimens. Usually, a lower percentage of air voids in an SGC-compacted specimen has the effect of indicating "better" mechanical property results (higher shear stiffness, lower permanent shear strain). Thus, specimens from the Optimum Plus cells would have lower percentages of air voids at the same compaction as specimens from the Optimum cells. As a result, the Optimum Plus cells could indicate better-than-expected mechanical properties despite a significantly higher (0.8%) asphalt binder content.

The "100 Gyrations" and "160 Gyrations" analyses were conducted entirely on specimens compacted at 100 and 160 gyrations, respectively. These analyses were selected because they better represented the likely use of an SGC parameter in mix design and field QC operations (specimens are compacted to a specified number of gyrations, not a target percentage of air voids).

Tables 33 through 35 provide data from the statistical analyses. Factors that are considered statistically significant (at the 5% significance level) are indicated for each of the response variables.

Of the response variables, the compaction slope (k) and number of gyrations at the maximum stress ratio ($N\text{-}SR_{max}$) were most affected by the input variables. As expected, the compaction slope was affected by every main factor, except for asphalt binder stiffness. However, the actual effect on the compaction slope was mixed and not intuitive. For example, the compaction slope increased as the percentage of sand decreased from 40% to 0%. This would lead to the expectation that a higher compaction slope is better (higher sand percentage is expected to lower mixture shear resistance). Unfortunately, the compaction slope also increases as the asphalt binder content increases. This result does not coincide with the effect of sand percentage.

TABLE 33 Statistical analysis—"equal voids"

	Input Variable					
Response Variable	**Aggregate**	**Gradation**	**Size**	**Sand Percentage**	**Binder Stiffness**	**Binder Content**
K	Y	Y	Y	Y		Y
$DEI_{92\text{-}96}$	Y			Y		Y
SR_{max}	Y		Y	Y	Y	
$SR_{final} \div SR_{max}$				Y	Y	
$SR_{160} \div SR_{max}$			Y			Y
$N\text{-}SR_{max}$				Y	Y	Y
$\%G_{mm}$ @ SR_{max}			Y		Y	Y
PF_{final}	Y			Y	Y	

TABLE 34 Statistical analysis—"100 gyrations"

	Input Variable					
Response Variable	**Aggregate**	**Gradation**	**Size**	**Sand Percentage**	**Binder Stiffness**	**Binder Content**
K	Y	Y	Y	Y		Y
$DEI_{92\text{-}96}$						Y
SR_{max}			Y	Y	Y	
$SR_{final} \div SR_{max}$				Y	Y	Y
$SR_{160} \div SR_{max}$	*Cannot evaluate this parameter for specimens compacted to 100 gyrations.*					
$N\text{-}SR_{max}$	Y	Y	Y	Y	Y	Y
$\%G_{mm}$ @ SR_{max}		Y			Y	Y
PF_{final}			Y	Y	Y	

TABLE 35 Statistical analysis—"160 gyrations"

	Input Variable					
Response Variable	**Aggregate**	**Gradation**	**Size**	**Sand Percentage**	**Binder Stiffness**	**Binder Content**
K	Y		Y	Y		Y
$DEI_{92\text{-}96}$	Y			Y		Y
SR_{max}			Y	Y		
$SR_{final} \div SR_{max}$			Y			Y
$SR_{160} \div SR_{max}$	*Same evaluation as previous parameter for specimens compacted to 160 gyrations.*					
$N\text{-}SR_{max}$			Y	Y	Y	Y
$\%G_{mm}$ @ SR_{max}			Y		Y	Y
PF_{final}		Y		Y		Y

The $N\text{-}SR_{max}$ values were affected by every main factor in the "100 Gyrations" analysis, and by the Binder Content, Sand Percentage, and Binder Stiffness in the other two analyses. Directionally, the analysis also makes sense for most of the variables as indicated in Table 36.

As indicated in Table 36, the number of gyrations at the maximum stress ratio is negatively affected by an increase in sand, increase in asphalt binder content, use of a crushed gravel instead of limestone, and use of smaller nominal maximum aggregate size. If a negative effect on $N\text{-}SR_{max}$ correlates with poorer expected rutting performance, then all four of these effects match expectations (changing the gradation from Fine to Coarse negatively affects $N\text{-}SR_{max}$). However, it is not intuitive that this effect will necessarily correlate with rutting performance.

The only counter-intuitive effect is that $N\text{-}SR_{max}$ decreases as a PG 76 asphalt binder is used instead of a PG 64 asphalt binder. This would seem to indicate that a PG 64 asphalt binder would have better rutting performance than a PG 76 asphalt binder.

Based on the findings of the statistical analysis on the compaction data, the number of gyrations at the maximum stress ratio ($N\text{-}SR_{max}$) appeared to be a strong possibility as the SGC parameter most related to rutting potential. This hypothesis was further tested by the addition of the mechanical property test results.

Mechanical Property Testing

Specimens were either compacted to 100 (Optimum Plus) or 160 gyrations (Optimum) to achieve approximately the same percentage of air voids. After collection of the compaction data, the specimens were sawed to a height of 50 mm for testing using the SST.

TABLE 36 Effect of input variables on $N\text{-}SR_{max}$ values ("100 gyrations" analysis)

As ___ INCREASES from	___	to	___	N-SR_{max} ___	By ____ gyrations
Sand	0%		40%	DECREASES	29
Binder Stiffness	PG 64		PG 76	DECREASES	19
Gradation	Coarse		Fine	INCREASES	11
Binder Content	Opt		Opt+	DECREASES	10
Aggregate	Gravel		Limestone	INCREASES	7
Nominal Max. Aggr. Size	9.5mm		19mm	INCREASES	6

Mechanical property testing consisted of determining mixture shear stiffness (G^*) at three temperatures (40, 46, and 52°C) and ten loading frequencies (10 Hz to 0.01 Hz). Following FSCH testing, the specimens were tested to determine permanent shear strain and estimated rut depth, using the RSCH test at 58°C.

Shear stiffness data at 10 Hz is presented for the 16 cells in the first two fractional factorials in Tables 37 through 39. Data on the estimated rut depth at 58°C (from the RSCH test) is presented in Table 40. The relationship between estimated rut depth and high-temperature shear stiffness for all 16 cells (43 data points) is illustrated in Figure 40.

Preliminary analysis indicates a decent correlation (R^2 = 0.63) between the complex shear modulus (10 Hz loading frequency) of the mixtures at 52°C and the estimated rut depth (determined from the RSCH test) at 58°C. Data from Cells 31, 39, and 53 have the greatest difference between the actual data and the trendline. In all, the six data points from the three cells indicate estimated rut depth values much higher than are indicated by the mixture shear stiffness. An examination of the main factors indicate that Cells 31, 39, and 53 have only two main factors in common—optimum asphalt binder content and 40% sand. It is possible that the 40% sand content has a stiffening effect on the asphalt mixtures that does not translate into shear resistance.

A statistical analysis was conducted on the mechanical property test data to determine the effects of the main factors (and significant interactions) on the shear stiffness and estimated rut depth of the asphalt mixtures. Because the mechanical property testing was only conducted on specimens compacted to approximately equal percentages of air voids, only the "Equal Voids" analysis was conducted.

With the compaction data, the main effects of the factors dominated with some evidence of the existence of interactions. With the mechanical property data, some interactions appear to have significant effects. Statistically significant factors (at 5% significance level) are Binder Stiffness, Size, Sand Percentage, and Binder Content. However, because of interactions between these factors, the main effect of each factor differs depending on the values of the other factors.

For estimated rut depth at 58°C, effects were determined for the following interactions:

Binder Stiffness Interaction with Size

- For PG 64-22 asphalt binders, the estimated rut depth increases by 4.5 mm as the size of the mixture decreases from 19 mm to 9.5 mm.
- For PG 76-22 asphalt binders, the estimated rut depth increases by 1.5 mm as the size of the mixture decreases from 19 mm to 9.5 mm.

TABLE 37 Complex shear modulus (MPa) at 10 Hz and 40°C

				PG 64-22		PG 76-22	
Aggregate	**Gradation**	**Size, mm**	**% Sand**	**Opt.**	**Opt. +**	**Opt.**	**Opt. +**
Limestone	Coarse	9.5	0	504			
			40				372
		19	0				434
			40	533			
	Fine	9.5	0			501	
			40		274		
		19	0		324		
			40			591	
Gravel	Coarse	9.5	0		174		
			40			479	
		19	0			654	
			40		389		
	Fine	9.5	0				319
			40	374			
		19	0	557			
			40				622

TABLE 38 Complex shear modulus (MPa) at 10 Hz and 46°C

				PG 64-22		PG 76-22	
Aggregate	**Gradation**	**Size, mm**	**% Sand**	**Opt.**	**Opt. +**	**Opt.**	**Opt. +**
Limestone	Coarse	9.5	0	282			
			40				229
		19	0				225
			40	294			
	Fine	9.5	0			330	
			40		131		
		19	0		190		
			40			325	
Gravel	Coarse	9.5	0		124		
			40			261	
		19	0			452	
			40		201		
	Fine	9.5	0				163
			40	229			
		19	0	312			
			40				389

TABLE 39 Complex shear modulus (MPa) at 10 Hz and 52°C

				PG 64-22		PG 76-22	
Aggregate	**Gradation**	**Size, mm**	**% Sand**	**Opt.**	**Opt. +**	**Opt.**	**Opt. +**
Limestone	Coarse	9.5	0	168			
			40				137
		19	0				126
			40	145			
	Fine	9.5	0			186	
			40		63		
		19	0		109		
			40			175	
Gravel	Coarse	9.5	0		89		
			40			130	
		19	0			274	
			40		82		
	Fine	9.5	0				93
			40	128			
		19	0	162			
			40				245

TABLE 40 Estimated rut depth (mm) from RSCH at 58°C

				PG 64-22		PG 76-22	
Aggregate	**Gradation**	**Size, mm**	**% Sand**	**Opt.**	**Opt. +**	**Opt.**	**Opt. +**
Limestone	Coarse	9.5	0	7.8			
			40				4.8
		19	0				7.8
			40	5.8			
	Fine	9.5	0			3.7	
			40		16.9		
		19	0		7.2		
			40			8.0	
Gravel	Coarse	9.5	0		11.3		
			40			9.8	
		19	0			3.6	
			40		9.9		
	Fine	9.5	0				8.5
			40	13.4			
		19	0	6.9			
			40				3.1

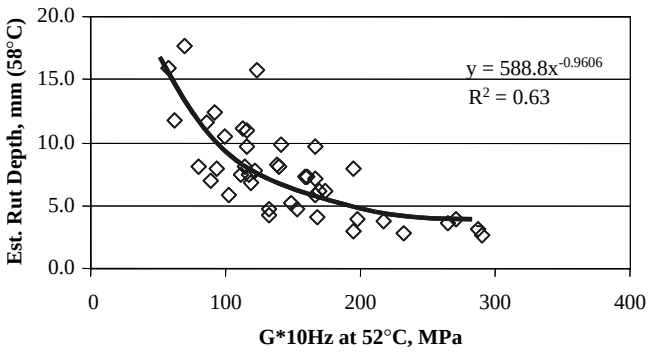

Figure 40. Relationship between high temperature shear stiffness and rut depth.

Sand Percentage Interaction with Size

- For 0% Sand mixtures, the estimated rut depth increases by 1.4 mm as the size of the mixture decreases from 19 mm to 9.5 mm.
- For 40% Sand mixtures, the estimated rut depth increases by 4.3 mm as the size of the mixture decreases from 19 mm to 9.5 mm.

Sand Percentage Interaction with Binder Stiffness

- For 0% Sand mixtures, the estimated rut depth increases by 2.4 mm using a PG 64-22 asphalt binder instead of a PG 76-22 asphalt binder.
- For 40% Sand mixtures, the estimated rut depth increases by 4.8 mm using a PG 64-22 asphalt binder instead of a PG 76-22 asphalt binder.

Sand Percentage Interaction with Binder Content

- For 0% Sand mixtures, the estimated rut depth increases by 3.2 mm using the Optimum-Plus asphalt binder content instead of the Optimum asphalt binder content.
- For 40% Sand mixtures, the estimated rut depth decreases by 1.4 mm using the Optimum-Plus asphalt binder content instead of the Optimum asphalt binder content.

In the analysis, most of the data appear reasonable, except for the last significant interaction (Sand Percentage with Binder Content). In this case, the Optimum-Plus condition of the 40% Sand mixtures indicates better estimated rutting performance than the 40% Sand mixtures with Optimum asphalt binder contents. An examination of the data indicates that this result is caused by the performance of the mixtures in Cell 64 and Cell 8. The Cell 64 mixture has the best overall rutting performance (lowest estimated rut depth) of all sixteen mixtures. The Cell 8 mixture has the fourth best overall rutting performance. It is not clear why these mixtures perform better than expected. One possible reason is that the average percentage of air voids in the test specimens in Cells 8 and 64 were considerably lower (1.7%) than the average of the rest of the test specimens from the remaining cells (3.1%).

For shear stiffness (G^*_{10Hz}) at 52°C, effects were determined for the following interactions:

Binder Stiffness Interaction with Size

- For PG 64-22 asphalt binders, the shear stiffness increases by 12 MPa as the size of the mixture increases from 9.5 mm to 19 mm.
- For PG 76-22 asphalt binders, the shear stiffness increases by 71 MPa as the size of the mixture increases from 9.5 mm to 19 mm.

Sand Percentage Interaction with Binder Content

- For 0% Sand mixtures, the shear stiffness increases by 93 MPa using the Optimum asphalt binder content instead of the Optimum-Plus asphalt binder content.
- For 40% Sand mixtures, the shear stiffness decreases by 2 MPa using the Optimum asphalt binder content instead of the Optimum-Plus asphalt binder content.

Once again, most of the data appear reasonable, except for the last significant interaction (Sand Percentage with Binder Content). In this case, the Optimum-Plus condition of the 40% Sand mixtures indicates better shear stiffness than the 40% Sand mixtures with Optimum asphalt binder contents. An examination of the data again indicates that this is caused by the performance of the mixture in Cell 64, which has the second highest shear stiffness at 52°C.

In general, the estimated rut depth follows expectations. For instance, the average rut depth of mixtures made with PG 64-22 asphalt binders is higher (9.5 mm) than the average rut depth of mixtures made with PG 76-22 asphalt binders (6.0 mm).

An examination of the entire data set indicates that the only significant correlation occurs between shear stiffness (G^*_{10Hz} at 52°C) and N-SR_{max} for the mixtures made with PG 64-22 asphalt binder. This is illustrated in Figure 41.

Unfortunately, other main effects are not as clear for mixtures made with PG 76-22 asphalt binders as PG 64-22 asphalt binders. This is indicated in Tables 41 and 42, where the effects of Sand Percentage and Binder Content are separated by Binder Stiffness.

The data in Tables 41 and 42 indicate that the mixtures made with PG 64-22 asphalt binders respond rationally to changes in Binder Content and Sand Percentage. Estimated rut depth increases and shear stiffness decreases as Sand Percentage increases (0% to 40%) or Binder Content increases (Optimum to Optimum-Plus). Mixtures made with PG 76-22 asphalt binders react much less to these changes.

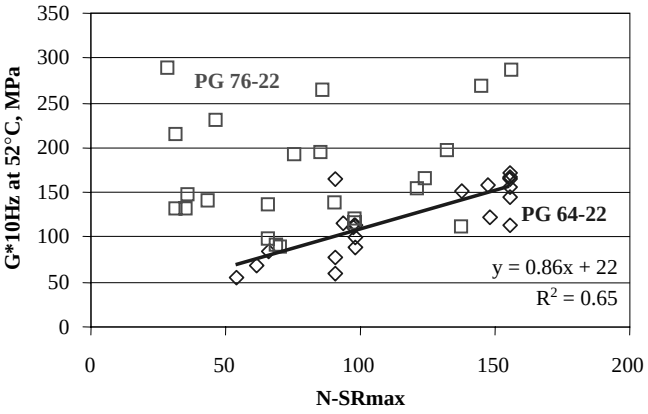

Figure 41. Relationship between shear stiffness and N-SR$_{max}$ (equal voids analysis).

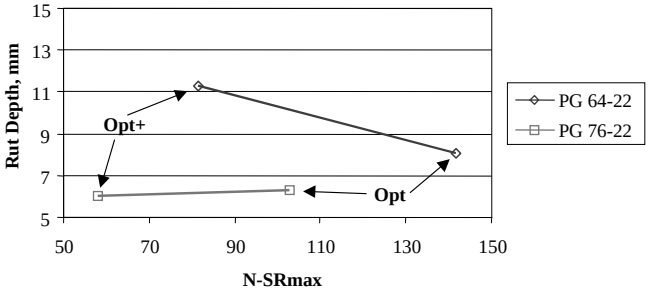

Figure 42. Effect of binder content—relationship between N-SR$_{max}$ and rut depth (equal voids analysis).

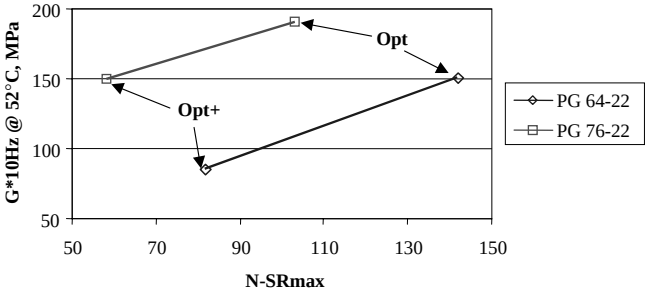

Figure 43. Effect of binder content—relationship between N-SR$_{max}$ and stiffness (equal voids analysis).

Because *N-SR*$_{max}$ values react significantly to changes in Sand Percentage and Binder Content, Figures 42 through 45 were created to show the relative relationship between *N-SR*$_{max}$ and mechanical property test results.

Figures 42 through 45 indicate that, for the mixtures made with the PG 64-22 asphalt binder, there is some apparent relationship between the *N-SR*$_{max}$ values and the mixture mechanical property tests. The relative insensitivity of the mixtures made with the PG 76-22 asphalt binder indicates that the binder stiffness dominates the mixture performance at the test temperatures (52°C for shear stiffness and 58°C for estimated rut depth).

Based on the test results and subsequent discussions with the project statistician, *N-SR*$_{max}$ value measured during SGC compaction was selected as the parameter with the greatest potential for identifying mixtures with poor rutting potential. This potential was further explored in Part B (field validation) experiments.

Selection of *N-SR*$_{max}$ Parameter

In the main laboratory experiment, the only significant correlation occurred between high temperature shear stiffness (G^*_{10Hz} at 52°C) and *N-SR*$_{max}$ (hereafter designated as *N-SR*$_{max}$) for the mixtures made with PG 64-22 asphalt binder (see Figure 41).

One of the possible problems with the poor correlation, in general, between the *N-SR*$_{max}$ parameter and mechanical properties was attributed to the determination of *N-SR*$_{max}$. The spreadsheet used to calculate the *N-SR*$_{max}$ value searches for the absolute maximum value and the number of gyrations at which this value occurs. This approach treats the stress ratio graph as a series of discrete data points rather than as a curve. An example of this is illustrated in Figure 46.

As illustrated in Figure 46, the stress ratio is oscillating between high and low values on consecutive gyrations.

TABLE 41 Effect of sand percentage on mechanical property results

	Est. Rut Depth @ 58°C, mm			G^*_{10Hz} @ 52°C, MPa		
	0%	40%	Δ	0%	40%	Δ
PG 64-22	8.3	11.1	+2.8	132	104	-28
PG 76-22	5.9	6.4	+0.5	170	172	+2

TABLE 42 Effect of binder content on mechanical property results

	Est. Rut Depth @ 58°C, mm			G^*_{10Hz} @ 52°C, MPa		
	Opt	Opt+	Δ	Opt	Opt+	Δ
PG 64-22	8.1	11.3	+3.2	151	86	-65
PG 76-22	6.3	6.0	-0.3	191	150	-41

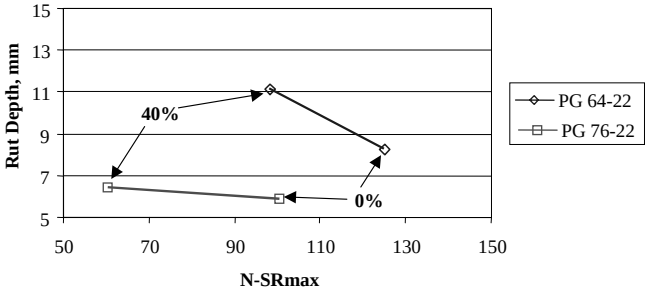

Figure 44. Effect of sand content—relationship between N-SR_{max} and rut depth (equal voids analysis).

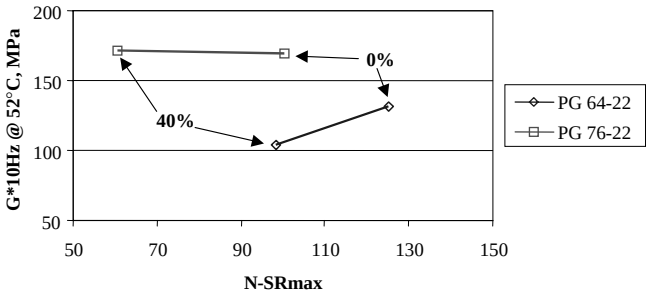

Figure 45. Effect of sand content—relationship between N-SR_{max} and stiffness (equal voids analysis).

There also is an apparent early peak (SR = 0.95707 at the 87th gyration) and a late peak (SR = 0.95723 at the 137th gyration), which is the location of the actual maximum stress ratio value. Between the two peaks, the curve dips into a trough. The cause of this behavior is not clear, but is illustrated also with one of the two remaining replicates from this cell. Because the mixture is a coarse 19-mm mixture, it is possible that this behavior may be caused by the coarse aggregate interlock.

Replicate 2 in Figure 47 illustrates the same behavior as Replicate 1 in Figure 46. The stress ratio curve reaches a peak, then decreases to a minimum before increasing again. Replicate 3 reaches a peak, then appears to slowly decline. The unusual behavior in Figures 46 and 47 resulted in $N\text{-}SR_{max}$ values of 137, 93, and 90 gyrations for Cell 13. Although the range of $N\text{-}SR_{max}$ values was 47 gyrations, the corresponding estimated rut depth values only had a spread of 2 mm (4.8 mm to 6.8 mm). This discrepancy allowed for poor correlation between $N\text{-}SR_{max}$ and estimated rut depth.

In an effort to improve the repeatability of the $N\text{-}SR_{max}$ values within a set of three specimens for each mixture and eliminate false peaks caused by identifying absolute maximum values, the stress ratio curve was plotted from 10 gyrations to the maximum (160 gyrations) on a normal, arithmetic scale. A second-order polynomial was then fit to the data. The $N\text{-}SR_{max}$ value was identified as the point where the derivative of the equation (dSR/dN) was equal to zero. This approach is illustrated in Figure 48 for the data shown in Figure 46.

When the curve fitting (regression) approach was used for the specimens in Cell 13, the $N\text{-}SR_{max}$ values were 108, 107, and 104 gyrations. The average value (106 gyrations) was nearly identical to the average value obtained without the regression (107 gyrations), but the repeatability was significantly improved. The coefficient of variation for the curve-fit data was 2% compared with 20% for the actual (not regressed) data.

The $N\text{-}SR_{max}$ values determined using a second-order polynomial regression are indicated in Table 43.

The data in Table 43 also include the "goodness of fit" or R^2 value of each of the regressions. As an arbitrary regression quality criterion, values of R^2 less than 0.75 were considered suspect. Using this criterion, 12 of the 48 specimens had unacceptable regressions. This included all three specimens in Cells 19 and 53. Examination of the data in these cells indicated that there was a sudden transition in the stress ratio early in the compaction sequence (less than 20 gyrations), coupled with data scatter late in the compaction sequence (greater than 100 gyrations). This is illustrated in Figure 49.

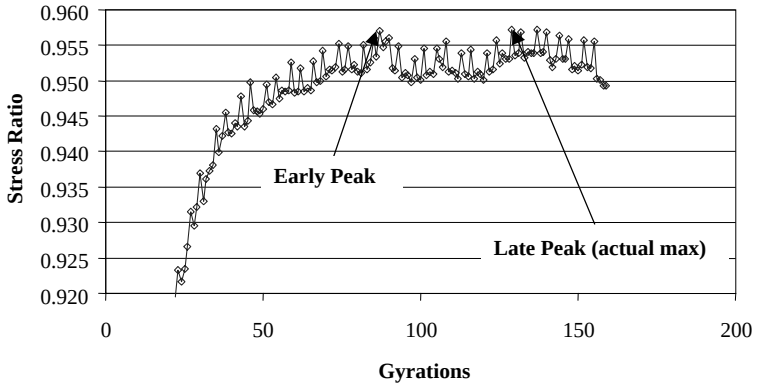

Figure 46. Expanded stress ratio curve—two peaks (19-mm Limestone Coarse, 40NS, PG 64-22, Opt, Rep 7-14-10 [Cell 13]).

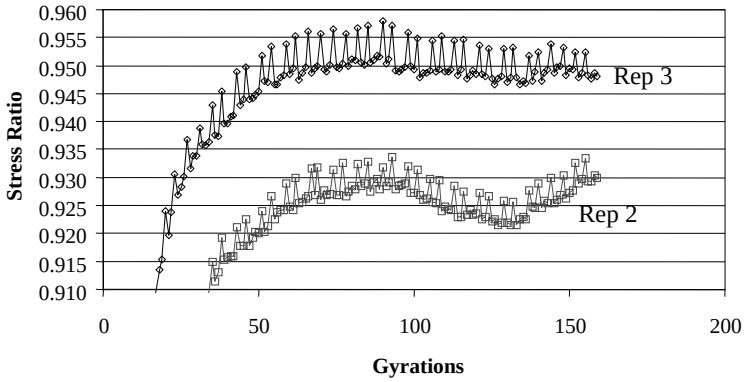

Figure 47. Expanded stress ratio curve—two replicates from Cell 13 (19-mm Limestone Coarse, 40NS, PG 64-22, Opt).

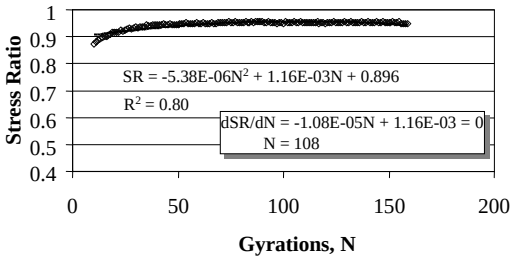

Figure 48. N-SR_{max} determined using second-order polynomial regression (19-mm Limestone Coarse, 40NS PG 64-22, Opt, Rep 7-14-10 [Cell 13]).

All three specimens from Cell 19 experienced an increase in stress ratio of approximately 0.07 after completion of the 17th gyration. All three specimens from Cell 53 experienced the same magnitude of increase in stress ratio after completion of the 12th gyration. The two mixtures are somewhat dissimilar. The Cell 19 mixture is a 9.5-mm Limestone Fine mix with 0% sand. The Cell 53 mixture is a 9.5-mm Gravel Fine mix with 40% sand. Both mixtures were produced at the optimum asphalt binder content.

The behavior illustrated in Figure 49 may be traced to the performance factor measurements for each mixture. This performance factor measurement is calculated using data collected from the modified Pine AFG1 SGC. For all mixtures, the performance factor graph indicates a sudden transition between 9 and 18 gyrations. This transition may be caused by a change in the software control algorithm used to calculate the performance factor. For the mixtures in Cells 19 and 53, the transition in the performance factor curve occurs at the exact instant as the transition in the stress ratio curve. This suggests that the problem illustrated in Figure 49 is not a material problem, but a problem with the control and data acquisition software.

The hypothesis that this was a control or data acquisition software problem rather than a material problem was somewhat validated through the compaction of additional specimens from Cell 53. Figure 50 provides an illustration of the original compaction data from October 2000 (with sudden stress ratio transition and data scatter). Figure 51 represents

TABLE 43 *N-SR*$_{max}$ determined from regression

	N-SR_{max}					R^2			
	Replicate					Replicate			
Cell	1	2	3	Average	CV	1	2	3	Average
1	130	132	142	**135**	**4%**	0.96	0.94	0.93	**0.94**
8	32	42	38	**37**	**11%**	0.98	0.99	0.99	**0.99**
12	136	132	126	**131**	**3%**	0.94	0.96	0.96	**0.95**
13	108	107	104	**106**	**2%**	0.80	0.79	0.77	**0.79**
19	108	98	102	**103**	**4%**	0.73	0.53	0.62	**0.63**
22	78	93	107	**93**	**13%**	0.54	0.67	0.80	**0.67**
26	117	121	129	**122**	**4%**	0.97	0.98	0.96	**0.97**
31	104	109	91	**101**	**7%**	0.75	0.92	0.67	**0.78**
34	101	96	62	**86**	**20%**	0.96	0.91	0.97	**0.95**
39	121	95	86	**101**	**15%**	0.83	0.61	0.53	**0.66**
43	104	134	113	**117**	**11%**	0.81	0.78	0.83	**0.81**
46	111	96	109	**105**	**6%**	0.86	0.66	0.90	**0.81**
52	77	76	65	**73**	**7%**	0.97	0.98	0.97	**0.97**
53	102	109	98	**103**	**4%**	0.42	0.50	0.30	**0.41**
57	121	117	130	**123**	**4%**	0.87	0.92	0.95	**0.91**
64	45	66	55	**55**	**15%**	0.94	0.79	0.85	**0.86**

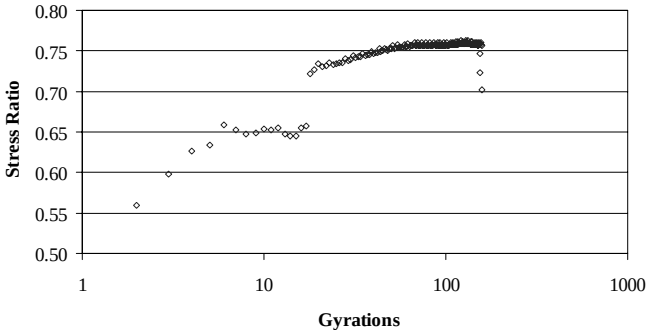

Figure 49. Example of sudden stress ratio transition with data scatter (9.5-mm Limestone Fine, 0NS PG 76-22, Opt, Rep 9-28-6 [Cell 19]).

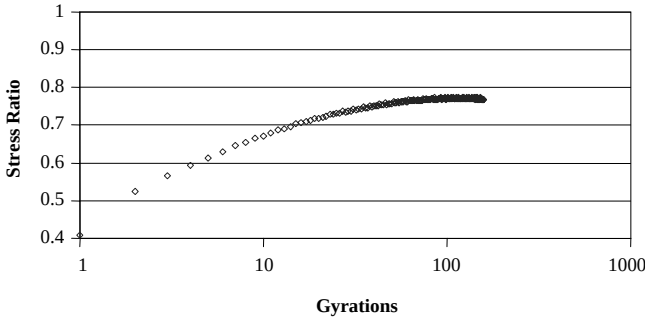

Figure 51. Cell 53 specimen compacted in June 2001 (9.5-mm Gravel Fine, 40NS PG 64-22, Opt [6.3%], Rep 1 [Cell 53]).

data from specimens compacted at the Asphalt Institute laboratory using the same compactor in June 2001. If the problem was simply related to the mixture, then the two graphs should have the same shape.

Clearly, the data in Figure 51 represent a much smoother transition. The correlation was poor for the data in Figure 50 ($R^2 = 0.42$) and its companion specimens compared with the data in Figure 51 ($R^2 = 0.89$), but the average $N\text{-}SR_{max}$ values were approximately the same. The data in Figure 50 yielded an average $N\text{-}SR_{max}$ value of 103. The data in Figure 51 resulted in an average $N\text{-}SR_{max}$ value of 107.

An examination of the other cells with poor regression correlation values indicates that the second-order polynomial did not adequately capture the initial curvature of the stress ratio curve. No sudden transition in the stress ratio or significant data scatter was noted.

A comparison of the $N\text{-}SR_{max}$ values determined from the actual data and the regression is presented in Table 44.

The data in Table 44 indicates that the regression can result in a significant reduction in the coefficient of variation (CV) within a mixture—thus indicating an improvement in repeatability. The average CV for the $N\text{-}SR_{max}$ regression values is 8%, compared with 19% for the actual $N\text{-}SR_{max}$ values. The overall effect of the regression appears to be, as expected, a normalizing effect. On average, high $N\text{-}SR_{max}$ values are slightly lower using the regression, while low $N\text{-}SR_{max}$ values are slightly higher. The improvement in repeatability, however, offsets this normalizing effect and, in the opinion of the research team, improves the utility of the $N\text{-}SR_{max}$ parameter as a mixture performance-screening tool.

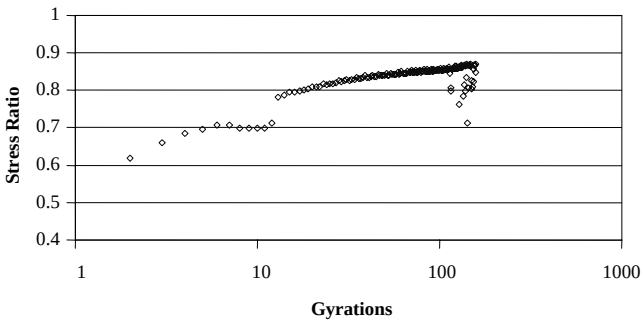

Figure 50. Cell 53 specimen compacted in October 2000 (9.5-mm Gravel Fine, 40NS PG64-22, Opt, Rep 10-16-4 [Cell 53]).

With the improvement in repeatability, a relationship was once again sought between mixture mechanical (performance) properties and $N\text{-}SR_{max}$. The average estimated rut depth for each mixture is illustrated as a function of $N\text{-}SR_{max}$ in Figure 52. The average high temperature shear stiffness is illustrated as a function of $N\text{-}SR_{max}$ in Figure 53.

The data in Figures 52 and 53 illustrate similar responses. In each case, there is no significant relationship between the performance of the PG 76-22 asphalt mixtures and $N\text{-}SR_{max}$ values. This may be due to the inability of the SGC, operating at high temperatures, to capture the effects of the modified PG 76-22 asphalt binder adequately.

Figures 52 and 53 also indicate some relationship between mechanical properties $N\text{-}SR_{max}$ values for the PG 64-22 asphalt mixtures. In each case, the trend is in the correct direction—increasing $N\text{-}SR_{max}$ results in better high temperature stiffness and lower estimated rutting. Although neither correlation is strong, the use of the calculated $N\text{-}SR_{max}$ values rather than the "actual" peak values does provide some improvement, as illustrated in Figure 54.

The data illustrated in Figure 54 indicate that the use of the "actual" $N\text{-}SR_{max}$ values results in a poorer correlation and a flatter slope (less sensitivity of estimated rut depth to changes in $N\text{-}SR_{max}$ values) than the use of the "regressed" $N\text{-}SR_{max}$ values.

Although the use of regressed (or calculated) $N\text{-}SR_{max}$ values improves the correlation with mechanical properties, the predictive relationship is still generally weak. In other words, the regression equations cannot be used to accurately predict the high temperature shear stiffness or estimated rut depth of a mixture from the $N\text{-}SR_{max}$ values obtained during the SGC compaction process. However, while the relationship between $N\text{-}SR_{max}$ values and mixture mechanical properties may not be good enough to get an accurate estimate of the rut depth of an

TABLE 44 Comparison of $N\text{-}SR_{max}$ (actual data) and $N\text{-}SR_{max}$ (regression)

	Actual $N\text{-}SR_{max}$					Regressed $N\text{-}SR_{max}$				
Cell	**1**	**2**	**3**	**Average**	**CV**	**1**	**2**	**3**	**Average**	**CV**
1	155	155	155	**155**	**0%**	130	132	142	**135**	**4%**
8	31	39	31	**34**	**11%**	32	42	38	**37**	**11%**
12	140	155	124	**140**	**9%**	136	132	126	**131**	**3%**
13	137	93	90	**107**	**20%**	108	107	104	**106**	**2%**
19	124	75	132	**110**	**23%**	108	98	102	**103**	**4%**
22	53	69	159	**94**	**50%**	78	93	107	**93**	**13%**
26	121	122	148	**130**	**10%**	117	121	129	**122**	**4%**
31	66	121	85	**91**	**25%**	104	109	91	**101**	**7%**
34	93	98	59	**83**	**21%**	101	96	62	**86**	**20%**
39	137	66	43	**82**	**49%**	121	95	86	**101**	**15%**
43	86	156	145	**129**	**24%**	104	134	113	**117**	**11%**
46	155	62	124	**114**	**34%**	111	96	109	**105**	**6%**
52	69	66	53	**63**	**11%**	77	76	65	**73**	**7%**
53	148	155	155	**153**	**2%**	102	109	98	**103**	**4%**
57	155	147	155	**152**	**2%**	121	117	130	**123**	**4%**
64	39	59	43	**47**	**18%**	45	66	55	**55**	**15%**

asphalt mixture, it may be good enough to identify gross mixture instability, thus serving as a screening test for further mechanical property tests.

To explore the potential of the $N\text{-}SR_{max}$ value as an indicator of mixture performance rather than as a predictor of mixture performance, the data from the PG 64-22 asphalt mixtures was examined.

Mixture Performance Screening Using $N\text{-}SR_{max}$

All of the mixtures in the main experiment were designed using 100 gyrations ($N_{maximum}$ = 160 gyrations). Because N_{design} was intended to represent the design traffic loading for the mixtures, it was hypothesized that values of $N\text{-}SR_{max}$ less than N_{design} (100 gyrations) would represent a potentially weak mixture. Similarly, values of $N\text{-}SR_{max}$ greater than the next higher N_{design} level (125 gyrations) should represent a strong mixture. Using these criteria, the data from the 24 specimens of the eight PG 64-22 asphalt mixtures were separated into categories as indicated in Table 45.

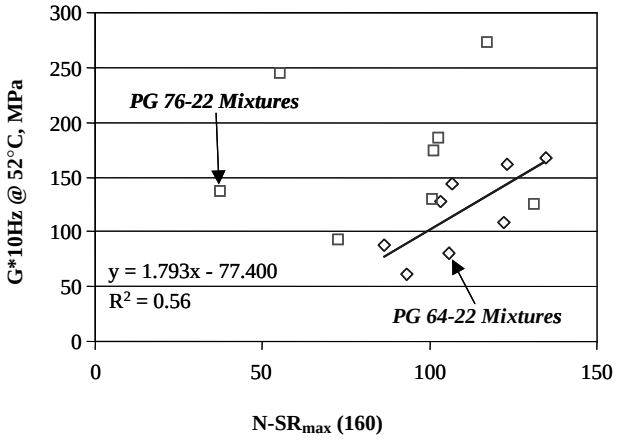

Figure 53. High temperature shear stiffness (G^*_{10Hz} at 52°C) as a function of $N\text{-}SR_{max}$.

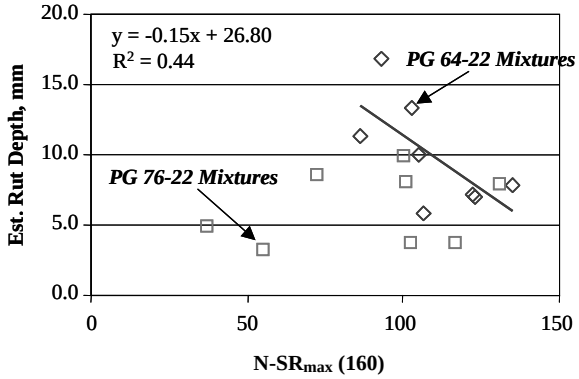

Figure 52. Estimated rut depth (from RSCH test at 58°C) as a function of $N\text{-}SR_{max}$.

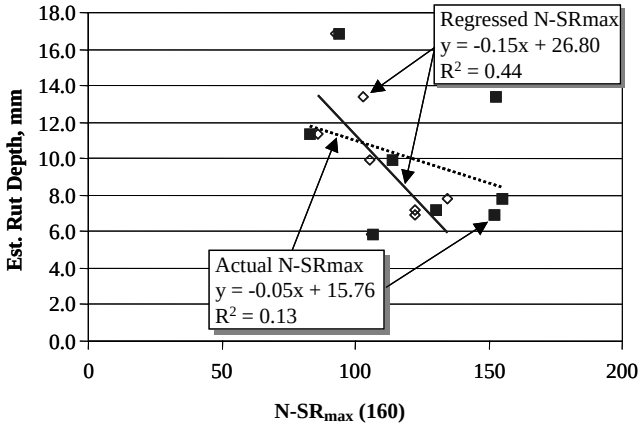

Figure 54. Estimated rut depth as a function of actual and regressed $N\text{-}SR_{max}$ values.

TABLE 45 $N\text{-}SR_{max}$ performance categories

$N\text{-}SR_{max}$	Expected Performance
> 125	Good
100 - 125	Fair
< 100	Poor

Using the criteria in Table 45, the $N\text{-}SR_{max}$ values indicated Good expected performance for five specimens. $N\text{-}SR_{max}$ values indicated Fair expected performance for 13 specimens and Poor expected performance for 6 specimens. Table 46 indicates the average estimated rut depth and high-temperature shear stiffness for each of the three performance groups.

As indicated in Table 46, the general categories established by the $N\text{-}SR_{max}$ values relate well to the actual, measured performance. For example, the average estimated rut depth of the five specimens that indicated Good performance was much lower than the average estimated rut depth of the six specimens that indicated Poor performance. Likewise, the shear stiffness of the Good group was considerably higher than the shear stiffness of the Poor group.

The measured performance of the specimens was also generally categorized. For estimated rut depth, it was assumed that values less than 6.25 mm at 5,000 cycles (roughly 3-million ESALs using the SHRP A-003A transfer function) were Good. Estimated rut depth values greater than 12.5 mm were categorized as Poor. Estimated rut depth values between 6.25 and 12.5 mm were categorized as Fair.

Using the relationship illustrated in Figure 40 between estimated rut depth and high-temperature shear stiffness, corresponding values of shear stiffness were calculated for Good, Fair, and Poor performance. Any value of G^*_{10Hz} at 52°C greater than 150 MPa was considered Good, while any value less than 75 MPa was considered Poor. Values between 75 and 150 MPa were considered Fair.

Table 47 provides $N\text{-}SR_{max}$ predicted performance data and actual, measured performance data for the 24 specimens produced using PG 64-22 asphalt binder. The data in Table 47 can be examined to determine the number of times the $N\text{-}SR_{max}$ performance matches the actual measured performance. These data are presented in Table 48.

The data in Table 48 indicate that approximately 75 to 80% of the time, the $N\text{-}SR_{max}$ parameter indicates either the same performance as measured by the mechanical property tests or worse performance than indicated by the mechanical property tests. In this respect, it appears that the $N\text{-}SR_{max}$ parameter provides a conservative estimate of the actual mixture performance. The $N\text{-}SR_{max}$ parameter never provides a Good result when the mechanical properties are Poor, or a Poor result when the mechanical properties are Good.

The six Poor results in Table 47 (indicated by $N\text{-}SR_{max}$ value less than 100) were obtained from four mixtures: two specimens each from Cells 22 and 34, and one specimen each from Cells 46 and 53. These four mixtures also exhibited the four highest estimated rut depth values. Consequently, it was decided that a single Poor result could be indicative of Poor mixture mechanical properties, for a given mixture, even when the average $N\text{-}SR_{max}$ value is acceptable.

Based on the findings from the experiment (PG 64-22 asphalt mixtures), a procedure was developed for screening the performance of an asphalt mixture during compaction.

The following procedure may be used as a screening test for the anticipated performance of an asphalt mixture. (Currently, the screening procedure evaluates aggregate structure and asphalt binder volume effects. Asphalt binder stiffness effects [i.e., using a PG 76-22 instead of the climate-only recommended grade of PG 64-22] are not accounted for.)

1. Compact three specimens to $N_{maximum}$ using an SGC with the capability to measure shear stress during compaction. This may involve the use of the Servopac, Pine Modified AFG1, or other compactor with a shear plate or other shear stress measurement capability. The stress ratio is determined at each gyration as the measured shear stress divided by the applied normal stress (nominally 600 kPa).
2. Plot the stress ratio as a function of gyrations on a normal arithmetic scale from 10 gyrations to $N_{maximum}$.
3. Fit a second-order polynomial curve to the stress ratio data ($SR = aN^2 + bN + c$). Determine the regression equation and correlation (R^2).
4. If the R^2 of the regression is less than 0.75, examine the data. If the low correlation is the result of data scatter, then the specimen should be discarded and a replacement specimen made (if necessary). If the low correlation is the result of the inability of the regression equation to account for the initial curvature (below 20 gyrations), then keep the specimen results and make a note of the reason for the low correlation.
5. Determine the number of gyrations where the slope of the curve is flat. This is done by taking the derivative of the equation, setting it equal to zero ($dSR/dN = 0 =$

TABLE 46 Expected performance (from $N\text{-}SR_{max}$) compared with actual performance

$N\text{-}SR_{max}$ Expected Performance	Est. Rut Depth (58°C), mm	G^*_{10Hz} at 52°C, MPa
Good	7.4	157
Fair	9.4	121
Poor	11.5	91

TABLE 47 Predicted and actual performance indicators

		Compaction Properties		Mechanical Properties			
Cell	**Rep**	**N-SR$_{max}$**	**Perf.**	**Est. RD @ 58°C, mm**	**Perf.**	**G*10Hz @ 52°C, MPa**	**Perf.**
1	A	130	**Good**	6.25	**Good**	173	**Good**
13	A	108	**Fair**	4.76	**Good**	153	**Good**
22	A	78	**Poor**	16.03	**Poor**	57	**Poor**
26	A	117	**Fair**	5.98	**Good**	102	**Fair**
34	A	101	**Fair**	11.80	**Fair**	62	**Poor**
46	A	111	**Fair**				
53	A	102	**Fair**	15.76	**Poor**	123	**Fair**
57	A	121	**Fair**	7.30	**Fair**	158	**Good**
1	B	132	**Good**	7.26	**Fair**	166	**Good**
13	B	107	**Fair**	6.82	**Fair**	117	**Fair**
22	B	93	**Poor**				
26	B	121	**Fair**	8.14	**Fair**	114	**Fair**
34	B	96	**Poor**	12.43	**Fair**	91	**Fair**
46	B	96	**Poor**	8.16	**Fair**	79	**Fair**
53	B	109	**Fair**			145	**Fair**
57	B	117	**Fair**	7.31	**Fair**	159	**Good**
1	C	142	**Good**	9.83	**Fair**	165	**Good**
13	C	104	**Fair**	5.92	**Good**	166	**Good**
22	C	107	**Fair**	17.68	**Poor**	68	**Poor**
26	C	129	**Good**	7.44	**Fair**	111	**Fair**
34	C	62	**Poor**	9.80	**Fair**	115	**Fair**
46	C	109	**Fair**	11.73	**Fair**	85	**Fair**
53	C	98	**Poor**	11.06	**Fair**	115	**Fair**
57	C	130	**Good**	6.24	**Good**	169	**Good**

TABLE 48 Comparison of *N-SR*$_{max}$ performance with actual performance

	Number of Specimens	
N-SR$_{max}$ Indicates Performance:	**Est. Rut Depth @ 58°C, mm**	**G*$_{10Hz}$ @ 52°C, MPa**
Same as Actual	9	11
Worse than Actual	7	7
Better than Actual	5	4

$2aN + b$), and solving for N ($N = -b/2a$). This value of N is the number of gyrations at which the maximum stress ratio occurs. It is identified as $N\text{-}SR_{max}$.

6. If the ratio of the log of $N\text{-}SR_{max}$ to the log of $N_{maximum}$ is greater than or equal to 0.95, the specimen is likely to have good high-temperature performance properties. Further performance testing may not be necessary. Table 49 presents the $N\text{-}SR_{max}$ value corresponding to a 0.95 ratio for each N_{design} level.
7. If $N\text{-}SR_{max}$ is less than N_{design}, the specimen is likely to have poor high-temperature performance properties. High-temperature performance testing is recommended.
8. If $N\text{-}SR_{max}$ is between N_{design} and the value for $N\text{-}SR_{max}$ ≥ 0.95 in the previous table, the specimen is likely to have fair high-temperature performance properties. The user should evaluate the mixture application before deciding if further high-temperature performance testing is required.
9. If in a set of three specimens any single "Poor" result is obtained ($N\text{-}SR_{max}$ less than N_{design} for any single specimen), high-temperature performance testing of the mixture is recommended.

TABLE 49 *N-SR*$_{max}$ at N_{design} level

Traffic, ESAL (10^6)	**N_{design}**	**$N_{maximum}$**	**$N\text{-}SR_{max} \geq 0.95$**
< 0.3	50	75	60
< 3	75	115	90
< 30	100	160	125
≥ 30	125	205	155

The screening procedure is indicated in the form of a flowchart in Figure 55.

VALIDATION EXPERIMENTS: *N-SR*$_{MAX}$ RELATIONSHIP TO RUTTING POTENTIAL

Four validation experiments were executed to evaluate the performance of different asphalt mixtures on several field projects. The Initial (or Mix Design) Validation was focused

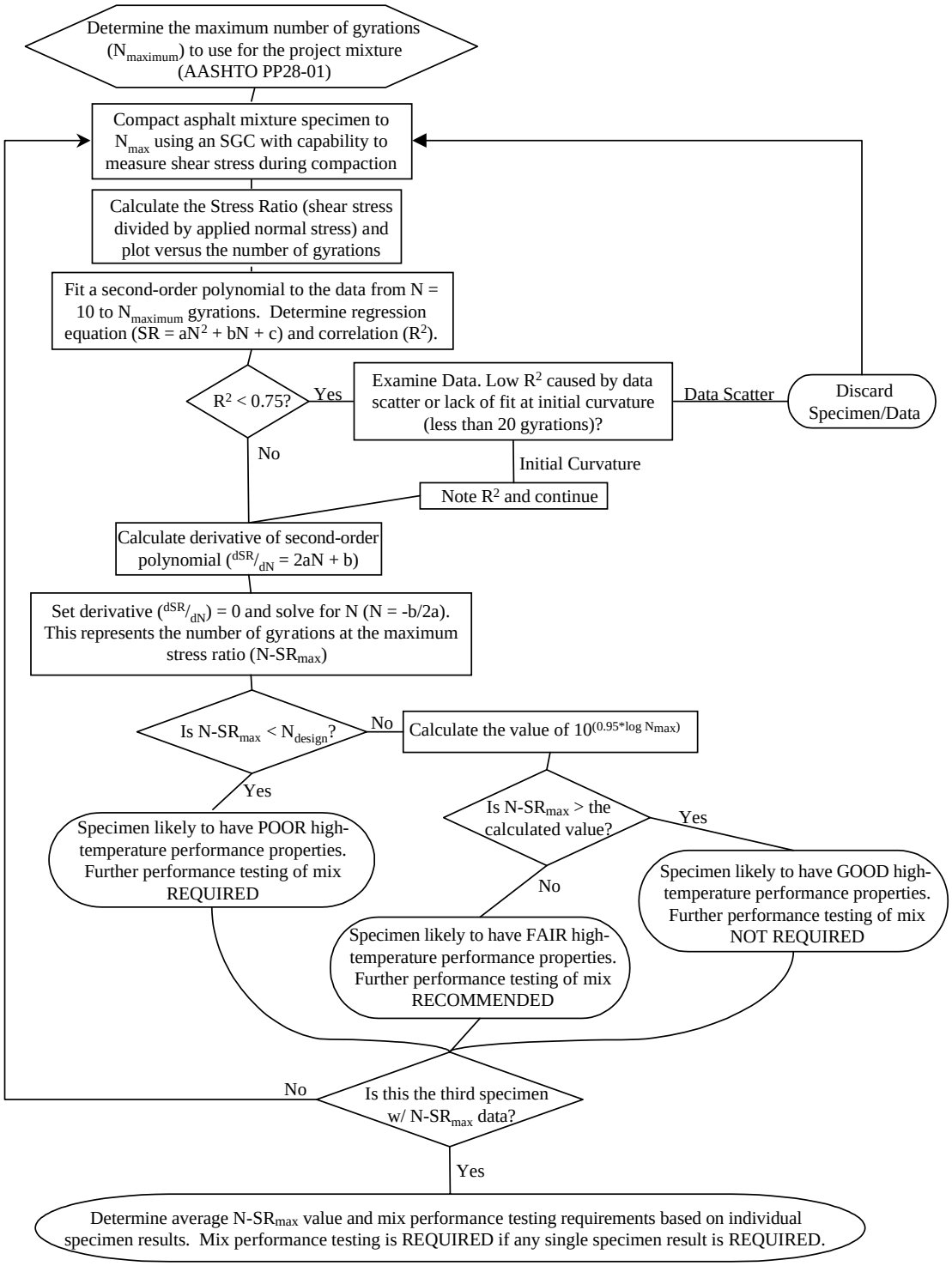

Figure 55. Mix performance screening using the SGC (with shear stress measurements).

on simulating a mix design in the laboratory for two different mixtures. The SPS-9 Validation was focused on the performance of the four SPS-9 mixtures placed in 1992. The WesTrack Validation was focused on the range of performance for several different WesTrack mixtures. The GPS Validation was focused on the GPS sections used during the SHRP experiment to develop the original N_{design} table. Each of these validation experiments is described in the following sections.

TABLE 50 N-SR_{max} data—Mixes A and N

	Mix A		Mix N	
Asphalt Content	**N-SR$_{max}$**	**Rating**	**N-SR$_{max}$**	**Rating**
Low (Opt – 0.8%)	122	Fair	114	Fair
	107	Fair	100	Fair
	115	**Fair**	**107**	**Fair**
Optimum	126	Good	110	Fair
	130	Good	104	Fair
	128	**Good**	**106**	**Fair**
High (Opt + 0.8%)	99	Poor	77	Poor
	87	Poor	67	Poor
	93	**Poor**	**72**	**Poor**

Mix Design Validation

An initial experiment was established to validate the SGC Performance Screening procedure using two of the mixes from the main laboratory experiment at multiple asphalt binder contents. This validation effort was designed to identify the effects of asphalt binder content and mixture type on N-SR_{max} values.

The two mixes selected for evaluation were Mix A (9.5-mm Limestone Coarse, 0% Sand) and Mix N (9.5-mm Gravel Fine, 40% Sand). The design asphalt binder content (selected at 4% air voids using an N_{design} of 100 gyrations) was previously determined for Mix A as 5.3% and for Mix N as 6.3%.

The mixes were selected to have different mechanical properties using the same asphalt binder stiffness. In the laboratory experiments, the estimated rut depths at 58°C for Mix A and Mix N were 7.8 mm and 13.4 mm, respectively. The high-temperature shear stiffnesses (G^*_{10Hz} at 52°C) were 168 MPa and 128 MPa, respectively.

Each mix design consisted of the compaction of two specimens each at three asphalt binder contents, including the design asphalt binder content and ± 0.8%. For Mix A, two specimens were compacted to $N_{maximum}$ (160 gyrations) at each of the three asphalt binder contents (4.5%, 5.3%, and 6.1%). For Mix N, two specimens were compacted to $N_{maximum}$ (160 gyrations) at each of the three asphalt binder contents (5.5%, 6.3%, and 7.1%). Following compaction, the N-SR_{max} value was determined.

For each mixture, four specimens were prepared at each asphalt binder content to an air voids content of approximately 3% for further mechanical property testing. The intent of the testing was to determine if the N-SR_{max} value indicated during the mix design corresponded with the expected mixture performance. Table 50 indicates the N-SR_{max} data for Mixes A and N.

The data in Table 50 indicate that the values of N-SR_{max} for the Low and Optimum asphalt binder contents were about the same. In each case, Fair performance is indicated, although the N-SR_{max} values are close to N_{design}. At the High asphalt binder content, the N-SR_{max} value of Mix N is much lower than N_{design}, thus indicating a poor-performing mixture.

For Mix A, the N-SR_{max} values for the Low asphalt binder content are actually slightly lower than the values for the Optimum asphalt binder content. The indicated performance at the Low asphalt binder content is Fair, while the indicated performance at the Optimum asphalt binder content is Good. At the High asphalt binder content, the N-SR_{max} values are lower than N_{design}, thus indicating Poor performance.

Comparing Mix A and Mix N, it is apparent that the N-SR_{max} values for Mix N are generally lower than for Mix A. With Good performance indicated for Mix A at the Optimum asphalt binder content, additional high-temperature testing to verify the mixture performance might be unnecessary. For Mix N, Fair performance is indicated at the Optimum asphalt binder content. Considering that only Fair performance is indicated at the Low asphalt binder content as well, the expected mixture performance should be verified through other high-temperature (or rutting) tests.

Figure 56 indicates the results of repeated shear testing (RSCH) on Mix A and Mix N. Values for N-SR_{max} are indicated next to the data points. Figure 57 indicates a general relationship between N-SR_{max} and estimated rutting using the RSCH test at 58°C. The data in Figures 56 and 57 generally indicate that the lower values of N-SR_{max} are associated with higher estimated rut depths in the asphalt mixtures.

The same data generated at 160 gyrations were also used to determine the N-SR_{max} values for Mixes A and N if they were to be used on a lower volume roadway (N_{design} = 75 gyrations rather than 100 gyrations). In this instance, the data

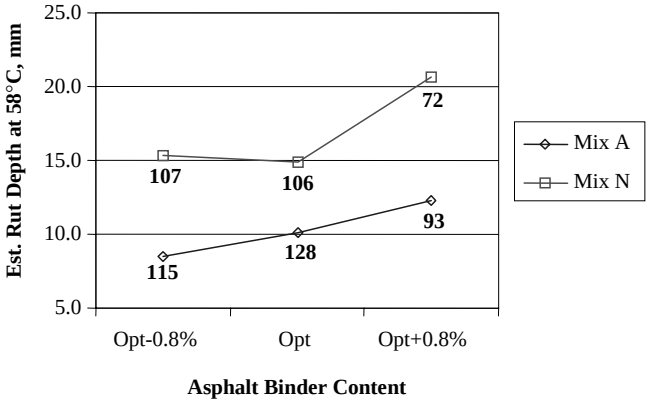

Figure 56. Estimated rut depth at multiple asphalt binder contents.

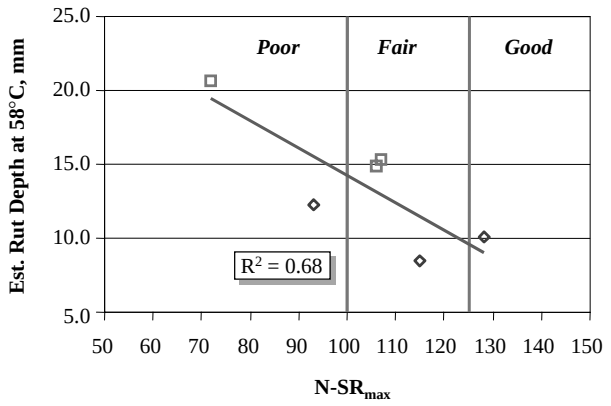

Figure 57. Relationship between estimated rut depth (RSCH) and N-SR_{max}.

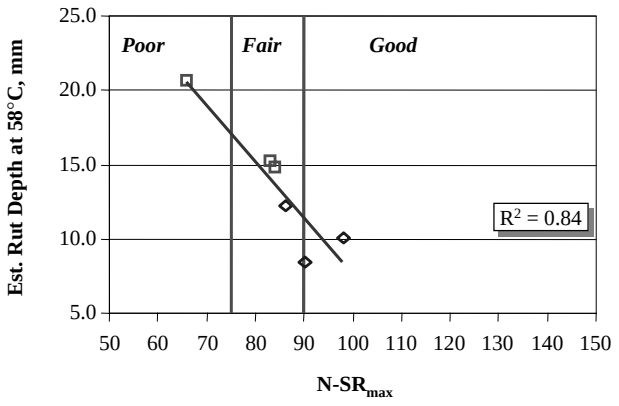

Figure 58. Relationship between estimated rut depth (RSCH) and N-SR_{max} (N_{design} = 75).

from the stress ratio curve were stopped at 115 gyrations rather than 160 gyrations and analyzed. The results are indicated in Table 51.

The data in Table 51 indicate that decreasing the number of design gyrations (or lowering the estimated traffic loading) improves the acceptance of the mixture. For Mix A, the High asphalt binder content (Optimum + 0.8%) becomes acceptable when N_{design} is decreased. This matches expectations because compaction at a lower N_{design} allows a weaker mix (higher asphalt binder content or weaker aggregate structure) to be accepted. Mix N remains only a Fair mix at the Optimum asphalt binder content. Because a decrease of 25 gyrations corresponds with approximately a 0.35% increase in asphalt binder content, the "Optimum" asphalt binder content (based on N_{design} = 100 gyrations) is actually 0.3 to 0.4% lower than optimum (based on N_{design} = 75 gyrations), while the High asphalt binder content is actually 0.4 to 0.5% higher than optimum (based on N_{design} = 75 gyrations). In other words, Mix N would still be considered a marginal-Poor mixture for a lower volume roadway.

The relationship between *N-SR*$_{max}$ and estimated rut depth (from the RSCH test) is illustrated in Figure 58.

The data in Figure 58 confirm the relationship indicated in Figure 57. Mix N remains a marginal-Poor mixture, even for a lower volume roadway.

TABLE 51 *N-SR*$_{max}$ data using $N_{maximum}$ = 115 gyrations (Mixes A and N)

	Mix A		Mix N	
Asphalt Content	**N-SR_{max}**	**Rating**	**N-SR_{max}**	**Rating**
Low (Opt – 0.8%)	92	Good	87	Fair
	88	Fair	79	Fair
	90	**Good**	**83**	**Fair**
Optimum	99	Good	86	Fair
	97	Good	82	Fair
	98	**Good**	**84**	**Fair**
High (Opt + 0.8%)	88	Fair	68	Poor
	83	Fair	64	Poor
	86	**Fair**	**66**	**Poor**

SPS-9 Mixtures Validation

Another field validation experiment involves validation of the *N-SR*$_{max}$ parameter with the 1992 SPS-9 mixtures. The estimated rutting rates of all these mixtures are all relatively low. The highest rutting rate is the Maryland IH-70 mixture, which has a rutting rate of 0.00325 mm/ESAL$^{1/2}$ (6-mm rutting after the application of approximately 3.5 million ESALs).

Previously compacted mixture specimens from each project were heated and combined. The combined loose mixture sample was then split to appropriate size for an SGC specimen (approximately 4,500 to 5,000 gm). Three mixture specimens were compacted from each mixture in the modified Pine AFG1 SGC. Data from the four surface mixtures are indicated in Table 52. The average stress ratio for each mixture is plotted versus gyrations in Figure 59.

The data in Table 52 and Figure 59 indicate that the Wisconsin IH-43 and Wisconsin IH-94 mixtures have the highest values of *N-SR*$_{max}$ and lowest rut depth (and rutting rate) values. Using the mix performance screening procedure described earlier, the Indiana IH-65 and Maryland IH-70 surface mixtures would require mix performance testing before being accepted for use on the project.

TABLE 52 1992 SPS-9 validation—surface mixtures

Project/Mixture	Rut Depth, mm	Rutting Rate (mm/ESAL$^{1/2}$)	N-SR_{max}
Wisconsin IH-43	2	0.00106	112
Wisconsin IH-94	2	0.00074	107
Indiana IH-65	5	0.00123	60
Maryland IH-70	6	0.00325	32

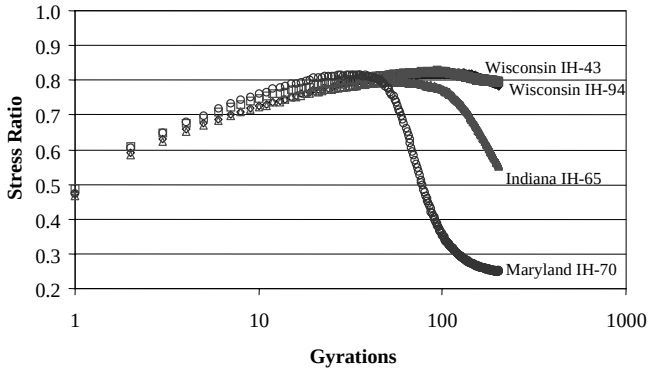

Figure 59. Average stress ratio for 1992 SPS-9 surface mixtures.

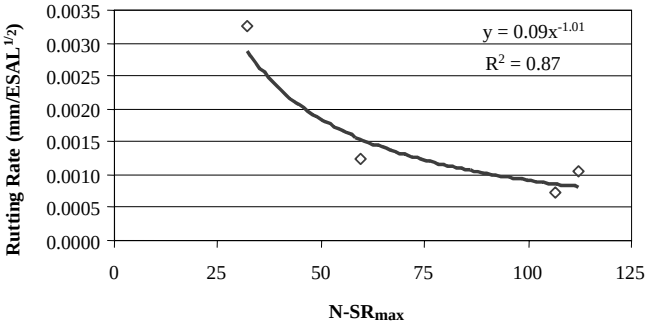

Figure 60. 1992 SPS-9 validation—relationship between rutting rate and N-SR_{max}.

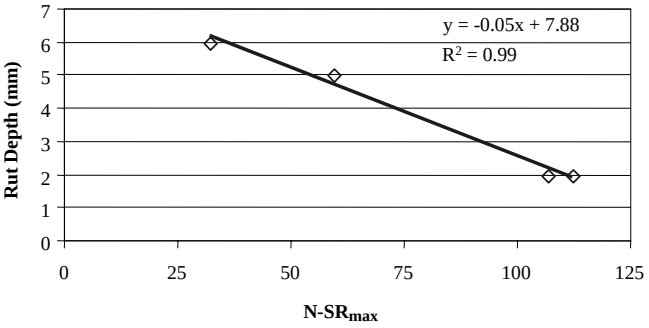

Figure 61. 1992 SPS-9 validation—relationship between rut depth and N-SR_{max}.

Figure 60 illustrates the relationship between the rutting rate of the project mixtures and the *N-SR*$_{max}$ values. Figure 61 illustrates the relationship between rut depth on the project mixtures and *N-SR*$_{max}$.

In Figure 60, a power law regression resulted in the best fit ($R^2 = 0.87$), although a linear regression also provided a reasonable fit ($R^2 = 0.73$). Figure 61 also indicates a direct relationship between rut depth and *N-SR*$_{max}$. Even though the correlation is high, the relationship was developed with only four data points. Still, the *N-SR*$_{max}$ values do correctly rank the good performance of the 1992 SPS-9 mixtures.

WesTrack Mixtures Validation

Each 5-gal bucket of WesTrack mixture was heated until the sample was loose enough for quartering. Three 4,500- to 5,000-gm samples were obtained from each mixture and heated to 135°C. Each specimen was then compacted using the modified Pine AFG1 SGC and *N-SR*$_{max}$ was determined. A summary of the test data is provided in Table 53.

Of the six WesTrack mixes, only Mix 07 (Fine, Low AC) had *N-SR*$_{max}$ values high enough to be classified as "Good" (assuming $N_{design} = 125$ gyrations). This mix, placed on Section 16 of the test track, exhibited 9 mm of rutting after the application of 2.8 million ESALs. Only 3 of the 26 test sections, including the same mix placed at lower initial construction air voids, provided better service. Of the remaining mixtures, only Mix 06 (Fine, Optimum AC) and Mix 15 (Fine Plus, Low AC) would not have required mix performance testing following the mixture screening procedure. These three mixes (07, 06, and 15) had an average rut depth of 10.3 mm. The other six mixtures (09, 14, 16, 24, 25, and 26) had an average rut depth of 20 mm.

Mix 09 did not match expectations according to the *N-SR*$_{max}$ values. This mixture had a relatively low *N-SR*$_{max}$ value (92) but good rutting performance on the test track. Although the *N-SR*$_{max}$ values follow the trend of lower values with higher asphalt content, the actual rutting performance for the Fine mix did not follow this trend. For instance, 0.8% additional asphalt binder causes the *N-SR*$_{max}$ to drop from 151 to 92. The rut depth for the Fine mix with 0.8% higher asphalt binder content is

TABLE 53 WesTrack validation

			N-SR_{max}				Rut Rate
Mix	**Gradation**	**AC**	**Rep. 1**	**Rep. 2**	**Rep. 3**	**Average**	**(mm/ESAL$^{1/2}$)**
07	Fine	Low	169	173	189	**177**	0.0054
06	Fine	Optimum	154	160	139	**151**	0.0060
09	Fine	High	98	92	84	**92**	0.0042
15	Fine Plus	Low	140	129	151	**140**	0.0072
16	Fine Plus	Optimum	102	107	122	**110**	0.0066
14	Fine Plus	High	15	20	23	**19**	0.0245
26	Coarse	Low	136	136	122	**131**	0.0114
24	Coarse	Optimum	130	128	117	**125**	0.0155
25	Coarse	High	124	126	122	**124**	0.0220

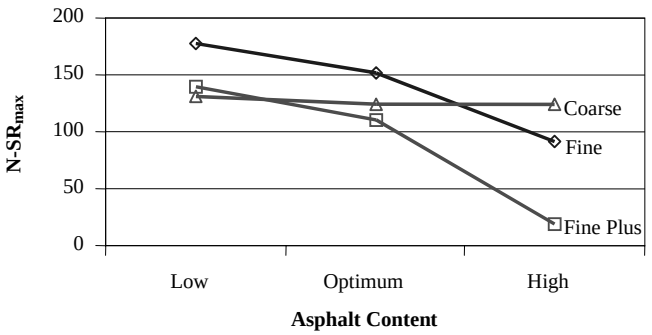

Figure 62. WesTrack mixtures—sensitivity of N-SR_{max} to asphalt binder content.

actually 3 mm less than the rut depth of the mix produced with optimum asphalt binder content. This does not match expectations and may be related to the construction air voids.

The sensitivity of *N-*SR_{max} values to changes in asphalt binder content varies by mixture. This is indicated in Figure 62. Both the Fine and Fine-Plus mixtures have similar sensitivity (same curve shape). The *N-*SR_{max} of the Coarse mixture appears to be relatively unaffected by asphalt binder content.

GPS Mixtures Validation

The fourth validation experiment involved the use of paving cores and mix from the GPS projects used in the original N_{design} experiment during SHRP.

After the research was completed, materials were retained, including compacted specimens, cores (that were not extracted), loose mix (after the core was heated and separated), and recovered aggregate. After taking an inventory of the retained materials, SHRP research reports were reviewed and the LTPP DataPave 2.0 software was used to determine the estimated rutting and accumulated traffic (through 1990) on the projects. This information is shown in Table 54.

The work plan for the GPS validation experiment was as follows:

1. Recover and combine aggregates from each layer for each project in Table 54. Determine the asphalt binder content of the mixture.
2. Split the recovered aggregate into batches of approximately 4,250 to 4,750 gm. This will enable the compacted SGC specimen to have a height of 100 mm or greater. Prepare more than one specimen if possible.

TABLE 54 GPS information

ID	State	Location	Years (-1990)	Rut Depth, mm	ESALs (x 10^3)	Rutting Rate, mm/$ESAL^{1/2}$
101450	DE	Kent Co.	25	5	9,269	0.00164
417018	OR	Salem	25	12	28,713	0.00224
068535	CA	Imperial Co.	19	8	7,255	0.00297
181028	IN	Spencer Co.	15	17	26,123	0.00333
041003	AZ	Phoenix	15	16	22,907	0.00334
481070	TX	Kaufman Co.	13	6	2,606	0.00372
041021	AZ	Kingman	13	13	12,809	0.00376
531801	WA	Vancouver	17	4	767	0.00464
041022	AZ	Mohave Co.	12	20	13,271	0.00549
401015	OK	Seminole	13	6	1,055	0.00594
321030	NV	Las Vegas	15	7	821	0.00773
231001	ME	Penobscott Co.	18	17	3,070	0.00970
211034	KY	Barren Co.	17	8	550	0.01079

TABLE 55 GPS validation

				N-SR_{max}			Average	
ID	State	$N_{maximum}$	Rut Rate, mm/$ESAL^{1/2}$	Rep 1	Rep 2	Rep 3	N-SR_{max}	PI
101450	DE	160	0.00164	139	121		130	0.959
417018	OR	205	0.00224	91	45		68	0.782
068535	CA	160	0.00297	68	75		71	0.841
181028	IN	205	0.00333	43	33	**68**	48	0.718
041003	AZ	205	0.00334	119	175	**96**	130	0.908
481070	TX	160	0.00372	92	27		59	0.754
041021	AZ	205	0.00376	137	126		131	0.917
531801	WA	115	0.00464	82	80	**54**	72	0.898
041022	AZ	205	0.00549	74	85	**39/46**	61	0.763
401015	OK	160	0.00594	13	8	**15**	12	0.483
321030	NV	115	0.00773	59	29	**53**	47	0.801
231001	ME	160	0.00970	42			42	0.734
211034	KY	115	0.01079	19	19		19	0.619

Third replicate values (numbers in **bold** in column Rep 3) are from different layer, but still within top 100 mm.

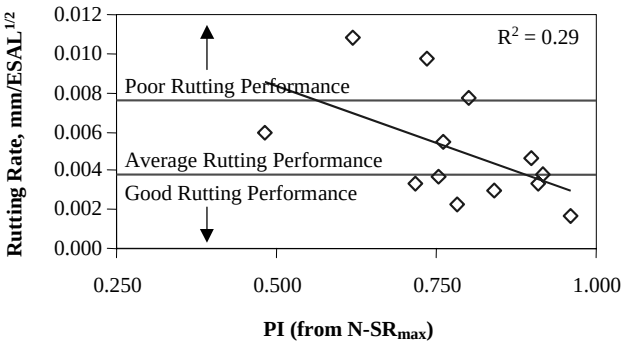

Figure 63. GPS validation experiment—rutting rate versus N-SR_{max}.

3. Mix the recovered/combined aggregate at the appropriate asphalt binder content using the PG 64-22 asphalt binder used in the laboratory experiments. By selecting a standard asphalt binder, the original research team assumed that the actual asphalt binder used on the various projects had an appropriate stiffness for the climate in which the mix was placed (i.e., AC-10 for Maine; AC-20 for Kentucky; AC-30/40 for Arizona).
4. Compact the mix using the modified Pine AFG1 SGC. Use maximum compaction levels of 115, 160, and 205 gyrations for Low, Medium, and High traffic, respectively.
5. Determine the *N-SR*$_{max}$ value for each mixture specimen. Because each mixture may be compacted to a different $N_{maximum}$, calculate the ratio of the log of *N-SR*$_{max}$ to the log of $N_{maximum}$ (ratio identified as the Performance Index, or PI) and compare with the calculated rutting rate.

TABLE 56 *N-SR*$_{max}$ expected performance for GPS mixtures

PI (from N-SR$_{max}$)	Expected Performance
> 0.90	Good
0.75 – 0.9	Fair
< 0.75	Poor

Data from the GPS Validation Experiment are presented in Table 55 and Figure 63.

The data in Figure 63 indicate that there is little relationship (R^2 = 0.29) between the PI (Performance Index determined from *N-SR*$_{max}$ – normalized for $N_{maximum}$) and the rutting rate *(26)* for the GPS mixtures. This is similar to the finding from the main laboratory experiment. However, when the mixtures are separated into groups according to PI value (Table 56), there is an apparent relationship. The *N-SR*$_{max}$ values indicated Good expected performance for three mixtures. *N-SR*$_{max}$ values indicated Fair expected performance for six mixtures and Poor expected performance for four mixtures. Table 57 indicates the average rutting rate and PI for each of the three performance groups.

The data in Table 57 appear very similar to the data reported for the main laboratory experiment. Using the criteria in Table 56, no mixture that had poor rutting performance in the field would have resulted in good *N-SR*$_{max}$ values. Conversely, only the Indiana mixture exhibited acceptable rutting performance in the field and a poor *N-SR*$_{max}$ value. It should be noted, however, that this mixture had exhibited 17 mm of rutting after 15 years of service. Thus, it is possible that most of the rutting occurred early in the life of the mixture when the rutting rate would have been higher (indicating less acceptable performance).

TABLE 57 Expected performance (from *N-SR*$_{max}$) compared with actual performance

N-SR$_{max}$ Expected Performance	PI (from N-SR$_{max}$)	Rutting Rate, mm/ESAL$^{1/2}$
Good	0.928	0.00291
Fair	0.806	0.00447
Poor	0.639	0.00744

CHAPTER **3**

INTERPRETATION, APPRAISAL, AND APPLICATIONS

SUMMARY OF RESEARCH

Examination of conventional SGC compaction data from past Superpave asphalt mixtures indicated that compaction slope was not related to asphalt mixture stiffness or rutting resistance because the compaction slope was insensitive to changes in asphalt binder content. However, the research did indicate that the product of compaction slope and percentage of air voids ($k \times AV$) was sensitive to changes in asphalt binder content. Another parameter that appeared marginally related to changes in asphalt content and, by extension, mixture stiffness was the terminal densification index from 92% to 98% density.

The main laboratory experiment concentrated on determining if any of the conventional SGC compaction parameters or selected other compaction parameters (from a modified SGC) were adequately responsive to changes in mixture components that were expected to change mixture stiffness and rutting resistance. Separate, smaller experiments were developed to examine other potential SGC compaction parameters. These included the use of the LPI and the use of the Servopac gyratory compactor at a higher angle of gyration. Other experiments were developed to examine any correlation of the $k \times AV$ parameter to asphalt mixture rutting resistance and to ascertain if changes in the SGC compaction procedure would improve the ability of the compaction parameters to discern asphalt binder stiffness.

LPI

Testing conducted using the LPI indicates that the LPI may have potential as a parameter for identifying poor rutting performance. As with some of the other parameters, there is not a strong relationship with the high-temperature mechanical property test results believed to be related to rutting. The best LPI parameter may be the change in residual pressure as the air voids content is reduced from 7% to 4%. This parameter is based on the assumption that stable mixes will densify without significantly changing the residual pore pressure. Analysis of the experimental mixes indicated that only 2 of 16 mixes did not have any replicate with negative change or change greater than 14 kPa. Negative change in residual pressure or change in residual pressure greater than 14 kPa were criteria believed to be related to unstable mixtures. Although there were only two asphalt mixtures that met these criteria, both mixes had estimated rut depths (from the repeated shear test at constant height) of 3.6 mm. Only one mixture had better estimated rutting resistance than those of the mechanical property tests.

The LPI value at N_{design}, 100 gyrations, did not appear to be strongly related to the rutting resistance of the asphalt mixtures. Using an LPI value of 200 kPa as a criterion (poor mixes having LPI values greater than 200 kPa), asphalt mixtures with LPI values greater than 200 kPa had an average rut depth of 7.8 mm. Asphalt mixtures with LPI values less than 200 kPa had an average rut depth of 8.2 mm. This is insufficient separation in performance for an indicator parameter.

One of the biggest questions surrounding the use of the LPI may be the repeatability of the test. The use of regression on the raw data values could improve the repeatability. If the repeatability issues cannot be solved by regression or other means, then it appears that the values for LPI and residual pressure are too variable to discriminate adequately between the rutting potential of different asphalt mixtures.

Servopac Gyratory Compactor

Testing conducted at the University of Florida with the Servopac gyratory compactor indicated no specific advantage by compacting at 2.5 deg (suggested by some research) than at the standard compaction angle of 1.25 deg. At 2.5 deg, compaction is quicker, but the air voids content controls mixture response. Specifically, the number of gyrations at which the maximum shear stress occurs is different for the specimens compacted at 2.5 deg than for those compacted at 1.25 deg, but the air voids content at which the maximum shear stress occurs is the same. Based on the limited number of mixtures tested, the number of gyrations at the maximum shear stress tracked the expected rutting performance when the aggregate structure or asphalt binder content was changed. Changing the asphalt binder stiffness did not affect the test result.

Product of Compaction Slope and Percentage of Air Voids ($k \times AV$)

Testing indicated that the product of compaction slope and air voids, $k \times AV$, was related to the rutting performance of the two mixtures studied, but only for the mixtures made with PG 64-22 binder. Unfortunately, this finding was not validated in

the main experiment. Testing in the main laboratory experiment to assess the effects of changes in mixture components on compaction parameters indicated that the $k \times AV$ parameter was related to high-temperature shear stiffness (G^*_{10Hz} at 52°C) for PG 64-22 mixtures ($R^2 = 0.77$), but was not related to estimated rut depth ($R^2 = 0.17$). This mixed response was unexpected because analysis of the experimental data indicated that high-temperature shear stiffness is weakly related to estimated rut depth from the repeated shear test ($R^2 = 0.63$).

More research and validation work is needed to determine if the $k \times AV$ parameter has value for routine testing. In the interim, users should be suspicious of $k \times AV$ values less than 20. From the two experiments (PG 64-22 asphalt binder only), the average estimated rut depth of the eight mixtures having $k \times AV$ values less than 20 was 12.8 mm. The average rut depth of the eight mixtures having $k \times AV$ values greater than 20 was 9.1 mm. The $k \times AV$ parameter is calculated as follows:

$$k \times AV = \frac{P_a * (C_{des} - C_{ini})}{(\mathrm{Log}(N_{des}) - Log(N_{ini}))}$$

In the equation, C_{des} and C_{ini} are the compaction values at the design number of gyrations (N_{des}) and initial number of gyrations (N_{ini}) expressed as a percentage (i.e., 96.5 rather than 0.965), and P_a is the percentage of air voids in the specimen expressed as a percentage (i.e., 3.5 rather than 0.035).

Finally, similar to the number of gyrations at the maximum shear stress, the $k \times AV$ parameter does not adequately capture effects of asphalt binder stiffness. The $k \times AV$ parameter is weakly related ($R^2 = 0.59$) to the $N\text{-}SR_{max}$ parameter from the main experiment.

Changing SGC Compaction Procedure to Discriminate Asphalt Binder Stiffness

Testing was conducted on a limited subset of asphalt mixtures to determine if changing any operational parameters of the Superpave gyratory compaction procedure could better discern the effects of asphalt binder stiffness on the mixture's rutting resistance. The analysis indicated that slowing the rotational speed to 6 rpm from 30 rpm and lowering the compaction temperature to 60°C did have some effect on the ability of the SGC compaction parameters to identify the use of a stiffer asphalt binder. However, the change in $N\text{-}SR_{max}$ was relatively small for the large procedural changes required. As such, the research team believed that the slight improvement in discerning stiffer asphalt binders was outweighed by the impact of significant changes in compaction procedure.

Number of Gyrations at Maximum Shear Stress ($N\text{-}SR_{max}$)

The best parameter identified by the research appears to be the number of gyrations at which the peak shear stress occurs during compaction, $N\text{-}SR_{max}$. This parameter was determined during the research with an AFG1 SGC from Pine Instruments modified to measure shear stress. It should be possible to measure this parameter with any compactor with shear stress measurement capability. The GLPA also may provide the same information, but will require more validation work. The main laboratory experiment (PG 64-22 mixes only) indicates that the $N\text{-}SR_{max}$ parameter never indicates good performance when mechanical properties are poor and never indicates poor performance when mechanical properties are good (i.e., it has a low rate of false negatives or positives). Out of 24 specimens, only 6 indicate poor performance (from four mixes). These four mixes have the worst rutting performance according to the repeated shear test. Validation efforts generally confirm the results of the main laboratory experiment. The first Superpave field mixtures, the SPS-9 mixes from 1992, are correctly ranked by $N\text{-}SR_{max}$ according to actual rutting performance. The WesTrack Fine and Fine-Plus mixtures also follow the expected trend. However, the WesTrack Coarse mixtures indicate $N\text{-}SR_{max}$ values that are relatively unaffected by the change in asphalt binder content. The GPS mixtures used in some of the SHRP experiments also generally confirm the results of the main laboratory experiments. For these mixtures, the $N\text{-}SR_{max}$ parameter appears capable of properly separating mixes into groups of good, fair, and poor performance.

WHAT THE FINDINGS MEAN

Although there were limitations identified during the research and more validation is needed, the number of gyrations at the maximum shear stress, $N\text{-}SR_{max}$, appears to be a workable parameter related to mixture stiffness and rutting resistance. The $N\text{-}SR_{max}$ parameter can be determined from any SGC with shear stress measurement capability. This includes the modified version of the AFG1 Superpave gyratory compactor from Pine Instruments (used in the research), as well as the Servopac gyratory compactor. It is expected, although it has not been validated, that the GLPA or shear testing plate developed at the University of Wisconsin—Madison will provide the same information.

The $N\text{-}SR_{max}$ should serve as a preliminary indicator of mixture instability without the necessity of routine mechanical property or performance testing. The $N\text{-}SR_{max}$ data should be available immediately after the asphalt mixture specimen has been compacted. The bulk specific gravity of the specimen or the percentage of air voids is not needed for the determination of the $N\text{-}SR_{max}$ value. If the user does not have an SGC with the capability to measure shear stress, the interaction of compaction slope (linear on semi-logarithmic scale of $\%G_{mm}$ as a function of the number of gyrations) and the percentage of air voids in the specimen, identified as $k \times AV$, may provide similar information, but this is not a preferred

option because the $k \times AV$ parameter does not correlate strongly with $N\text{-}SR_{max}$.

EXPECTED USE

It is expected that the $N\text{-}SR_{max}$ parameter can be used in both mix design and routine QC procedures to identify gross mixture instability in an asphalt mixture. As part of the Superpave mix design procedure, the $N\text{-}SR_{max}$ parameter can be used in addition to volumetric properties during the trial blend evaluations to select the best design aggregate structure for the combinations of aggregates available. The $N\text{-}SR_{max}$ parameter can also be used in the mix design procedure during the determination of the design asphalt binder content. By monitoring the change in the $N\text{-}SR_{max}$ value as the asphalt binder content changes, the user should be able to identify the potential sensitivity of the design asphalt mixture to changes in asphalt binder content during production.

During mix production, the $N\text{-}SR_{max}$ parameter can be used to identify potential mixture instability rapidly. Because the $N\text{-}SR_{max}$ value is available immediately following compaction, the user can identify a potentially poor asphalt mixture within 10 min of sampling the mix and splitting it to the appropriate size. This quick response minimizes the amount of poor-quality material being placed before corrective action can be taken.

In both mix design and QC applications, the procedure illustrated in Figure 61 can be applied. If conducting a mix design, $N\text{-}SR_{max}$ values that are Poor at the design asphalt binder content indicate that the asphalt mixture should be subjected to performance testing before the asphalt mixture is approved for the project. $N\text{-}SR_{max}$ values that are Fair at the design asphalt binder content indicate that the asphalt mixture may be subjected to performance testing at the discretion of the user. Mixtures that will be used on high-traffic or high-stress roadways should have additional performance testing conducted. Mixtures that will be placed on lower volume roads may not require additional performance testing.

In conducting QC operations, $N\text{-}SR_{max}$ values that are Poor indicate that the remainder of the asphalt mixture sample should be retained for performance testing. The urgency of the performance testing will be at the discretion of the client (i.e., the state highway agency for most projects). $N\text{-}SR_{max}$ values that are Fair at the design asphalt binder content indicate that the asphalt mixture may be subjected to performance testing at the discretion of the user. During the initial production of the asphalt mixture, the $N\text{-}SR_{max}$ values should be obtained and compared with the design $N\text{-}SR_{max}$ values along with volumetric properties, aggregate gradation, and asphalt binder content information. Once the contractor has made appropriate set-up adjustments, the $N\text{-}SR_{max}$ values from the initial production will be established as the baseline for the remainder of production. Significant deviation (i.e., $\Delta\ N\text{-}SR_{max} \geq 20$) from the initial production values will indicate a significant change in material components or volumetric properties, or both. For example, the mix validation experiment indicated that an increase in asphalt binder content of 0.8% above the design asphalt content decreased the $N\text{-}SR_{max}$ value by 35.

LIMITATIONS

The biggest limitation of the $N\text{-}SR_{max}$ parameter as an indicator of mixture rutting potential is its apparent inability to differentiate between the stiffnesses of different asphalt binders. Thus, a mixture made with a PG 64-22 asphalt binder will appear to have an $N\text{-}SR_{max}$ value, and thereby similar expected performance, as the same mixture made with a PG 76-22 asphalt binder. Consequently, it is expected that the $N\text{-}SR_{max}$ will only provide information on the aggregate structure and asphalt binder volume in an asphalt mixture. The insensitivity to asphalt binder stiffness may also present a problem for asphalt mixtures with high film thickness, because the stiffness of the mastic in the mixture may not be adequately evaluated by the $N\text{-}SR_{max}$ parameter. Because of this, it is not known how SMA or open graded friction course mixtures will perform using the $N\text{-}SR_{max}$ parameter.

IMPLEMENTATION ISSUES

The $N\text{-}SR_{max}$ parameter and the procedure used to determine the $N\text{-}SR_{max}$ value for an asphalt mixture have several implications for implementation. First, only a few commercial models of SGCs are available that currently have shear stress measurement capability. Retrofitting may be an option for some models, but others may require a re-design. This is a significant implementation issue with the large number and variety of SGCs currently in use in the United States.

One possibility to alleviate the problem of retrofitting or redesigning SGCs is to use the GLPA. Although this procedure has not been validated by mixture testing, it is likely that the GLPA will provide a similar response as the shear stress measurements. The problem with the GLPA, other than the need for validation, is that the data require considerable processing through data collection software before they can be analyzed. The “unfriendly” data collection and analysis of the GLPA will need to be improved before it can be expected to be used routinely in mix design and quality control.

Eventually, automated data collection and analysis of the shear stress measurements will speed the use of the $N\text{-}SR_{max}$ parameter. Currently, the AFG1 compaction data are saved immediately onto a diskette. The text file can then be opened into a spreadsheet and, with some manipulation, be used to determine the $N\text{-}SR_{max}$ value for the asphalt mixture. It should be possible for the data to be manipulated within a control

software program so that the user only sees the final $N\text{-}SR_{max}$ immediately after compaction.

Another issue with implementation involves the procedure for determining $N\text{-}SR_{max}$. Based on the research, the recommended procedure requires that specimens be compacted to $N_{maximum}$ rather than N_{design}. This differs from the current standard practice (compacting specimens to N_{design}) for determining the volumetric properties of an asphalt mixture. Using the current practice, an asphalt mixture specimen compacted to determine volumetric properties cannot be used to determine $N\text{-}SR_{max}$ and an asphalt mixture specimen compacted to determine $N\text{-}SR_{max}$ cannot be used to determine volumetric properties. Although specimens were compacted to $N_{maximum}$ in the original Superpave mix design procedure, the procedure was changed following the recommendation of the Mixtures Expert Task Group and the NCHRP 9-9 research *(27)*.

Another implementation issue that should be considered is the reproducibility of the test data. It is expected that some of the current issues surrounding the SGC—specifically, the effect of variation in angle of gyration (internal versus external angle)—will impact the determination of $N\text{-}SR_{max}$. As noted in the research, the use of a polynomial regression improves the repeatability of the $N\text{-}SR_{max}$ data within a set of specimens. However, there is no information currently available on the reproducibility of $N\text{-}SR_{max}$ values between different users or compactors.

CHAPTER **4**

CONCLUSIONS AND SUGGESTED RESEARCH

The primary objectives of this research project were to (1) determine the relationship between mix properties measurable during Superpave gyratory compaction and permanent deformation of pavements in service and (2) recommend any practical modifications to existing SGCs, test methods, or both, to measure the identified properties.

Literature review, analyses of past compaction data, execution of controlled laboratory experiments to identify an appropriate compaction parameter, and validation experiments have resulted in a compaction parameter available from some SGCs that appears related to the stiffness and rutting resistance of an asphalt mixture. The compaction parameter is the number of gyrations at which the maximum shear stress occurs during compaction in an SGC (with shear stress measurement capability), identified as $N\text{-}SR_{max}$. This parameter is available from SGCs having shear stress measurement capability. Although this research did not validate its use, it is likely that the GLPA may be used for $N\text{-}SR_{max}$ determination for those SGCs without the capability to perform shear stress measurements during compaction.

Further research is needed to validate the potential of the LPI developed at Worcester Polytechnic Institute. The research conducted on the LPI as part of this project indicated some potential as a mixture screening tool. Further research may also be needed to explore the concepts suggested by the research conducted at Washington State University *(28)*.

Efforts to better differentiate the stiffness and rutting resistance of asphalt mixtures with asphalt binders having different stiffnesses indicated that lowering the compaction temperature to approximately 60°C and/or slowing the rotational speed to 6 rpm provided some differentiation between binder stiffnesses. The minimal apparent differentiation of asphalt binder stiffnesses seemed to be outweighed by the impracticality of changing the compaction procedure. Further research may be needed to determine if it is even practical to assume that asphalt binder stiffness will have a significant effect on any compaction parameter used to determine the rutting resistance of an asphalt mixture.

Finally, although the $N\text{-}SR_{max}$ parameter appears promising, further research is needed to validate that the parameter is correlated with asphalt mixture rutting performance. The limiting criteria may also require adjustment after validation experiments.

ABBREVIATIONS AND ACRONYMS

$\%G_{mm}@SR_{max}$	Density (expressed as a percentage of the maximum) at the time when the maximum stress ratio occurs
AASHTO	American Association of State Highway and Transportation Officials
AI	Asphalt Institute
ALF	Accelerated Loading Facility
APT	Accelerated Pavement Test(er)
ARRB	Australian Road Research Board
AV	Air voids
C_{des}, C_{ini}	Compaction at design number of gyrations; compaction at initial number of gyrations
CEI_{92}	Construction energy index (from start of compaction to 92% density)
$CEI_{Nini-92}$	Construction energy index (from $N_{initial}$ to N_{92})
CV	Coefficient of variation
DEI_{92-96}	Densification energy index (from N_{92} to N_{96})
DOT	Department of Transportation
ESAL	Equivalent Single Axle Load
ETG	Expert Task Group
FAA	Fine aggregate angularity
FHWA	Federal Highway Administration
FSCH	Frequency Sweep (shear) at Constant Height
FST	Field Shear Tester
G^*	Complex shear modulus
G^*_{10Hz}	Complex shear modulus at 10Hz loading frequency
GLPA	Gyratory Load Cell Plate Assembly
G_{mm}	Maximum theoretical specific gravity of an asphalt mixture
GPS	General Paving Studies (used during SHRP)
GTM	Gyratory Test Machine (Corps of Engineers)
HMA	Hot mix asphalt
IH	Interstate Highway
K	Compaction slope (semi-logarithmic)
$k \times AV$	Combined factor of compaction slope and percentage of air voids
kPa	
LCPC	Laboratoire Central des Ponts et Chaussées (France's central lab for highways)
LPI	Lateral Pressure Indicator (Index)
LTPP	Long-Term Pavement Performance
LWT	Loaded Wheel Test(er)
NCHRP	National Cooperative Highway Research Program
N_{des}, N_{ini}	Design number of gyrations; Initial number of gyrations
N_{design}, $N_{maximum}$	Design number of gyrations; Maximum number of gyrations
NMAS	Nominal maximum aggregate size
$N\text{-}SR_{max}$,	Number of gyrations at the maximum stress ratio
N_{xx}	Number of gyrations to xx% density (e.g. 92% = N_{92})
N_{xx}/N_{yy}	Ratio of number of gyrations at xx% density to number of gyrations at yy% density
PF_{final}	Performance Factor at the final number of gyrations
PG	Performance Grade
PI	Performance Index (ratio of logarithm of $N\text{-}SR_{max}$ to logarithm of $N_{maximum}$)
PMAC	Polymer Modified Asphalt Cement
QC	Quality Control
R^2	Correlation coefficient
RAP	Reclaimed Asphalt Pavement
Rpm	revolutions per minute
RSCH	Repeated Shear at Constant Height
RZ	Restricted Zone
SBS	Styrene-Butadiene-Styrene polymer
SGC	Superpave gyratory compactor
SHRP	Strategic Highway Research Program
SMA	Stone mastic asphalt
SPS-9	Specific Paving Studies (used during SHRP)
SR	Stress ratio
SR_{160}/SR_{max}	Ratio of stress ratio at 160 gyrations to the stress ratio at the maximum number of gyrations
SR_{final}/SR_{max}	Ratio of stress ratio at the final number of gyrations to the stress ratio at the maximum number of gyrations
SR_{max}	Maximum stress ratio
SSCH	Simple Shear at Constant Height
SST	Superpave Shear Tester
TDI_{92-98}	Terminal densification index (from N_{92} to N_{98})
TDI_{96-98}	Terminal densification index (from N_{96} to N_{98})
$T_{eff}(PD)$	Effective temperature for characterizing permanent deformation
TRB	Transportation Research Board
TRIS	Transportation Research Information Services
VFA	Voids Filled with Asphalt
VTM	Voids in Total Mixture (see AV)
WPI	Worcester Polytechnic Institute
γ_{5000}	Permanent shear strain at 5,000 loading cycles

REFERENCES

1. McGennis, R. B., R. M. Anderson, D. Perdomo, and P. A. Turner. "Issues Pertaining to Use of Superpave Gyratory Compactor," *Transportation Research Record 1543,* Transportation Research Board, National Research Council, Washington, DC (1996) pp. 139–144.
2. Khatri, A., and H. U. Bahia. "Compaction Temperatures for Asphalt Mixtures Produced with Modified Binders," paper submitted for presentation at 2000 Annual Meeting of the Transportation Research Board, Washington, DC (2000).
3. Cominsky, R. J., G. A. Huber, T. W. Kennedy, and R. M. Anderson. "The Superpave Mix Design Manual for New Construction and Overlays," *SHRP Report A-407,* Strategic Highway Research Program, Washington, DC (1994).
4. Anderson, R. M., and H. U. Bahia. "Evaluation and Selection of Aggregate Gradations for Asphalt Mixtures Using Superpave," *Transportation Research Record 1583,* Transportation Research Board, National Research Council, Washington, DC (1997) pp. 91–97.
5. Anderson, R. M., J. R. Bukowski, and P. A. Turner. "Using Superpave Performance Tests To Evaluate Asphalt Mixtures," *Transportation Research Record 1681,* Transportation Research Board, National Research Council, Washington, DC (1999) pp. 106–112.
6. McGennis, R. B. "Evaluation of Materials from Northeast Texas Using Superpave Mix Design Technology," *Transportation Research Record 1583,* Transportation Research Board, National Research Council, Washington, DC (1997) pp. 98–105.
7. Anderson, R. M., R. J. Cominsky, and B. M. Killingsworth. "Sensitivity of Superpave Mixture Tests to Changes in Mixture Components," *Asphalt Paving Technology,* Vol. 67, Association of Asphalt Paving Technologists (1998).
8. De Sombre, R., D. E. Newcomb, B. Chadbourn, and V. Voller. "Parameters to Define the Laboratory Compaction Temperature Range of Hot-Mix Asphalt," *Asphalt Paving Technology,* Vol. 67, Association of Asphalt Paving Technologists (1998).
9. Mallick, R. B. "Use of Superpave Gyratory Compactor to Characterize Hot-Mix Asphalt (HMA)," *Transportation Research Record 1681,* Transportation Research Board, National Research Council, Washington, DC (1999) pp. 86–96.
10. Bahia, H. U., T. Friemel, P. Peterson, and J. Russell. "Optimization of Constructability and Resistance to Traffic: A New Design Approach for HMA Using the Superpave Gyratory Compactor," *Asphalt Paving Technology,* Vol. 67, Association of Asphalt Paving Technologists (1998).
11. Langlois, P., and M. Beaudoin. "The Correlation Between Rutting Resistance and Hot-Mix Design With a Gyratory Compactor," *Proceedings,* Canadian Technical Asphalt Association (1998).
12. Tarn, J. C., J. D. Lin, and J. R. Chang. "The Study on Asphalt Concrete Performance with Different Gradations Using SGC in SHRP," *Proceedings of the 9th REAAA Conference,* Wellington, New Zealand, 1998.
13. Anderson, R. M., E. R. Brown, and M. S. Buchanan. "Evaluation of the Effect of Short-Term Temperature on the Volumetric and Densification Properties of Specimens Compacted with the Superpave Gyratory Compactor," *Proceedings,* Canadian Technical Asphalt Association (1999).
14. Vavrik, W. R., and S. H. Carpenter. "Calculating Air Voids at Specified Number of Gyrations in Superpave Gyratory Compactor," *Transportation Research Record 1630,* Transportation Research Board, Washington, DC (1998) pp. 117–125.
15. Butcher, M. "Determining Gyratory Compaction Characteristics Using Servopac Gyratory Compactor," *Transportation Research Record 1630,* Transportation Research Board, National Research Council, Washington, DC (1998) pp. 87–97.
16. West, R. C., and B. E. Ruth. "Compaction and Shear Strength Testing of Stone Matrix Asphalt Mixtures in the Gyratory Testing Machine," *Asphalt Paving Technology,* Vol. 64, Association of Asphalt Paving Technologists (1995).
17. Guler, M., H. U. Bahia, P. J. Bosscher, and M. E. Plesha. "Device for Measuring Shear Resistance of Hot-Mix Asphalt in Gyratory Compactor," *Transportation Research Record 1723,* Transportation Research Board, National Research Council, Washington, DC (2000) pp. 116–124.
18. Anderson, R. M., G. A. Huber, D. E. Walker, and X. Zhang. "Mixture Testing, Analysis, and Field Performance of the Pilot Superpave Projects: The 1992 SPS-9 Mixtures," *Asphalt Paving Technology,* Vol. 69, Association of Asphalt Paving Technologists (2000).
19. Cominsky, R. J., B. M. Killingsworth, R. M. Anderson, D. A. Anderson, and W. W. Crockford. *NCHRP Report 409: Quality Control and Acceptance of Superpave-Designed Hot Mix Asphalt,* Transportation Research Board, National Research Council, Washington, DC (1998).
20. Sousa, J. B., S. L. Weissman, J. A. Deacon, J. Harvey, G. Paulsen, and C. L. Monismith. "Permanent Deformation Response of Asphalt Aggregate Mixes, Part II—Development of Permanent Deformation Tests and Associated Analyses; Extended Test Program," *SHRP Report A-415,* Strategic Highway Research Program, Washington, DC (1994).
21. Cominsky, R. J., R. B. Leahy, and E. T. Harrigan. "Level One Mix Design: Materials Selection, Compaction, and Conditioning," *SHRP Report A-408,* Strategic Highway Research Program, Washington, DC (1994).
22. Stuart, K. D., W. S. Mogawar, and P. Romero. "Validation of Asphalt Binder and Mixture Tests that Measure Rutting Susceptibility Using the Accelerated Loading Facility," *FHWA Report RD-99-204,* Federal Highway Administration, McLean, VA (1999).

23. Minutes of the Mixtures Expert Task Group Meeting, March 2000.
24. Barksdale, R. D., J. Alba, N. P. Khosla, R. Kim, P. C. Lambe, and M. S. Rahman. "Laboratory Determination of Resilient Modulus for Flexible Pavement Design, NCHRP 1-28 Final Report," *NCHRP Web Document 14*, National Cooperative Highway Research Program, Transportation Research Board, National Research Council, Washington, DC (1997).
25. Sousa, J. B., and S. L. Weissman. "Modeling Permanent Deformation of Asphalt-Aggregate Mixtures," *Journal of the Association of Asphalt Paving Technologists,* Vol. 63 (1994).
26. Brown, E. R., and S. A. Cross. "A National Study of Rutting in Hot Mix Asphalt (HMA) Pavements," *Journal of the Association of Asphalt Paving Technologists,* Vol. 61 (1992).
27. Brown, E. R., and M. S. Buchanan. "Consolidation of the Ndesign Compaction Matrix and Evaluation of Gyratory Compaction Requirements," *Asphalt Paving Technology*, Vol. 68, Association of Asphalt Paving Technologists (1999).
28. Dessouky, S., E. Masad, and F. Bayomy. *Performance Prediction of Asphalt Mixes Using the Superpave Gyratory Compactor—Final Report,* Washington State University, February (2002).
29. Moutier, F., J. F. Corte, and J. Bonnot. "Comparison of the Use of the Gyratory Compactor in the French Mix Design Method and in Superpave Level 1," *Proceedings of the Conference on Road Safety in Europe and Strategic Highway Research Program*. Prague, The Czech Republic, September 20–22, 1995.
30. Hall, K. D., S. Dandu, and G. V. Gowda. "Effect of Specimen Size on Compaction and Volumetric Properties in Gyratory Compacted Hot-Mix Asphalt Concrete Specimens," *Transportation Research Record 1545*, Transportation Research Board, National Research Council, Washington, DC (1996) pp. 126–132.
31. Habib, A., M. Hossain, R. Kaldate, and G. A. Fager. "Comparison of Superpave and Marshall Mixtures for Low-Volume Roads and Shoulders," *Transportation Research Record 1609*, Transportation Research Board, National Research Council, Washington, DC (1998) pp. 44–50.

APPENDIXES A, B, AND C

The following appendixes are available on request from NCHRP:

- Appendix A: NCHRP 9-7 Field Projects;
- Appendix B: Additional Details from LPI Experiment; and
- Appendix C: Experiment Evaluating the Effect of Binder Stiffness on SGC Properties.

The entire contractor's final report is also planned for publication in the CRP CD-ROM Bituminous Materials Research Series.

APPENDIX D

DRAFT AASHTO PROCEDURE FOR ESTIMATING THE RUTTING PERFORMANCE OF ASPHALT MIXTURES USING SHEAR STRESS MEASUREMENTS DURING COMPACTION IN THE SUPERPAVE GYRATORY COMPACTOR

STANDARD TEST METHOD FOR ESTIMATING THE RUTTING PERFORMANCE OF ASPHALT MIXTURES USING SHEAR STRESS MEASUREMENTS DURING COMPACTION IN THE SUPERPAVE GYRATORY COMPACTOR

AASHTO DESIGNATION TPXX-02

1. SCOPE

1.1 This standard provides a procedure (illustrated in Figure D-1) for estimating the rutting potential of an asphalt mixture during compaction in the Superpave gyratory compactor. The procedure can be used to evaluate different mixtures with the same (or similar) asphalt binders. It should not be used to compare the estimated rutting potential of mixtures with different asphalt binder grades because the procedure appears relatively insensitive to changes in asphalt binder grade.

1.2 This standard is applicable to specimens compacted from either laboratory-produced or plant-produced asphalt mixture.

1.3 This practice may involve hazardous materials, operations, and equipment. It does not purport to address all the safety problems associated with its use. It is the responsibility of whoever uses this practice to consult and establish appropriate safety and health practices and determine the applicability of regulatory limitations prior to its use.

2. REFERENCED DOCUMENTS

2.1 AASHTO Standards

- T312 Preparing and Determining the Density of Hot Mix Asphalt (HMA) Specimens by Means of the Superpave Gyratory Compactor
- M231 Weighing Devices Used in Testing of Materials
- PP2 Short and Long Term Aging of Hot Mix Asphalt (HMA)
- PP28 Superpave Volumetric Design for Hot Mix Asphalt (HMA)
- T166 Bulk Specific Gravity of Compacted Asphalt Mixtures Using Saturated Surface-Dry Specimens

3. SIGNIFICANCE AND USE—The test procedures and associated analysis techniques described in this method can be used to estimate the rutting potential of an asphalt mixture during routine compaction in the Superpave gyratory compactor. This information can be collected on specimens compacted to determine mixture volumetric properties. Information on the estimated rutting potential is intended to serve as a rapid screening test for mixture instability. Additional performance testing is recommended when the screening procedure indicates a mixture with poor high-temperature properties (i.e., a rutting-susceptible mixture).

4. EQUIPMENT AND MATERIALS

4.1 Superpave Gyratory Compactor—An electrohydraulic or electromechanical compactor meeting the requirements of AASHTO T-312.

4.1.1 Shear Measurement System—A means shall be provided to continually measure (at least once per gyration) the shear stress imparted during compaction.

Note 1—Currently there are few models of SGCs that have the built-in capability to measure shear stress during compaction. The AFG1 SGC manufactured by Pine Instruments can be readily modified to measure shear stress during compaction. The Servopac SGC manufactured by Industrial Process Controls also has shear stress measurement capability. Other SGCs may be available or modified to measure shear stress. A self-contained measurement device similar to the Dynamic Angle Validation Kit may also be an option in the future.

4.2 Thermometers—Armored, glass, or dial-type thermometers with metal stems for determining the temperature of aggregates, binder, and HMA between 10°C and 232°C.

4.3 Balance—A balance meeting the requirements of M231, Class G5, for determining the mass of aggregates, binder, and HMA.

4.4 Oven—An oven, thermostatically controlled to ±3°C, for heating aggregates, binder, HMA, and equipment as required. The oven shall be capable of maintaining the temperature required for mixture conditioning in accordance with PP2.

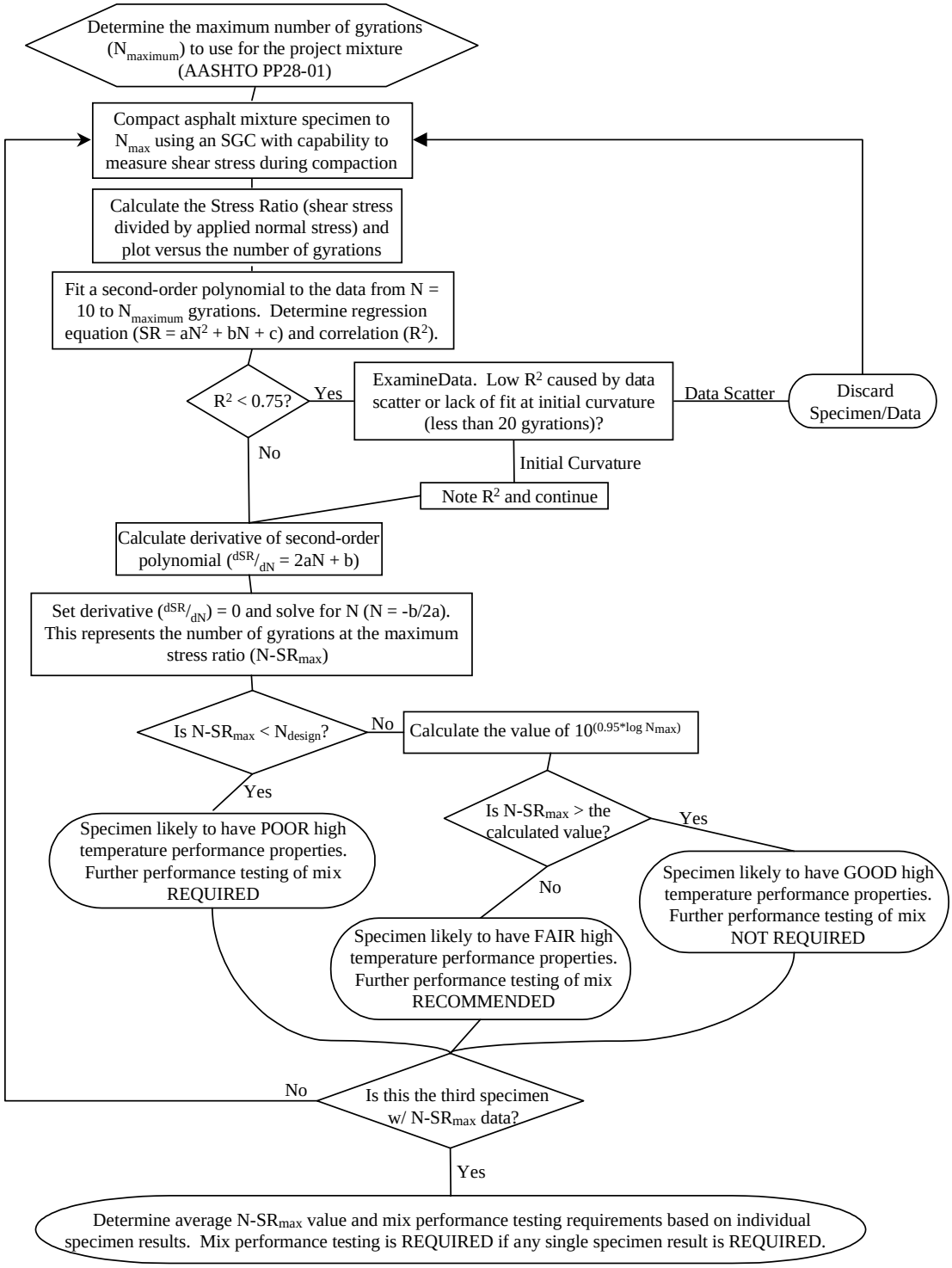

Figure D-1. Mix performance screening using the SGC (w/shear stress measurements).

4.5 Miscellaneous—Flat-bottom metal pans for heating aggregates, scoop for batching aggregates, containers (e.g., grill-type tins, beakers, and containers for heating asphalt), large mixing spoon or small trowel, large spatula, gloves for handling hot equipment, paper disks, mechanical mixer (optional), and lubricating materials recommended by the compactor manufacturer.

5. STANDARDIZATION

5.1 See AASHTO T-312, Section 6.

6. PREPARATION OF APPARATUS

6.1 See AASHTO T-312, Section 7.

7. HMA MIXTURE PREPARATION

7.1 See AASHTO T-312, Section 8.

8. COMPACTION PROCEDURE

8.1 When the compaction temperature is achieved, remove the heated mold, base plate, and upper plate (if required) from the oven. Place the base plate and a paper disk in the bottom of the mold.

8.2 Place the mixture into the mold in one lift. Care should be taken to avoid segregation in the mold. After all the mix is in the mold, level the mix, and place another paper disk and upper plate (if required) on top of the leveled material.

8.3 Load the charged mold into the compactor, verify the compaction parameters, and initialize the compaction sequence.

8.4 Allow the compaction to proceed to the maximum number of gyrations ($N_{maximum}$) specified in Table 1 of PP28 for the appropriate project traffic conditions.

8.5 After completion of compaction, either extrude the specimen and remove the mold from the compactor or remove the mold from the compactor and then extrude the specimen.

Note 2—No additional gyrations with the angle removed are required unless specifically called for in another standard referencing TP 4 (as in PP 2 Section 7.3.2.1.2). The extruded specimen may not be a right-angle cylinder. Specimen ends may need to be sawed to conform to the requirements of specific performance tests.

Note 3—The specimens can be extruded from the mold immediately after compaction for most HMA. However, a cooling period of 5 to 10 minutes in front of a fan may be necessary before extruding some specimens to ensure the specimens are not damaged.

8.6 Remove the paper disks from the top and bottom of the specimen.

Note 4—Before reusing the mold, place it in an oven for at least 5 minutes. The use of multiple molds will speed the compaction process.

9. PROCEDURE FOR ESTIMATING RUTTING PERFORMANCE

9.1 For each compacted specimen, determine the stress ratio at each gyration as the measured shear stress divided by the applied normal stress (nominally 600 kPa).

9.2 Plot the stress ratio as a function of gyrations on a normal arithmetic scale from 10 gyrations to $N_{maximum}$.

9.3 Fit a second-order polynomial curve to the stress ratio data ($SR = aN^2 + bN + c$). Determine the regression equation and correlation (R^2).

9.3.1 If the R^2 of the regression is less than 0.75, examine the data. If the low correlation is the result of data scatter, then the specimen should be discarded and a replacement specimen made (if necessary). If the low correlation is the result of the inability of the regression equation to account for the initial curvature (below 20 gyrations), then keep the specimen results and make a note of the reason for the low correlation.

9.4 Determine the number of gyrations where the slope of the curve is flat. This is done by taking the derivative of the equation, setting it equal to zero ($dSR/dN = 0 = 2aN + b$), and solving for N ($N = -b/2a$). This value of N is the number of gyrations at which the maximum stress ratio occurs. It is identified as $N\text{-}SR_{max}$.

9.5 Determine the logarithm of $N\text{-}SR_{max}$ and divide by the logarithm of $N_{maximum}$ (or the final number of gyrations). If the ratio is greater than or equal to 0.95, the specimen is likely to have good high-temperature performance properties. Further performance testing may not be necessary. Table D-1 presents the $N\text{-}SR_{max}$ value corresponding to a 0.95 ratio for each N_{design} level.

9.6 If $N\text{-}SR_{max}$ is less than N_{design}, the specimen is likely to have poor high-temperature performance properties. High-temperature performance testing is recommended.

9.7 If $N\text{-}SR_{max}$ is between N_{design} and the value where the ratio of the logarithm of $N\text{-}SR_{max}$ to the logarithm of $N_{maximum}$ is equal to 0.95 (Table D-1), the specimen is likely to have fair high-temperature performance properties. The user should evaluate the mixture application before deciding if further high-temperature performance testing is required.

Note 5—The decision to continue with high-temperature performance testing should be based on the application of the mixture. If the mixture is to be used on a project with high traffic or high stress, then further performance testing would be warranted. If the mixture is to be used on a project with relatively low traffic, then the user may opt to waive additional performance testing.

TABLE D-1 $N\text{-}SR_{max}$ Values Corresponding to Ratio of 0.95 (Log $N\text{-}SR_{max}$ / Log $N_{maximum}$)

Traffic, ESAL (10^6)	N_{design}	$N_{maximum}$	$N\text{-}SR_{max}$ value where the $\text{Log } N\text{-}SR_{max} / \text{Log } N_{maximum} \geq 0.95$
< 0.3	50	75	60
< 3	75	115	90
< 30	100	160	125
≥ 30	125	205	155

9.8 The compacted mix specimen may then be subjected to further testing to determine the bulk specific gravity of the compacted specimen in accordance with T166. Repeat the steps in Section 8 and Sections 9.1 through 9.7 until the $N\text{-}SR_{max}$ value has been determined for three specimens from the same mixture (or sample).

9.9 If any specimen in the set of three has an $N\text{-}SR_{max}$ value below N_{design}, then high-temperature performance testing is recommended for the asphalt mixture.

10. REPORT

10.1 For each test specimen report the following:

10.1.1 Mixture Identification

10.1.2 N_{design} and $N_{maximum}$

10.1.3 Calculated $N\text{-}SR_{max}$ value

10.1.4 Regression equation and R^2 value

10.1.5 Rating (Good, Fair, Poor) of estimated high-temperature mechanical properties

11. PRECISION AND BIAS

11.1 Precision—The research required to develop precision estimates for this procedure has not been conducted.

11.2 Bias—The research required to determine the bias of this procedure has not been conducted.

12. KEY WORDS—gyratory, compaction, shear stress, rutting potential.

APPENDIXES E AND F

The following appendixes are available on request from NCHRP:

- Appendix E: Literature Review Summaries; and
- Appendix F: Task 2 Data Sheets.

The entire contractor's final report is also planned for publication in the CRP CD-ROM Bituminous Materials Research Series.

Abbreviations used without definitions in TRB publications:

AASHO	American Association of State Highway Officials
AASHTO	American Association of State Highway and Transportation Officials
ASCE	American Society of Civil Engineers
ASME	American Society of Mechanical Engineers
ASTM	American Society for Testing and Materials
FAA	Federal Aviation Administration
FHWA	Federal Highway Administration
FRA	Federal Railroad Administration
FTA	Federal Transit Administration
IEEE	Institute of Electrical and Electronics Engineers
ITE	Institute of Transportation Engineers
NCHRP	National Cooperative Highway Research Program
NCTRP	National Cooperative Transit Research and Development Program
NHTSA	National Highway Traffic Safety Administration
SAE	Society of Automotive Engineers
TCRP	Transit Cooperative Research Program
TRB	Transportation Research Board
U.S.DOT	United States Department of Transportation